Heavy baryon-antibaryon molecules in effective field theory

Jun-Xu Lu,[1,2] Li-Sheng Geng,[1,*] and Manuel Pavon Valderrama[1,†]

[1]School of Physics and Nuclear Energy Engineering, International Research Center for Nuclei and Particles in the Cosmos and Beijing Key Laboratory of Advanced Nuclear Materials and Physics, Beihang University, Beijing 100191, China

[2]Institut de Physique Nucléaire, CNRS-IN2P3, Université Paris-Sud, Université Paris-Saclay, F-91406 Orsay Cedex, France

(Received 6 July 2017; revised manuscript received 24 February 2019; published 26 April 2019)

We discuss the effective field theory description of bound states composed of a heavy baryon and antibaryon. This framework is a variation of the ones already developed for heavy meson-antimeson states to describe the $X(3872)$ or the Z_c and Z_b resonances. We consider the case of heavy baryons for which the light quark pair is in S-wave and we explore how heavy quark spin symmetry constrains the heavy baryon-antibaryon potential. The one pion exchange potential mediates the low energy dynamics of this system. We determine the relative importance of pion exchanges, in particular the tensor force. We find that in general pion exchanges are probably nonperturbative for the $\Sigma_Q\bar{\Sigma}_Q$, $\Sigma_Q^*\bar{\Sigma}_Q$, and $\Sigma_Q^*\bar{\Sigma}_Q^*$ systems, while for the $\Xi_Q'\bar{\Xi}_Q'$, $\Xi_Q^*\bar{\Xi}_Q'$, and $\Xi_Q^*\bar{\Xi}_Q^*$ cases they are perturbative. If we assume that the contact-range couplings of the effective field theory are saturated by the exchange of vector mesons, we can estimate for which quantum numbers it is more probable to find a heavy baryonium state. The most probable candidates to form bound states are the isoscalar $\Lambda_Q\bar{\Lambda}_Q$, $\Sigma_Q\bar{\Sigma}_Q$, $\Sigma_Q^*\bar{\Sigma}_Q$, and $\Sigma_Q^*\bar{\Sigma}_Q^*$ and the isovector $\Lambda_Q\bar{\Sigma}_Q$ and $\Lambda_Q\bar{\Sigma}_Q^*$ systems, both in the hidden charm and hidden bottom sectors. Their doubly charmed and doubly bottom counterparts ($\Lambda_Q\Lambda_Q$, $\Lambda_Q\Sigma_Q^{(*)}$, $\Sigma_Q^{(*)}\Sigma_Q^{(*)}$) are also good candidates for binding.

DOI: 10.1103/PhysRevD.99.074026

I. INTRODUCTION

Heavy hadron molecules—bound states composed of heavy hadrons—are a type of exotic hadron. The theoretical basis for their existence is robust: in analogy with the nuclear forces that bind the nucleons, heavy hadrons can exchange light mesons, generating exchange forces that might be strong enough to bind them [1–5]. The discovery of the $X(3872)$ more than a decade ago [6] probably provides the most paradigmatic candidate for a molecular state. The $X(3872)$ turns out not to be alone: a series of similarly puzzling hidden charm (hidden bottom) states that do not fit in the charmonium (bottomonium) spectrum have been found in different experiments since then. They are usually referred to as XYZ states and a few are particularly good candidates for molecular states. In the hidden charm sector we have the $Z_c(3900)$ and $Z_c(4020)$ [7,8], which are suspected to be $D\bar{D}^*$, $D^*\bar{D}^*$ molecules [9,10], and the $P_c(4380)^+$ and $P_c(4450)^+$ pentaquark states [11], which might contain $\bar{D}\Sigma_c^*$, $\bar{D}^*\Sigma_c$, $\bar{D}^*\Sigma_c^*$, and even $\bar{D}\Lambda_c(2590)$ molecular components [12–18]. In the hidden bottom sector we have the $Z_b(10610)$ and $Z_b(10650)$ [19,20], which might be $B\bar{B}^*$, $B^*\bar{B}^*$ molecules [21,22]. If we consider the open charm sector, the $D_{s0}(2317)$ and $D_{s1}(2460)$ mesons [23,24] were discovered before the $X(3872)$ and have been theorized to have a large DK/D^*K molecular component [25–28].

We expect molecular states to be relatively narrow for states happening above the open charm threshold. For the moment the masses of the experimentally discovered states have reached the heavy meson-meson and heavy meson-baryon threshold (3.7 and 4.1/4.3 GeV for $D\bar{D}$ and $\Lambda_c\bar{D}/\Sigma_c\bar{D}$, respectively), but barely the heavy baryon-baryon threshold (4.5, 4.7, and 4.9 GeV for $\Lambda_c\bar{\Lambda}_c$, $\Lambda_c\bar{\Sigma}_c$, and $\Sigma_c\bar{\Sigma}_c$, respectively). A narrow resonance near the heavy baryon-baryon threshold would be an excellent candidate for a heavy baryon-antibaryon bound state. Though these states have not been found yet, it is fairly straightforward to extend the available descriptions of heavy meson-antimeson molecules to them and explore the relevant dynamics behind these states. In a few instances it might be possible to predict the location of heavy baryonium states, with the $\Lambda_c(2590)\bar{\Sigma}_c$ systems being an illustrative example [29].

*lisheng.geng@buaa.edu.cn
†mpavon@buaa.edu.cn

Heavy hadron-antihadron molecules are among the most interesting theoretical objects of hadronic physics. Owing to their heavy-light quark content, they are simultaneously subjected to isospin, SU(3)-flavor, chiral and heavy quark symmetry, a high degree of symmetry that can translate into a fairly regular spectrum [10,21,30–35]. This spectrum will not be fully realized in nature: unless these states are shallow they will be a mixture of molecule, charmonium and other exotic components. Yet these potential regularities in the molecular spectrum can be successfully exploited to uncover the nature of a few of the XYZ states. The most clear example probably is the Z_c's and Z_b's resonances, which seem to be related by different realizations of heavy quark symmetry [10].

Heavy hadron molecules possess another interesting quality: they show a separation of scales. On the one hand we have the size of the hadrons, which is of the order of 0.5 fm, while on the other we have the size of the bound state, which should be bigger than the individual hadrons within it. As a consequence heavy hadron molecules are amenable to an effective field theory (EFT) treatment, where all quantities can be expressed as an expansion of a light over a heavy energy scale. EFT descriptions of heavy hadron molecules have been exploited successfully in the past specifically in systems composed of heavy mesons and antimesons [31,36–38]. In this manuscript we extend the heavy hadron EFT formulated in Ref. [32] and put to use in Refs. [10,33,34] in the case of the heavy baryon-antibaryon molecules. As commented, these types of molecules might very well be discovered in the next few years. The purpose of this work is to explore the symmetry constraints and the kind of EFT that is to be expected in these systems, rather than to make concrete predictions of the possible location of these states. Yet we will speculate a bit about this later issue on the basis of the relative strength of the long-range pion exchange and the saturation of the EFT low energy constants by σ, ρ, ω and ϕ meson exchange.

The manuscript is structured as follows. In Sec. II we make a brief introduction to the EFT formalism. In Sec. III we present the leading order EFT potential for heavy baryon-antibaryon states, which consists of a series of contact four-baryon vertices plus the time-honored one pion exchange potential. In Sec. IV we explore the question of whether pions are perturbative or not for this type of hadron molecule. In Sec. V we discuss the possible power countings to describe molecular states. In Sec. VI we speculate about which heavy baryon-antibaryon molecules might be more probable. Finally in Sec. VII we present our conclusions. In Appendix A we present the complete derivation of the one pion exchange potential, in Appendix B we briefly explain the one eta and one kaon exchange potential, and in Appendix C we derive the heavy quark symmetry constraints for the four-baryon contact vertices.

II. EFFECTIVE FIELD THEORY FOR HEAVY BARYON MOLECULES

EFTs are generic and systematic descriptions of low energy processes. They can be applied to physical systems in which there is a distinct separation of scales, but where the underlying high energy theory for that system is unknown or unsolvable. Hadronic molecules are a good candidate for the EFT treatment: the separation among the hadrons forming a hadronic molecule is expected to be larger than the size of the hadrons. When the hadrons are close to each other they overlap and the ensuing description in terms of quantum chromodynamics (QCD) is unsolvable. But this is not the case when the hadrons are far away, in which case their interactions can be described in terms of well-known physics such as pion exchanges. In the following we will present a brief introduction to the application of the EFT framework to heavy baryon-antibaryon systems.

A. The effective field theory expansion

EFTs rely on the existence of a separation of scales, where a distinction is made between low and high energy physics and their respective characteristic momentum scales $M_{\rm soft}$ and $M_{\rm hard}$, which are sometimes called the soft (or light) and hard (or heavy) scales. The separation of scales can be used to express physical quantities at low energies as expansions in terms of the small parameter $M_{\rm soft}/M_{\rm hard}$. If we consider a system of heavy baryons for concreteness, there are two possible EFT expansions depending on which type of low energy symmetry we are considering:

(i) heavy quark spin symmetry (HQSS) and
(ii) chiral symmetry.

For HQSS the soft and hard scales are $\Lambda_{\rm QCD} \sim 200$ MeV and the mass of the heavy quark m_Q, which is either $m_c \sim 1.5$ GeV or $m_b \sim 4.5$ GeV. For chiral symmetry we call the soft and hard scales Q and M, where if there are no baryons we have $Q \sim m_\pi \sim q \sim 100$–$200$ MeV (with m_π the pion mass and q the momenta of the pions) and $M \sim 2\pi f_\pi \sim 1$ GeV. If there are baryons, Q includes the soft momenta of the baryons, while practical calculations in the two-baryon sector suggest a more conservative value of $M \sim 0.5$–1.0 GeV for the hard scale. We advance that the scale Q can contain more than the pion mass and the momenta of the pions and baryons, as we will discuss in Sec. II B.

Heavy baryons are nonrelativistic at the soft scales of either of the two previous symmetries. This implies that their interactions can be described in terms of an effective potential $V_{\rm EFT}$, which admits the double expansion

$$V_{\rm EFT} = \sum_{\mu,\nu} \hat{V}^{(\mu,\nu)} \left(\frac{\Lambda_{\rm QCD}}{m_Q}\right)^{\mu} \left(\frac{Q}{M}\right)^{\nu}, \tag{1}$$

where the indexes μ and ν indicate the order in the heavy quark and chiral expansion, respectively, with $\mu \geq 0$ and

$\nu \geq -1$ (this second point will be explained in Sec. II B). The HQSS expansion converges remarkably faster than the chiral expansion, owing to the sizes of the soft and hard scales involved in each of these expansions. For this reason from now on we will work in the $m_Q \to \infty$ limit and ignore any HQSS breaking effect. With this in mind, the expansion of the EFT potential simplifies to

$$V_{\rm EFT} = \sum_{\nu=\nu_0}^{\nu_{\rm max}} V^{(\nu)} + \mathcal{O}\left(\frac{Q}{M}\right)^{\nu_{\rm max}+1}, \tag{2}$$

which converges for $Q < M$ and where we have simplified the notation with respect to Eq. (1). The expansion begins at $\nu = \nu_0 \geq -1$ and we truncate it at $\nu = \nu_{\rm max}$, where the truncation error gives the uncertainty of a calculation. The lowest order $\nu = \nu_0$ is referred to as the leading order (LO). For a two-heavy-baryon system, the scale Q includes the external momenta of the hadrons, the pion mass, and the binding momentum of a potential bound state if there is any. The rules by which we decide the order of each contribution are called "power counting."

The degrees of freedom of the EFT we are constructing are the heavy baryons and the pion fields [or the pseudo Nambu-Goldstone boson fields if we consider SU(3) chiral symmetry]. This choice of light degrees of freedom actually implies that the EFT potential can be decomposed into two different contributions,

$$V_{\rm EFT} = V_C + V_F, \tag{3}$$

where V_C and V_F are the contact-range and finite-range potentials. While V_C only involves direct interactions between the heavy baryon fields (thus its contact-range nature), V_F involves the exchange of pions and has a finite range determined by the inverse of the mass of the pion. We can expand V_C and V_F according to power counting

$$V_C = \sum_{\nu=\nu_0(C)}^{\nu_{\rm max}} V_C^{(\nu)} + \mathcal{O}\left(\frac{Q}{M}\right)^{\nu_{\rm max}+1}, \tag{4}$$

$$V_F = \sum_{\nu=\nu_0(F)}^{\nu_{\rm max}} V_F^{(\nu)} + \mathcal{O}\left(\frac{Q}{M}\right)^{\nu_{\rm max}+1}, \tag{5}$$

where the power counting of V_C and V_F can differ: we introduce $\nu_0(C)$ and $\nu_0(F)$ to indicate that the expansion may begin at different orders.

For concreteness we will temporarily consider that (chiral) power counting is given by naive dimensional analysis (NDA). We warn that NDA is incompatible with the existence of bound states, but we will address this problem later. Within NDA the power counting of a contribution to the potential is determined by the powers of the heavy baryon momenta, pion momenta, and pion masses included in a particular contribution. In NDA the order of the LO contribution to the potential is $\nu = 0$. For the contact-range potential, this LO contribution is a momentum- and energy-independent interaction,

$$\langle \vec{p}\,'|V_C^{(0)}|\vec{p}\rangle = C^{(0)}, \tag{6}$$

with $C^{(0)}$ a coupling, which will depend on the quantum numbers of the two-body system under consideration and will involve spin and isospin operators. The LO piece of the finite-range potential is given by one pion exchange (OPE), which we write (again schematically) as

$$\langle \vec{p}\,'|V_F^{\rm LO}|\vec{p}\rangle = F^{(0)}\vec{I}_1 \cdot \vec{I}_2 \frac{\vec{a}_1 \cdot \vec{q}\,\vec{a}_2 \cdot \vec{q}}{q^2 + m_\pi^2}, \tag{7}$$

with $\vec{I}_1$ and $\vec{I}_2$ the isospin operators and $\vec{a}_1$ and $\vec{a}_2$ the spin operators of the heavy baryons. The couplings $C^{(0)}$ and $F^{(0)}$ have dimensions of $[\text{energy}]^{-2}$, which means that in NDA their size is given by[1]

$$C^{(0)} \sim \frac{1}{M^2}, \qquad F^{(0)} \sim \frac{1}{M^2}, \tag{8}$$

for which we have taken into account that the only scale from which we can construct the couplings is M (otherwise the counting of the LO potential will change and we will not be talking about NDA).

Other possible contributions to V_C and V_F appear at higher order in the EFT expansion. The subleading terms in V_C are derivative contact-range interactions; i.e., they involve positive powers of the external heavy baryon momenta. The subleading terms in V_F include multipion exchanges, by which it is meant irreducible diagrams involving the exchange of two or more pions. Here it is important to notice that iterations of the OPE potential indeed involve the exchange of two or more pions, but these diagrams are not irreducible: reducible multipion exchanges (iterated OPE) will be lower order than irreducible multipion exchanges.

We will not consider the subleading terms in this work: subleading interactions, in particular the contact-range ones, involve new free parameters which require additional data to be determined. These additional data are not expected to be experimentally available in the near future.

B. Bound states and power counting

Power counting is not unique. NDA is simply the most obvious choice for building a power counting, but not the only one. In particular, the existence of bound states requires modifications to the power counting [39–42], as we will illustrate below. Bound states are solutions of a

[1]Modulo numerical factors, which for nonrelativistic scattering will be multiples of 4π. As we are focusing on the scaling only, we do not include these factors explicitly.

dynamical equation, such as Schrödinger or Lippmann-Schwinger, and require nonperturbative physics. We can see this from the Lippmann-Schwinger equation as applied to bound states,

$$|\Psi_B\rangle = G_0 V |\Psi_B\rangle, \tag{9}$$

where $|\Psi_B\rangle$ is the bound state wave function and $G_0 = 1/(E - H_0)$ the resolvent operator, with H_0 the free Hamiltonian. When G_0 appears in loops it is counted as Q:

$$\int \frac{d^3\vec{l}}{(2\pi)^3} \frac{1}{E - \frac{l^2}{2\mu}} \sim \mu Q, \tag{10}$$

where μ refers to the reduced mass. Generating a bound state requires the iteration of the potential, which in terms of power counting is only consistent if

$$\mathcal{O}(V) = \mathcal{O}(VG_0V) = \mathcal{O}(VG_0VG_0V) = \ldots, \tag{11}$$

from which $V \sim Q^{-1}$ is required. To explain why the potential is counted this way we have to revisit the estimations of the size of the couplings $C^{(0)}$ and $F^{(0)}$ contained in Eq. (8). If any of these two couplings contains a light scale

$$C^{(-1)} \sim \frac{1}{MQ} \quad \text{and/or} \quad F^{(-1)} \sim \frac{1}{MQ}, \tag{12}$$

the LO potential will be promoted from Q^0 to Q^{-1}, allowing for the existence of bound states.[2] The light momentum scale that appears in $C^{(-1)}$ can be identified with the inverse scattering length of the two-body system [39–42], while the light scale in $F^{(-1)}$ is related with the strength of the OPE potential [45]. We stress that it is enough to promote one of the two couplings $C^{(0)}$ and $F^{(0)}$ from Q^0 to Q^{-1}, where for a more detailed discussion we refer to Sec. V.

C. Coupled channels

Now we consider the power counting of coupled channel effects. Heavy baryons can come in HQSS multiplets which are degenerate in the heavy quark limit, e.g., the Σ_c and the Σ_c^* in the charm sector or the Σ_b and the Σ_b^* in the bottom sector. If we take the Σ_c and the Σ_c^* heavy baryons as an example, the two-heavy-baryon system can have transitions of the type $\Sigma_c\Sigma_c \to \Sigma_c\Sigma_c^*$, $\Sigma_c\Sigma_c \to \Sigma_c^*\Sigma_c^*$, etc. In EFT, these transitions have a characteristic momentum scale,

$$\Lambda_{\rm CC} = \sqrt{2\mu\Delta_{\rm CC}}, \tag{13}$$

with μ the reduced mass of the system and $\Delta_{\rm CC}$ the energy difference of the transition. Coupled channel effects can be argued to be suppressed by a factor of

$$\left(\frac{Q}{\Lambda_{\rm CC}}\right)^2, \tag{14}$$

with $\Lambda_{\rm CC}$ the coupled channel scale. For the $\Sigma_c\Sigma_c$ family of systems, we have that $\Lambda_{\rm CC} = 400/564$ MeV depending on the transition, while for the $\Sigma_b\Sigma_b$ case we have $\Lambda_{\rm CC} = 350/495$ MeV. This scale is softer than M, but not much softer: we can effectively ignore the coupled channels at the price of reducing the range of applicability of the EFT.

That is, there are two choices for constructing the EFT in this case: (i) consider the coupled channel effects to be subleading (at the price of reducing the convergence radius of the EFT) or (ii) include them at leading order. Here we will opt for the first option, owing to its simplicity. Be that as it may, most of the results of this manuscript can be easily extended to the coupled channel case.

D. Kaon/eta exchanges and SU(3) symmetry

If we want to preserve SU(3) flavor symmetry, the exchange of kaons and eta mesons should be treated on equal footing as the exchange of pions, at least in principle. But the masses of the kaon and the eta meson are of the order of 0.5 GeV, which is comparable to the hard scale M. We have two choices: (i) ignore kaon and eta exchanges or (ii) include them explicitly.

In the first option, the contributions from kaon and eta exchange are implicitly included in the contact-range potential. There is a disadvantage, though: the contact-range potential breaks SU(3)-flavor symmetry in this case. We expect the size of this breaking to be parametrically small for heavy baryon-baryon and heavy baryon-antibaryon systems of the type $\Sigma_Q\Sigma_Q$, $\Sigma_Q\bar{\Sigma}_Q$, $\Xi'_Q\Xi'_Q$, $\Xi'_Q\bar{\Xi}'_Q$, etc., i.e., systems containing only one species of baryon. Besides the pion, this type of system only exchanges eta mesons, where their coupling to the heavy baryons is considerably weaker than that of the pions. Regarding the kaons, they are relevant for heavy baryon-baryon systems that involve different species: $\Sigma_Q\Xi'_Q$, $\Xi'_Q\Omega_Q$, etc. But if we consider instead a heavy baryon-antibaryon system, the exchange of a single kaon implies a transition between two-baryon states with different thresholds, which involves coupled channel effects. For example in the $\Xi'_c\bar{\Sigma}_c \to \Omega_c\bar{\Xi}'_c$ transition mediated by the exchange of a kaon/antikaon, the energy gap is $\Delta_{\rm CC} = 240$ MeV and the coupled channel scale is $\Lambda_{\rm CC} = 790$ MeV, which is certainly hard.

For these reasons we expect the exchange of kaon and eta mesons to have a small impact on the description of

[2]We mention in passing that the promotion can also be understood in terms of the *anomalous* dimension of the coupling C_0, i.e., of its scaling with respect to the cutoff [43,44].

heavy baryon-antibaryon systems in general. This suggests that ignoring explicit kaon and eta exchange, which amounts to including them implicitly in the contact-range couplings, is not likely to generate a sizable breakdown of SU(3) flavor in the contact-range potential. The implicit inclusion of eta and kaon effects in the contact-range couplings will change their values from the ones expected from exact SU(3)-flavor symmetry, but this change will probably be numerically smaller than the usual 20% uncertainty associated with SU(3)-flavor symmetry relations. This point is supported by an analysis of the strength of the eta and kaon exchanges in Appendix B, where we also present the kaon and eta exchange potentials in case one wants to include them explicitly in the EFT.

III. THE LEADING ORDER POTENTIAL

In this section we write down the heavy baryon-antibaryon potential at LO within the EFT expansion. This potential can contain a contact- and a finite-range piece,

$$V_{\rm EFT}^{(0)} = V_{\rm C}^{(0)} + V_{\rm F}^{(0)}, \tag{15}$$

where we are assuming NDA for the purpose of fixing the notation and simplifying the discussion. If there are bound states, the actual power counting of the heavy baryon-antibaryon system will differ from NDA; see Sec. II B. But we will address this problem later in Secs. IV and V.

The LO contact-range potential is a momentum- and energy-independent potential in momentum space (or a Dirac delta in coordinate space). The LO finite-range potential is the OPE potential.[3] For the contact-range component, we cannot determine if it is perturbative or not *a priori* without resorting to experimental or phenomenological input. For the finite-range components, i.e., the pion exchanges, the situation is different and we can, in fact, determine if they are perturbative; see Sec. IV. The discussion about the possible power countings that arise depending on which pieces of the EFT potential are perturbative and nonperturbative will be presented later in Sec. V.

This section is organized as follows. We begin by explaining the details of how the heavy baryons are organized in superfields that are well behaved according to HQSS in Sec. III A. Next we will consider the C- and G-parity properties of the heavy baryon-antibaryon system in Sec. III B. After this, we will first introduce the general form of the contact-range potential and the constraints imposed on it by heavy quark spin symmetry, SU(2)-isospin, and SU(3)-flavor symmetry in Sec. III C. Last, we will present the general form of the OPE potential and its partial wave projection in Sec. III D. Owing to the scope of the discussion, the notation will be complex. We overview the most used notation in this section in Table I.

A. The heavy baryon superfields

Heavy baryons have the structure

$$|Q(qq)\rangle, \tag{16}$$

where Q is the heavy quark and qq the light quark pair, which is in S-wave. The light quarks can couple their spin

TABLE I. List of the most used symbols in Sec. III.

Symbol	Meaning
$B_{\bar{3}}$	Antitriplet heavy baryon field
B_6	Sextet heavy baryon field, ground state ($J=\frac{1}{2}$)
B_6^*	Sextet heavy baryon field, excited state ($J=\frac{3}{2}$)
$M_{\bar{3}}$	Antitriplet heavy baryon mass
M_6	Sextet heavy baryon mass, ground state ($J=\frac{1}{2}$)
M_6^*	Sextet heavy baryon mass, excited state ($J=\frac{3}{2}$)
T	Antitriplet heavy baryon superfield
S	Sextet heavy baryon superfield
C	(i) C-parity (ii) Coupling of the momentum- and energy-independent contact interaction
G	G-parity
$A_{S_L}^{(M)}$	Antitriplet-antitriplet (A), antitriplet-sextet (B), and sextet-sextet (C) contact interactions
$B_{S_L D}^{(M)}$, $B_{S_L D}^{(M)}$	M refers to the SU(3)-flavor representation, S_L to total light quark spin, and
$C_{S_L}^{(M)}$	D and E to whether it is a direct or exchange term
$\vec{I}_i$	Generic isospin operator for vertex $i=1,2$ of the two-body potential
$\vec{t}_i$	Isospin-0 to isospin-1 transition matrices
$\vec{\tau}_i$	Isospin-$\frac{1}{2}$ Pauli matrices
$\vec{T}_i$	Isospin-1 matrices
$\vec{a}_i$	Generic spin operator for vertex $i=1,2$ of the two-body potential
$\vec{\sigma}_i$	Spin-$\frac{1}{2}$ Pauli matrices
$\vec{S}_i$, $\vec{S}_i^+$	Spin-$\frac{1}{2}$ to spin-$\frac{3}{2}$ transition matrices
$\vec{\Sigma}_i$	Spin-$\frac{3}{2}$ angular momentum matrices
C_{12}	Spin-spin operator ($\vec{a}_1\cdot\vec{a}_2$)
S_{12}	Tensor operator ($3\vec{a}_1\cdot\hat{r}\vec{a}_2\cdot\hat{r}-\vec{a}_1\cdot\vec{a}_2$)
$^{2S+1}L_J$	Spectroscopic notation for partial waves with S the spin, L the orbital angular momentum, and J the total angular momentum
$\mathbf{C}_{12}$	Matrix elements of the spin-spin operator in the partial wave basis
$\mathbf{S}_{12}$	Matrix elements of the tensor operator in the partial wave basis

[3]Regarding the exchange of the other $SU(3)$ Nambu-Goldstone bosons, we refer to the discussion in Sec. II D.

to $S_L = 0, 1$. If the light spin is $S_L = 0$, we have a $J^P = \frac{1}{2}^+$ heavy baryon:

$$B_{\bar{3}} = |Q(qq)_{S_L=0}\rangle. \tag{17}$$

This type of heavy baryon belongs to the $\bar{3}$ representation of the $SU(3)$ flavor group. If the light spin is $S_L = 1$, we have instead a $J^P = \frac{1}{2}^+$ or a $J^P = \frac{3}{2}^+$ baryon,

$$B_6 = |Q(qq)_{S_L=1}\rangle|_{J=1/2}, \tag{18}$$

$$B_6^* = |Q(qq)_{S_L=1}\rangle|_{J=3/2}, \tag{19}$$

which belong to the 6 representation of $SU(3)$.

If the heavy quark within the heavy baryons is a charm quark, $Q = c$, the flavor components of the $B_{\bar{3}}$ field are

$$B_{\bar{3}} = \begin{pmatrix} \Xi_c^0 \\ -\Xi_c^+ \\ \Lambda_c^+ \end{pmatrix}, \tag{20}$$

where we follow the convention of Cho [46]. For the B_6 field, the flavor components are

$$B_6 = \begin{pmatrix} \Sigma_c^{++} & \frac{1}{\sqrt{2}}\Sigma_c^+ & \frac{1}{\sqrt{2}}\Xi_c^{+\prime} \\ \frac{1}{\sqrt{2}}\Sigma_c^+ & \Sigma_c^0 & \frac{1}{\sqrt{2}}\Xi_c^{0\prime} \\ \frac{1}{\sqrt{2}}\Xi_c^{+\prime} & \frac{1}{\sqrt{2}}\Xi_c^{0\prime} & \Omega_c^0 \end{pmatrix}. \tag{21}$$

For the B_6^* baryons we have exactly the same components as for B_6, but with a star to indicate that they are spin-3/2 baryons. Depending on the case, it can be practical to simply consider the $SU(2)$-isospin structure rather than the complete $SU(3)$-flavor one.

The fields $B_{\bar{3}}$, B_6, and B_6^* can be organized into the superfields T and S, which have good transformation properties under the rotation of the heavy quark. For nonrelativistic heavy baryons we write the superfields as [46]

$$T = B_{\bar{3}}, \qquad \vec{S} = \frac{1}{\sqrt{3}}\vec{\sigma}B_6 + \vec{B}_6^*, \tag{22}$$

where the letters T and S stands for (anti-)triplet and sextet. The definition of the nonrelativistic superfield T is redundant (it acts merely as a second name for $B_{\bar{3}}$), but we include it for completeness. Notice that we have written the spin-3/2 heavy baryon field as a vector: $\vec{B}_6^*$. The reason is that this is a Rarita-Schwinger field, where the spin-3/2 nature of this field is taken into account by *coupling* a spatial vector with a Dirac spinor and then projecting to the spin-3/2 channel with the condition $\vec{\sigma}\cdot\vec{B}_6^* = 0$. Under rotations of the heavy quark spin, the superfields behave as

$$T \to e^{\frac{i}{2}\vec{\epsilon}\cdot\vec{\sigma}_Q}T, \qquad \vec{S} \to e^{\frac{i}{2}\vec{\epsilon}\cdot\vec{\sigma}_Q}\vec{S}. \tag{23}$$

For a more complete account of the heavy baryon fields and superfields, we refer to Appendix A.

B. C- and G-parity

We are considering heavy baryon-antibaryon states. If a state is electrically neutral and does not have strangeness, then C-parity will be a well-defined quantum number. If the heavy baryon and antibaryon have identical S_L and J^P, i.e., if they have the structure

$$|B_{\bar{3}}\bar{B}_{\bar{3}}\rangle, \qquad |B_6\bar{B}_6\rangle, \qquad |B_6^*\bar{B}_6^*\rangle, \tag{24}$$

then the C-parity of the system is

$$C = (-1)^{L+S}, \tag{25}$$

with L and S the orbital angular momentum and spin.[4] Examples of this type of heavy baryon-antibaryon system are $\Lambda_c^+\Lambda_c^-$, $\Sigma_c^0\bar{\Sigma}_c^0$, and $\Sigma_c^{*+}\Sigma_c^{*-}$.

If the light quark spin S_L and spin-parity J^P of the heavy baryon and antibaryon are not identical, we first have to choose a C-parity convention, for instance,

$$C|B_{\bar{3}}\rangle = +|\bar{B}_{\bar{3}}\rangle, \tag{26}$$

$$C|B_6\rangle = +|\bar{B}_6\rangle, \tag{27}$$

$$C|B_6^*\rangle = -|\bar{B}_6^*\rangle, \tag{28}$$

where there is a relative minus sign for the C-parity transformation of the spin-$\frac{3}{2}$ fields with respect to the spin-$\frac{1}{2}$ fields. With this convention we define the states

$$|B_{\bar{3}}\bar{B}_6(\eta)\rangle = \frac{1}{\sqrt{2}}[|B_{\bar{3}}\bar{B}_6\rangle + \eta|B_6\bar{B}_{\bar{3}}\rangle], \tag{29}$$

$$|B_{\bar{3}}\bar{B}_6^*(\eta)\rangle = \frac{1}{\sqrt{2}}[|B_{\bar{3}}\bar{B}_6^*\rangle + \eta|B_6^*\bar{B}_{\bar{3}}\rangle], \tag{30}$$

$$|B_6\bar{B}_6^*(\eta)\rangle = \frac{1}{\sqrt{2}}[|B_6\bar{B}_6^*\rangle + \eta|B_6^*\bar{B}_6\rangle], \tag{31}$$

where $\eta = \pm 1$, for which the C-parity is

$$C = \eta(-1)^{L+S}, \tag{32}$$

where L (S) is the total orbital angular momentum (spin) of the heavy baryon-antibaryon pair.[5] Examples of this type of molecule include $\Lambda_c^+\Sigma_c^-$, $\Xi_c^{\prime 0}\bar{\Xi}_c^0$, and $\Xi_c^{\prime +}\Xi_c^{*-}$.

[4]This comes from multiplying the intrinsic C-parity of a fermion-antifermion system with the symmetry factors of exchanging the particles, i.e., $C = (-1)\times(-1)^L\times(-1)^{S+1}$.

[5]The C-parity is the product of the intrinsic C-parity and the symmetry factor of exchanging the particles, which now includes a contribution from η, i.e., $C = (+\eta)\times(-1)\times(-1)^L\times(-1)^{S+1}$ for $B_{\bar{3}}B_6$ and $C = (-\eta)\times(-1)\times(-1)^L\times(-1)^S$ for $B_{\bar{3}}B_6^*/B_6B_6^*$.

For a heavy baryon-antibaryon state that is not electrically neutral but has no strangeness and belongs to the same $SU(2)$ isospin representation as a neutral state, C-parity is not a well-defined quantum number but there exists an extension that includes isospin. This extension is G-parity [47], which can be defined as follows:

$$G = Ce^{i\pi I_2}, \tag{33}$$

that is, a C-parity transformation combined with a rotation in isospin space.[6] For an electrically charged state, the G-parity is well defined and its eigenvalues are

$$G = C(-1)^I, \tag{34}$$

where I is the isospin of the electrically charged state and C is the C-parity of the electrically neutral component of the isospin multiplet. For example, if we consider $\Sigma_c^{++}\bar{\Sigma}_c^0$, its isospin is $I = 2$ and the neutral component of its isospin multiplet is a linear combination of $\Sigma_c^0\bar{\Sigma}_c^0$, $\Sigma_c^+\Sigma_c^-$, and $\Sigma_c^{++}\Sigma_c^{--}$: the G-parity of $\Sigma_c^{++}\bar{\Sigma}_c^0$ is then $G = (-1)^I C = (-1)^{L+S}$.

C. The contact-range potential

The LO contact-range potential takes the generic form

$$\langle p'|V_C^{(0)}|p\rangle = C, \tag{35}$$

with C a coupling constant and where p (p') is the center-of-mass momentum of the incoming (outgoing) heavy baryon-antibaryon pair. In principle, there should be one independent coupling C for each J^{PC} quantum number and type of heavy baryon-antibaryon molecule. But the contact-range potential is constrained by HQSS and $SU(3)$-flavor symmetry, which greatly reduces the number of possible couplings. We first consider the HQSS structure of the contact-range potential and then the $SU(3)$ flavor one.

1. HQSS structure

The application of HQSS to the heavy baryon-antibaryon system implies that the contact-range coupling does not depend on the heavy quark spin, only on the light quark spin. This means that the coupling C can be decomposed in terms of light quark components,

$$C = \sum d_{S_L} C_{S_L}, \tag{36}$$

where S_L is the total light quark spin of the heavy baryon-antibaryon system. The d_{S_L}'s are coefficients that depend on the heavy and light quark decomposition of the specific heavy baryon-antibaryon molecule; see Appendix C for details.

The contact-range couplings of the $T\bar{T}$, $S\bar{T}$, and $S\bar{S}$ molecules are independent and we will use a different notation for each case: A, B, and C respectively. For the $T\bar{T}$ system we write the contact-range potential as

$$\langle T\bar{T}|V_C^{(0)}|T\bar{T}\rangle = A_0, \tag{37}$$

where we are already taking into account that the total light quark spin is always $S_L = 0$ (we also ignore the coefficient because there is actually no decomposition). For the $S\bar{T}$ system we write

$$\langle S\bar{T}|V_C^{(0)}|S\bar{T}\rangle = d_{1D}B_{1D}, \tag{38}$$

$$\langle S\bar{T}|V_C^{(0)}|T\bar{S}\rangle = d_{1E}B_{1E}, \tag{39}$$

where the total light spin is always $S_L = 1$, but where we have to make the distinction between a diagonal and nondiagonal potential. For the $S\bar{S}$ system we have

$$\langle S\bar{S}|V_C^{(0)}|S\bar{S}\rangle = d_0C_0 + d_1C_1 + d_2C_2, \tag{40}$$

where the total light spin is $S_L = 0$, 1, 2. We list the contact-range potential for heavy baryon-antibaryon molecules with well-defined C-parity in Table II, which also applies by extension to the molecules with well-defined G-parity.

If the molecules do not have well-defined C- or G-parity (i.e., molecules with strangeness), the form of the contact-range potential depends on the particular case. For the family of molecules

$$|B_{\bar{3}}\bar{B}_{\bar{3}}\rangle, \quad |B_6\bar{B}_6\rangle, \quad |B_6^*\bar{B}_6^*\rangle \tag{41}$$

(e.g., $\Lambda_c\bar{\Xi}_c$, $\Sigma_c\bar{\Xi}_c'$, $\Sigma_c^*\bar{\Xi}_c^*$), the contact-range couplings are exactly as shown in Table II for the case in which C-parity is well defined. For the molecules involving different types of heavy hadrons, the contact-range potentials are defined in coupled channels. If we consider the bases

$$\mathcal{B}_1 = \{|B_{\bar{3}}\bar{B}_6\rangle, |B_6\bar{B}_{\bar{3}}\rangle\}, \tag{42}$$

$$\mathcal{B}_2 = \{|B_{\bar{3}}\bar{B}_6^*\rangle, |B_6^*\bar{B}_{\bar{3}}\rangle\}, \tag{43}$$

$$\mathcal{B}_3 = \{|B_6\bar{B}_6^*\rangle, |B_6^*\bar{B}_6\rangle\}, \tag{44}$$

[6]Notice that the G-parity transformation is sometimes defined as $G = Ce^{-i\pi I_2}$ with a minus sign. For particles with integer isospin, this is equivalent to the definition with a plus sign, $G = Ce^{+i\pi I_2}$. For particles with half-integer isospin, each of these conventions generates antiparticle states that differ by a sign. This has no observable consequence, as it amounts to a global redefinition of the amplitudes by a phase.

TABLE II. HQSS decomposition of the contact-range couplings for heavy baryon-antibaryon molecules with well-defined C-parity. A, B, and C refer to the couplings of the $T\bar{T}$, $S\bar{T}$, and $S\bar{S}$ systems, respectively, with the subscript indicating the light quark spin decomposition. For the cases where C-parity is not well defined, we refer to the explanations in the main text.

System	J^P/J^{PC}	V_C (HQSS)
$B_{\bar{3}}\bar{B}_{\bar{3}}$	0^{-+}	A_0
$B_{\bar{3}}\bar{B}_{\bar{3}}$	1^{--}	A_0
$B_{\bar{3}}\bar{B}_6$	0^{-+}	$B_{1D}-B_{1E}$
$B_{\bar{3}}\bar{B}_6$	0^{--}	$B_{1D}+B_{1E}$
$B_{\bar{3}}\bar{B}_6$	1^{-+}	$B_{1D}-\frac{1}{3}B_{1E}$
$B_{\bar{3}}\bar{B}_6$	1^{--}	$B_{1D}+\frac{1}{3}B_{1E}$
$B_{\bar{3}}\bar{B}_6^*$	1^{-+}	$B_{1D}+\frac{1}{3}B_{1E}$
$B_{\bar{3}}\bar{B}_6^*$	1^{--}	$B_{1D}-\frac{1}{3}B_{1E}$
$B_{\bar{3}}\bar{B}_6^*$	2^{-+}	$B_{1D}-B_{1E}$
$B_{\bar{3}}\bar{B}_6^*$	2^{--}	$B_{1D}+B_{1E}$
$B_6\bar{B}_6$	0^{-+}	$\frac{1}{3}C_0+\frac{2}{3}C_1$
$B_6\bar{B}_6$	1^{--}	$\frac{1}{27}C_0+\frac{6}{27}C_1+\frac{20}{27}C_2$
$B_6\bar{B}_6^*$	1^{-+}	C_1
$B_6\bar{B}_6^*$	1^{--}	$\frac{16}{27}C_0+\frac{6}{27}C_1+\frac{5}{27}C_2$
$B_6\bar{B}_6^*$	2^{-+}	$\frac{1}{3}C_1+\frac{2}{3}C_2$
$B_6\bar{B}_6^*$	2^{--}	C_2
$B_6^*\bar{B}_6^*$	0^{-+}	$\frac{2}{3}C_0+\frac{1}{3}C_1$
$B_6^*\bar{B}_6^*$	1^{--}	$\frac{10}{27}C_0+\frac{15}{27}C_1+\frac{2}{27}C_2$
$B_6^*\bar{B}_6^*$	2^{-+}	$\frac{2}{3}C_1+\frac{1}{3}C_2$
$B_6^*\bar{B}_6^*$	3^{--}	C_2

we end up with the following contact-range potentials:

$$V_{\mathcal{B}_1}(0^-)=\begin{pmatrix} B_{1D} & -B_{1E} \\ -B_{1E} & B_{1D}\end{pmatrix}, \tag{45}$$

$$V_{\mathcal{B}_1}(1^-)=\begin{pmatrix} B_{1D} & \frac{1}{3}B_{1E} \\ \frac{1}{3}B_{1E} & B_{1D}\end{pmatrix}, \tag{46}$$

$$V_{\mathcal{B}_2}(1^-)=\begin{pmatrix} B_{1D} & -\frac{1}{3}B_{1E} \\ -\frac{1}{3}B_{1E} & B_{1D}\end{pmatrix}, \tag{47}$$

$$V_{\mathcal{B}_2}(2^-)=\begin{pmatrix} B_{1D} & -B_{1E} \\ -B_{1E} & B_{1D}\end{pmatrix}, \tag{48}$$

$$V_{\mathcal{B}_3}(1^-)=\begin{pmatrix} \frac{16C_0+33C_1+5C_2}{54} & \frac{16C_0-21C_1+5C_2}{54} \\ \frac{16C_0-21C_1+5C_2}{54} & \frac{16C_0+33C_1+5C_2}{54}\end{pmatrix}, \tag{49}$$

$$V_{\mathcal{B}_3}(2^-)=\begin{pmatrix} \frac{1}{6}C_1+\frac{5}{6}C_2 & \frac{1}{6}C_1-\frac{1}{6}C_2 \\ \frac{1}{6}C_1-\frac{1}{6}C_2 & \frac{1}{6}C_1+\frac{5}{6}C_2\end{pmatrix}. \tag{50}$$

Examples of bases 1, 2, and 3 are the $\Xi_c\bar{\Sigma}_c-\Xi_c'\bar{\Lambda}_c$, $\Xi_c\bar{\Sigma}_c^*-\Xi_c^*\bar{\Lambda}_c$, and $\Xi_c'\bar{\Sigma}_c^*-\Xi_c^*\bar{\Sigma}_c$ systems.

2. SU(3)-flavor structure

Besides HQSS, heavy baryon-antibaryon systems also have SU(3)-flavor symmetry. In SU(3) flavor, the T and S heavy baryons belong to the antitriplet and sextet representation ($\bar{3}$ and 6), respectively. For the $T\bar{T}$, the HQSS coupling is further divided into the SU(3)-flavor representations $\bar{3}\otimes 3=1\oplus 8$, a singlet and an octet. That is, there are two independent SU(3)-flavor contact interactions

$$A_0\to\{A_0^{(1)},A_0^{(8)}\}. \tag{51}$$

For the $S\bar{T}$ case, we have $6\otimes 3=8\oplus 10$:

$$B_{1D}\to\{B_{1D}^{(8)},B_{1D}^{(10)}\}, \tag{52}$$

$$B_{1E}\to\{B_{1E}^{(8)},B_{1E}^{(10)}\}. \tag{53}$$

Finally for the $S\bar{S}$ case we have $6\otimes\bar{6}=1\oplus 8\oplus 27$:

$$C_{S_L}\to\{C_{S_L}^{(1)},C_{S_L}^{(8)},C_{S_L}^{(27)}\}. \tag{54}$$

The decomposition for a specific molecule can be found in Table III, which has been obtained from the SU(3) Clebsch-Gordan coefficients for the $\bar{3}\otimes 3$, $6\otimes 3$, and $6\otimes\bar{6}$ of Ref. [48]. Notice that we are not explicitly considering the SU(2)-isospin structure as it is a subgroup of SU(3) flavor.

TABLE III. SU(3)-flavor decomposition of the contact-range couplings depending on the type heavy baryon-antibaryon molecule. Notice that the HQSS structure of the couplings is independent of the SU(3) one, which is why we do not show the light spin indices for the couplings. For the S heavy baryons we show the decomposition for the lightest member of the HQSS multiplet only.

System	Type	Isospin	V_C
$\Lambda_c\bar{\Lambda}_c$	$T\bar{T}$	0	$\frac{1}{3}A^{(1)}+\frac{2}{3}A^{(8)}$
$\Xi_c\bar{\Xi}_c$	$T\bar{T}$	0	$\frac{2}{3}A^{(1)}+\frac{1}{3}A^{(8)}$
$\Xi_c\bar{\Xi}_c$	$T\bar{T}$	1	$A^{(8)}$
$\Xi_c'\bar{\Xi}_c$	$S\bar{T}$	0	$B^{(8)}$
$\Xi_c'\bar{\Xi}_c$	$S\bar{T}$	1	$\frac{1}{3}B^{(8)}+\frac{2}{3}B^{(10)}$
$\Sigma_c\bar{\Lambda}_c$	$S\bar{T}$	1	$\frac{2}{3}B^{(8)}+\frac{1}{3}B^{(10)}$
$\Omega_c\bar{\Omega}_c$	$S\bar{S}$	0	$\frac{1}{6}C^{(1)}+\frac{8}{15}C^{(8)}+\frac{3}{10}C^{(27)}$
$\Xi_c'\bar{\Xi}_c'$	$S\bar{S}$	0	$\frac{1}{3}C^{(1)}+\frac{1}{15}C^{(8)}+\frac{3}{5}C^{(27)}$
$\Sigma_c\bar{\Sigma}_c$	$S\bar{S}$	0	$\frac{1}{2}C^{(1)}+\frac{2}{5}C^{(8)}+\frac{1}{10}C^{(27)}$
$\Xi_c'\bar{\Xi}_c'$	$S\bar{S}$	1	$\frac{1}{5}C^{(8)}+\frac{4}{5}C^{(27)}$
$\Sigma_c\bar{\Sigma}_c$	$S\bar{S}$	1	$\frac{4}{5}C^{(8)}+\frac{1}{5}C^{(27)}$
$\Sigma_c\bar{\Sigma}_c$	$S\bar{S}$	2	$C^{(27)}$

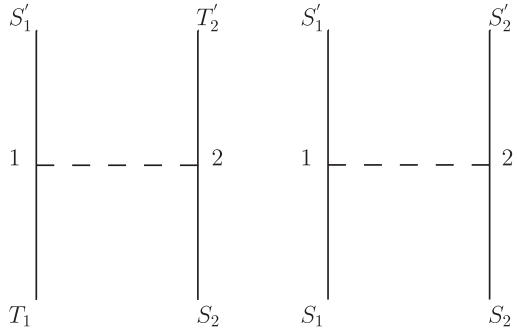

FIG. 1. Diagrams for OPE potential between two heavy hadrons. On the left we show the TS potential and on the right the SS potential, where T (S) is the heavy baryon with light spin $S_L = 0$ ($S_L = 1$).

Finally, we remind the reader that the SU(3)-flavor structure of the contact-range potential can be broken if the finite-range potential is not SU(3)-flavor symmetric. Whether this happens depends on two factors. The first is the particular power counting we are using and the order we are considering within the EFT expansion, e.g., if the contact-range interaction is leading, but the exchange of pions, kaons, and etas is subleading, the violations of SU(3)-flavor symmetry if we ignore kaon and eta exchanges will be subleading. The second factor is that kaon and eta exchanges are parametrically small, as was explained in Sec. II D, and a more detailed derivation can be found in Appendix B.

D. The one pion exchange potential

The OPE potential in momentum space reads

$$\langle T_1\bar{T}_2|V_{\rm F}^{(0)}|T_1'\bar{T}_2'\rangle = 0, \tag{55}$$

$$\langle T_1\bar{S}_2|V_{\rm F}^{(0)}|S_1'\bar{T}_2'\rangle = -R_1\bar{R}_2\frac{g_3^2}{2f_\pi^2}\vec{I}_1\cdot\vec{I}_2\frac{\vec{a}_1\cdot\vec{q}\vec{a}_2\cdot\vec{q}}{q^2+\mu_\pi^2}, \tag{56}$$

$$\langle S_1\bar{S}_2|V_{\rm F}^{(0)}|S_1'\bar{S}_2'\rangle = -R_1\bar{R}_2\frac{g_2^2}{2f_\pi^2}\vec{I}_1\cdot\vec{I}_2\frac{\vec{a}_1\cdot\vec{q}\vec{a}_2\cdot\vec{q}}{q^2+\mu_\pi^2}, \tag{57}$$

where we have chosen the specific notation above to cover all the possible combinations. The subscripts 1 and 2 are used to denote the vertices 1 and 2 in the diagrams of Fig. 1. In the equation above, R_1 and $\bar{R}_2$ are numerical factors which depend on the transition we are considering; see Table IV (the bar indicates an antibaryon to antibaryon transition). $\vec{I}_1$ and $\vec{I}_2$ are isospin matrices, while $\vec{a}_1$ and $\vec{a}_2$ spin matrices. For the couplings we have that g_2 is the axial coupling for the $S_L = 1$ heavy baryon, g_3 the coupling involved in $T \to S\pi$ transitions, and f_π the pion decay constant. μ_π is the effective pion mass for the vertices involved in the particular channel considered. Finally we notice that OPE vanishes for the $T\bar{T}$ molecules, which can be described solely in terms of contact interactions at lowest order.

TABLE IV. Numerical, isospin, and spin factors associated with each vertex in the $\langle S\bar{T}|V|T\bar{S}\rangle$ and $\langle S\bar{S}|V|S\bar{S}\rangle$ heavy baryon-antibaryon potential. The arrows are used to indicate the final baryon state in the vertex. The symbols $\vec{\tau}_i$ and $\vec{T}_i$ represent the Pauli matrices (in isospin space) and the isospin $I = 1$ matrices, respectively, while t_i is a special isospin matrix for connecting the isoscalar Λ_c with the isovector Σ_c and the pion. The symbols $\vec{\sigma}_i$ and $\vec{\Sigma}_i$ are the Pauli matrices and the spin $S = 3/2$ matrices, while $\vec{S}_i$ is a 2×4 matrix that is used for the transitions involving a spin-1/2 and spin-3/2 baryon. Notice that this table can also be used to compute the heavy baryon-baryon potential.

Vertex	R_i	$\bar{R}_i$	$\vec{I}_i$	$\vec{a}_i$
$\Lambda_c \to \Sigma_c$	$\sqrt{\frac{2}{3}}$	$-\sqrt{\frac{2}{3}}$	$\vec{t}_i$	$\vec{\sigma}_i$
$\Lambda_c \to \Sigma_c^*$	$\sqrt{2}$	$\sqrt{2}$	$\vec{t}_i$	$\vec{S}_i^\dagger$
$\Xi_c \to \Xi_c'$	$\sqrt{\frac{2}{3}}$	$-\sqrt{\frac{2}{3}}$	$\frac{1}{2}\vec{\tau}_i$	$\vec{\sigma}_i$
$\Xi_c \to \Xi_c^*$	$\sqrt{2}$	$\sqrt{2}$	$\frac{1}{2}\vec{\tau}_i$	$\vec{S}_i^\dagger$
$\Sigma_c \to \Sigma_c$	$\frac{2}{3}$	$-\frac{2}{3}$	$\vec{T}_i$	$\vec{\sigma}_i$
$\Sigma_c^* \to \Sigma_c$	$\frac{1}{\sqrt{3}}$	$\frac{1}{\sqrt{3}}$	$\vec{T}_i$	$\vec{S}_i$
$\Sigma_c \to \Sigma_c^*$	$\frac{1}{\sqrt{3}}$	$\frac{1}{\sqrt{3}}$	$\vec{T}_i$	$\vec{S}_i^\dagger$
$\Sigma_c^* \to \Sigma_c^*$	$\frac{2}{3}$	$-\frac{2}{3}$	$\vec{T}_i$	$\vec{\Sigma}_i$
$\Xi_c' \to \Xi_c'$	$\frac{2}{3}$	$-\frac{2}{3}$	$\frac{1}{2}\vec{\tau}_i$	$\vec{\sigma}_i$
$\Xi_c^* \to \Xi_c'$	$\frac{1}{\sqrt{3}}$	$\frac{1}{\sqrt{3}}$	$\frac{1}{2}\vec{\tau}_i$	$\vec{S}_i$
$\Xi_c' \to \Xi_c^*$	$\frac{1}{\sqrt{3}}$	$\frac{1}{\sqrt{3}}$	$\frac{1}{2}\vec{\tau}_i$	$\vec{S}_i^\dagger$
$\Xi_c^* \to \Xi_c^*$	$\frac{2}{3}$	$-\frac{2}{3}$	$\frac{1}{2}\vec{\tau}_i$	$\vec{\Sigma}_i$

Regarding the isospin structure of the OPE potential, we have that $\vec{I}_1$ and $\vec{I}_2$ are the isospin matrices corresponding to vertex 1 and 2. If we have a heavy baryon with isospin 1/2 at vertex i, we can simply make the substitution $\vec{I}_i = \frac{\vec{\tau}_i}{2}$, where $\vec{\tau}$ are the Pauli matrices. If the heavy baryon at vertex i has isospin 1, we use the $J = 1$ angular momentum matrices in isospin space, for which we use the notation $\vec{T}_i$; i.e., we make the substitution $\vec{I}_i = \vec{T}_i$. The exact isospin factor for each type of vertex can be found in Table IV.

Regarding the spin structure, we note that the spin operators a_1 and a_2 depend on which is the initial and final spin of the heavy baryons at vertex 1 and 2. If the initial and final heavy baryons at vertex 1(2) have spin 1/2, we have $\vec{a}_1 = \vec{\sigma}_1$ ($\vec{a}_2 = \vec{\sigma}_2$). If the initial and final heavy baryons at vertex 1 (2) have spin 3/2, we have $\vec{a}_1 = \vec{\Sigma}_1$ ($\vec{a}_2 = \vec{\Sigma}_2$), where $\vec{\Sigma}$ are the $S = 3/2$ spin matrices. If the initial and final heavy baryons at vertex 1 (2) switch from spin 1/2 to spin 3/2 (or vice versa), then $\vec{a}_1 = \vec{S}_1$ ($\vec{a}_2 = \vec{S}_2$), where $\vec{S}$ are special 2×4 spin matrices that describe the transition from a different initial to final spin (see their definition in Appendix A). As with isospin, the

exact spin matrix to use in each type of vertex can be checked in Table IV.

Regarding the axial couplings g_2 and g_3, we notice that the value of g_3 can be extracted from the $\Sigma_c^{++} \to \Lambda_c^+ \pi^+$ decay measured by Belle in Ref. [49], yielding $g_3 = 0.973^{+0.019}_{-0.042}$ [50] (notice that the previous reference originally uses the convention of Yan *et al.* [51] to define the axial couplings, instead of the one by Cho [46,52] that we employ here, and we have consequently adapted the numbers of Ref. [50] to our convention). In contrast, g_2 is experimentally unavailable, but on the basis of quark model relations one can estimate it to be $g_2 = -\sqrt{2} g_3 = -1.38$. If we consider the values of g_2 and g_3 from the lattice QCD calculation of Ref. [53], we obtain instead $g_2 = -0.84 \pm 0.20$ and $g_3 = 0.71 \pm 0.13$, where it is important to mention that they are calculated in the $m_Q = \infty$ limit (notice again that our convention for g_2 differs from the definition used in Ref. [53] by a sign, which has been taken into account). Had we applied the quark model relations to the lattice QCD value of g_3, we would have obtained $g_2 = -1.00$, which is considerably larger than the lattice QCD determination but yet within its error bar.

For the effective pion mass, we have that if the particles in the vertex 1 and 2 have the same mass, then $\mu_\pi = m_\pi$. On the other hand if they have different masses (e.g., $S_1 = B$, $S_1' = B'$) and the mass splitting is given by Δ, then we have that $\mu_\pi^2 = m_\pi^2 - \Delta^2$ (a relation that assumes heavy, non-relativistic baryons).

Finally we notice that we can also compute the heavy baryon-baryon potential by making the change

$$R_1 \bar{R}_2 \to R_1 R_2 \tag{58}$$

in Eqs. (56) and (57) and checking the proper values in Table IV.

The most explicit way to construct the potential for one particular channel is to make use of Table IV, where all the factors are listed. For instance if we are considering the $\Xi_c^* \bar{\Sigma}_c \to \Xi_c' \bar{\Sigma}_c^*$ potential, we can see that it contains a $\Xi_c^* \to \Xi_c'$ transition in vertex 1 and a $\bar{\Sigma}_c \to \bar{\Sigma}_c^*$ transition in vertex 2. If we use Table IV we find $R_1 = 1/\sqrt{3}$, $I_1 = \vec{\tau}_1/2$, $\vec{a}_1 = \vec{S}_1$ for vertex 1 and $\bar{R}_2 = 1/\sqrt{3}$, $I_2 = \vec{T}_1$, $\vec{a}_2 = \vec{S}_2^\dagger$ for vertex 2. Putting the pieces together, the potential reads

$$\langle \Xi_c^* \bar{\Sigma}_c | V_{\rm F}^{(0)} | \Xi_c' \bar{\Sigma}_c^* \rangle = -\frac{1}{3} \frac{g_3^2}{2 f_\pi^2} \frac{\vec{\tau}_1 \cdot \vec{T}_2}{2} \frac{\vec{S}_1 \cdot \vec{q} \vec{S}_2^\dagger \cdot \vec{q}}{q^2 + \mu_\pi^2}, \tag{59}$$

where $\mu_\pi^2 = m_\pi^2 - \Delta^2$, with $\Delta \simeq (m(\Xi_c^*) - m(\Xi_c')) \simeq (m(\Sigma_c^*) - m(\Sigma_c)) \simeq 70\,\text{MeV}$ and $\mu_\pi \sim 120$ MeV. The other cases can be obtained analogously.

1. The OPE potential in coordinate space

If we Fourier-transform the potential into coordinate space we obtain

$$\begin{aligned}\langle T_1 \bar{S}_2 | V_{\rm F}^{(0)}(\vec{r}) | S_1' \bar{T}_2' \rangle &= -R_1 \bar{R}_2 \vec{I}_1 \cdot \vec{I}_2 \frac{g_3^2}{6 f_\pi^2} C_{12} \delta^3(\vec{r}) + R_1 \bar{R}_2 \vec{I}_1 \cdot \vec{I}_2 [C_{12} W_C(r) \\ &\quad + S_{12}(\hat{r}) W_T(r)], \end{aligned} \tag{60}$$

$$\begin{aligned}\langle S_1 \bar{S}_2 | V_{\rm F}^{(0)}(\vec{r}) | S_1' \bar{S}_2' \rangle &= -R_1 \bar{R}_2 \vec{I}_1 \cdot \vec{I}_2 \frac{g_2^2}{6 f_\pi^2} C_{12} \delta^3(\vec{r}) + R_1 \bar{R}_2 \vec{I}_1 \cdot \vec{I}_2 [C_{12} W_C(r) \\ &\quad + S_{12}(\hat{r}) W_T(r)], \end{aligned} \tag{61}$$

where C_{12} and S_{12} are the spin-spin and tensor operators, defined as

$$C_{12} = \vec{a}_1 \cdot \vec{a}_2, \tag{62}$$

$$S_{12}(\hat{r}) = 3 \vec{a}_1 \cdot \hat{r} \vec{a}_2 \cdot \hat{r} - \vec{a}_1 \cdot \vec{a}_2. \tag{63}$$

The OPE potential contains a Dirac-delta contribution which can be reabsorbed into the contact-range potential if one wishes to. The spin-spin and tensor pieces of the potential W_C and W_T can be written as

$$W_C = \frac{g_i^2 \mu_\pi^3}{24\pi f_\pi^2} \frac{e^{-\mu_\pi r}}{\mu_\pi r}, \tag{64}$$

$$W_T = \frac{g_i^2 \mu_\pi^3}{24\pi f_\pi^2} \frac{e^{-\mu_\pi r}}{\mu_\pi r} \left(1 + \frac{3}{\mu_\pi r} + \frac{3}{(\mu_\pi r)^2}\right), \tag{65}$$

where $g_i = g_2$ or g_3 depending on the case and μ_π is the effective pion mass for the channel under consideration. The spin-spin piece of the OPE potential is often referred to as "central" OPE, a naming convention that often appears in nuclear physics for historical reasons and which permeates the notation W_C and W_T. *Central* is used in opposition to *tensor* to convey the idea that the central piece carries no orbital angular momentum (while the tensor piece carries two units of orbital angular momentum). The term "central OPE" is indeed convenient and we will use it in what follows (instead of the more accurate spin-spin OPE). We notice that the OPE potential also contains a contact-range contribution, which is mostly harmless: it can be reabsorbed into the EFT contact-range contribution to the potential by a redefinition of the couplings. Hence it can be simply ignored.

2. Partial wave projection of the OPE potential

We consider now the projection of the coordinate space potential into the partial wave basis. For that we work with baryon-antibaryon states with well-defined total angular momentum and parity J^P. If the total strangeness of the baryon-antibaryon state is zero, we will consider states with well-defined C-parity (for neutral systems) or G-parity (if

the system is not electrically neutral). Also, we will only consider states that contain an S-wave, as they are the more likely to form a bound state. If we use the spectroscopic notation $^{2S+1}L_J$ to denote the partial waves, we have the following combinations:

$$|B_Q\bar{B}_6(0^-)\rangle = \{^1S_0\}, \tag{66}$$

$$|B_Q\bar{B}_6(1^-)\rangle = \{^3S_1, ^3D_1\}, \tag{67}$$

$$|B_Q\bar{B}_6^*(1^-)\rangle = \{^3S_1, ^3D_1, ^5D_1\}, \tag{68}$$

$$|B_Q\bar{B}_6^*(2^-)\rangle = \{^3D_2, ^5S_2, ^5D_2, ^5G_2\}, \tag{69}$$

$$|B_6^*\bar{B}_6^*(0^-)\rangle = \{^1S_0, ^5D_0\}, \tag{70}$$

$$|B_6^*\bar{B}_6^*(1^-)\rangle = \{^3S_1, ^3D_1, ^7D_1, ^7G_1\}, \tag{71}$$

$$|B_6^*\bar{B}_6^*(2^-)\rangle = \{^1D_2, ^5S_2, ^5D_2, ^5G_2\}, \tag{72}$$

$$|B_6^*\bar{B}_6^*(3^-)\rangle = \{^3D_3, ^3G_3, ^7S_3, ^7D_3, ^7G_3, ^7I_3\}, \tag{73}$$

with $B_Q = B_{\bar{3}}$ or B_6. The calculation of the matrix elements is in general straightforward, where we refer to Appendix A for the details. The result of these calculations is that the C_{12} and $S_{12}(\hat{r})$ operators can be expressed as matrices, which we denote with the $\mathbf{C}_{12}$ and $\mathbf{S}_{12}$ notation. With this in mind for $r > 0$ we write the OPE potential as

$$V_{\rm F}^{(0)}(r) = R_1\bar{R}_2\vec{I}_1\cdot\vec{I}_2[\mathbf{C}_{12}W_C(r) + \mathbf{S}_{12}W_T(r)], \tag{74}$$

where the dimension of the matrices is set by the number of partial waves. The explicit matrices that apply in each case can be found in Appendix A, where it is also explained how they are calculated.

IV. HOW TO COUNT THE ONE PION EXCHANGE POTENTIAL

The LO EFT heavy baryon-antibaryon potential can in principle contain a contact- and a finite-range piece, where the latter is the well-known OPE potential. While there is no *a priori* way to determine if the contact-range potential is perturbative, this is not the case for the OPE potential where there exists a series of theoretical developments to evaluate its strength. In this section we will check how these ideas apply to the central and tensor pieces of the OPE potential. Before starting the discussion it is important to stress that we make a very explicit distinction between iterated OPE (or reducible multipion exchange) and irreducible multipion exchanges. The former is merely the outcome of iterating the EFT potential within the Schrödinger or Lippmann-Schwinger equations while the latter is a genuine contribution to the EFT potential, though a subleading one: the lowest order two pion exchange irreducible diagrams enter at order Q^2 in the chiral expansion.

A. The central potential

The perturbative nature of the central piece of OPE can be determined from the comparison of tree-level versus once-iterated central OPE, i.e., V and VG_0V in operator form. This type of comparison was made in Ref. [54] in the context of nucleon-nucleon scattering.[7] Here we are merely adapting it to the particular case of the heavy baryon-antibaryon system. The ratio of iterated vs tree-level OPE can be expressed as a ratio of scales,

$$\frac{\langle p|VG_0V|p\rangle}{\langle p|V|p\rangle} = \frac{Q}{\Lambda_C}, \tag{75}$$

where Q is a light scale (either the external momentum p or the pion mass m_π) and Λ_C is a scale that characterizes central OPE. The evaluation of this ratio at $p = 0$ leaves the pion mass as the only light scale left, in which case we obtain the following value for the central scale:

$$\Lambda_C = \frac{1}{|\sigma\tau|}\frac{24\pi f_\pi^2}{\mu|R_1\bar{R}_2|g_i^2}, \tag{76}$$

with μ the reduced mass of the system, σ and τ the evaluation of the spin and isospin operators corresponding to the particular case under consideration and where R_1 and $\bar{R}_2$ can be found in Table IV. For the charm and bottom sectors the values are, respectively,

$$\Lambda_C(Q = c) = \frac{1060\ \text{MeV}}{|\sigma\tau||R_1\bar{R}_2|g_i^2}, \tag{77}$$

$$\Lambda_C(Q = b) = \frac{450\ \text{MeV}}{|\sigma\tau||R_1\bar{R}_2|g_i^2}, \tag{78}$$

which depend on the value of the couplings g_2 and g_3.

The discussion about the values of the axial couplings, and in particular g_2, is important because it can change the value of Λ_C by a large factor. For the $T\bar{S}$ and $S\bar{S}$ molecules, the value of Λ_C in the charm sector is

$$\Lambda_C^{T\bar{S}}(Q = c) \sim \frac{1120^{+100}_{-40}\ \text{MeV}}{|\sigma\tau||R_1\bar{R}_2|}, \tag{79}$$

$$\Lambda_C^{S\bar{S}}(Q = c) \sim \frac{(560 - 1500)\ \text{MeV}}{|\sigma\tau||R_1\bar{R}_2|}, \tag{80}$$

where $\Lambda_C^{S\bar{S}}$ can change almost by a factor of 3 owing to the uncertainty of g_2 (notice that instead of a number with an

[7]Recently a more sophisticated method for determining the perturbativeness of OPE has been developed in Ref. [55] for peripheral waves with $L \geq 1$. Unfortunately it has not been extended yet to S-waves.

TABLE V. The central scale Λ_C (in units of MeV) for a few selected heavy baryon-antibaryon molecules. For momenta above this scale, $p > \Lambda_C$, the central force becomes nonperturbative. The scale Λ_C is inversely proportional to $\sigma\tau$, reaching its minimum for the channels with the lowest total spin and isospin and growing quickly for other configurations. The selection includes the heavy baryon-antibaryon states for which $\Lambda_C < 0.5$ GeV, most of which are of the $\Sigma_Q^{(*)}\bar{\Sigma}_Q^{(*)}$ type. In addition we include the $\Xi_Q^{(\prime/*)}\bar{\Xi}_Q^{(\prime/*)}$ molecule for which the central force is strongest and the antitriplet-sextet molecules. The uncertainty in the antitriplet-sextet case comes from the axial coupling, which is taken to be $g_3 = 0.973^{+0.019}_{-0.042}$ in the charm sector [50] and $g_3 = 0.71 \pm 0.13$ in the bottom one [53]. For the sextet-sextet case in the charm sector, the axial coupling is not well determined and we take it in the range $|g_2| \sim 0.84$–1.38, while in the bottom sector we have $g_2 = -0.84 \pm 0.20$ [53]. For comparison, in the deuteron channel of the two-nucleon system, the central scale is $\Lambda_C \simeq 590$ MeV.

Channel	I	Sign	Λ_C	Channel	I	Sign	Λ_C
$\Xi_c\bar{\Xi}_c'(0^{-\pm})$	0	$\mp$	720^{+70}_{-30}	$\Xi_b\bar{\Xi}_b'(0^{-\pm})$	0	$\mp$	580^{+290}_{-170}
$\Lambda_c\bar{\Sigma}_c(0^{-\pm})$	1	$\pm$	580^{+50}_{-20}	$\Lambda_b\bar{\Sigma}_b(0^{-\pm})$	1	$\pm$	450^{+220}_{-130}
$\Xi_c'\bar{\Xi}_c'(0^{-+})$	0	$-$	530–1420	$\Xi_b'\bar{\Xi}_b'(0^{-+})$	0	$-$	620^{+450}_{-210}
$\Sigma_c\bar{\Sigma}_c(0^{-+})$	0	$-$	210–560	$\Sigma_b\bar{\Sigma}_b(0^{-+})$	0	$-$	240^{+170}_{-80}
$\Xi_c^*\bar{\Xi}_c'(1^{-+})$	0	$-$	580–1560	$\Xi_b^*\bar{\Xi}_b'(1^{-+})$	0	$-$	680^{+490}_{-230}
$\Sigma_c^*\bar{\Sigma}_c(1^{-+})$	0	$-$	230–610	$\Sigma_b^*\bar{\Sigma}_b(1^{-+})$	0	$-$	260^{+190}_{-90}
$\Sigma_c^*\bar{\Sigma}_c(1^{--})$	0	$-$	280–750	$\Sigma_b^*\bar{\Sigma}_b(1^{--})$	0	$-$	320^{+230}_{-110}
$\Sigma_c^*\bar{\Sigma}_c(2^{--})$	0	$+$	280–750	$\Sigma_b^*\bar{\Sigma}_b(2^{--})$	0	$+$	320^{+230}_{-110}
$\Xi_c^*\bar{\Xi}_c^*(0^{-+})$	0	$-$	410–1100	$\Xi_b^*\bar{\Xi}_b^*(0^{-+})$	0	$-$	490^{+350}_{-170}
$\Sigma_c^*\bar{\Sigma}_c^*(0^{-+})$	0	$-$	160–440	$\Sigma_b^*\bar{\Sigma}_b^*(0^{-+})$	0	$-$	190^{+140}_{-70}
$\Sigma_c^*\bar{\Sigma}_c^*(1^{--})$	0	$-$	220–590	$\Sigma_b^*\bar{\Sigma}_b^*(1^{--})$	0	$-$	260^{+190}_{-90}
$\Sigma_c^*\bar{\Sigma}_c^*(3^{--})$	0	$+$	270–740	$\Sigma_b^*\bar{\Sigma}_b^*(3^{--})$	0	$+$	320^{+230}_{-110}

error, we have simply indicated a range of possible values). In the bottom sector it is instead more advisable to use the lattice QCD determination for g_2 and g_3, leading to

$$\Lambda_C^{T\bar{S}}(Q = b) \sim \frac{900^{+440}_{-260}\ \text{MeV}}{|\sigma\tau||R_1\bar{R}_2|}, \tag{81}$$

$$\Lambda_C^{S\bar{S}}(Q = b) \sim \frac{660^{+440}_{-220}\ \text{MeV}}{|\sigma\tau||R_1\bar{R}_2|}. \tag{82}$$

The previous values have to be combined with the $|\sigma\tau||R_1\bar{R}_2|$ factor. The maximum value of this factor happens for the channels with lowest spin and isospin. In Table V we list the scale Λ_C for a few representative heavy baryon-antibaryon molecules. In general $\Lambda_C \sim 0.5$ GeV (if not harder) in most cases, which means that we expect central OPE to be perturbative. The exceptions are the isoscalar 0^{-+} $\Sigma_Q\bar{\Sigma}_Q$ and 0^{-+}, 1^{--} $\Sigma_Q^*\bar{\Sigma}_Q^*$ molecules, at least in the bottom sector. In the charm sector the scale Λ_C varies considerably as a consequence of the uncertainty of the axial coupling g_2. In particular if the absolute value of the axial coupling $|g_2|$ is on the high end, i.e., the value $g_2 = -1.38$ deduced from the quark model, central OPE will be important for certain molecules in the hidden charm sector. In the bottom sector the situation is more clear: central OPE will be nonperturbative for the aforementioned $\Sigma_Q\bar{\Sigma}_Q$ and $\Sigma_Q^*\bar{\Sigma}_Q^*$ molecules. Finally for having a comparison with a well-known state, we mention that the central scale for OPE in the two-nucleon system is $\Lambda_C \simeq 590$ MeV.

B. The tensor potential

The tensor piece of the OPE potential requires a more involved analysis. A direct comparison of V and VG_0V is not possible. The reason is that the iteration of the tensor piece of OPE diverges; see, for instance, Refs. [32,55] for a detailed explanation. Thus we must resort to a method that does not involve the direct evaluation of the iterated tensor OPE.

The type of power-law behavior of the tensor OPE potential is analogous to the behavior of a few physical systems studied in atomic physics. The potential between two dipoles is of the $1/r^3$ type, just like the tensor force. The failure of standard perturbation theory for these systems is well known in atomic physics, where alternative techniques have been developed to deal with this type of potential. The work of Cavagnero [56] explains that the divergences of perturbation theory in these types of systems is similar to the role of *secular* perturbations in classical mechanics, i.e., a type of perturbation that is small at short timescales but ends up diverging at large timescales. The solution is to redefine (or, loosely speaking, *renormalize*[8]) some quantity in order to obtain a finite result again. For the perturbative series of the $1/r^3$ potentials, the quantity we renormalize is the angular momentum. The zeroth order term in the perturbative expansion of the wave function is now

$$\Psi_l^{(0)}(r;k) = \frac{J_{\nu(ka_3)}(kr)}{\sqrt{r}}, \tag{83}$$

instead of the standard $\frac{J_{l+1/2}(kr)}{\sqrt{r}}$, where $J_\nu(z)$ refers to the Bessel function of order ν. In the expression above, ν is the *renormalized* angular momentum, which happens to be a function of the momentum k and a length scale a_3 that is related to the strength of the potential (it will be defined later). The secular series is built not only by adding higher order terms but also by making $\nu(x)$ depend on $\kappa = ka_3$. If

[8]We simply adopt the terminology in use in the field of atomic physics for these redefinitions in secular perturbation theory, though it does not exactly correspond with the standard meaning of renormalization.

we switch off the potential and take $ka_3 = 0$, we have $\nu(0) = l + \frac{1}{2}$ and we recover the free wave function. For small enough values of κ we expect $\nu(\kappa)$ to be expansible in powers of x, i.e., to be perturbative. By reexpanding the secular series and the renormalized angular momentum we can recover the original perturbative series. However, the interesting feature of the series above is that we can determine the values of κ for which $\nu(\kappa)$ is analytic. When $\nu(\kappa)$ is not analytic, it does not admit a power series in κ anymore. This in turn means that there is no way to rearrange the secular series into the standard perturbative series, leading to its failure.

For the $1/r^3$ potential, which is equivalent to the tensor force for distances $m_\pi r < 1$, the secular series has been studied in detail by Gao [57] for the uncoupled channel case. Birse [45] extended the previous techniques for the coupled channel case and particularized them for the nucleon-nucleon system. In a previous publication by one of the authors [32], the analysis of Birse was applied to the heavy meson-antimeson system. In this work we extend it to the heavy baryon-antibaryon system.

We will consider the tensor force in the limit $m_\pi \to 0$, for which the OPE potential can be written as

$$2\mu \mathbf{V}(r) = \frac{a_3}{r^3}\mathbf{S}_j, \tag{84}$$

where the potential is a matrix in the coupled channel space and $\mathbf{S}_j$ is the tensor operator (in matrix form, as written in Sec. III D), with j referring to the total angular momentum. We have that μ is the reduced mass of the heavy baryon-antibaryon system and a_3 is the length scale that determines the strength of the tensor piece of the potential. The potential in this limit is amenable to the secular perturbative series developed in Refs. [32,45,57]. The corrections stemming from the finite value of m_π were considered in Ref. [32] and will be discussed later on in this section.

C. The renormalized angular momentum

Now we explain how the secular perturbation theory looks like and most importantly, how to calculate the renormalized angular momenta ν. We begin by writing the reduced Schrödinger equation in coupled channels (the uncoupled channel can be found in Ref. [32]) for the particular case of a pure $1/r^3$ potential,

$$-\mathbf{u}''_{k,j} + \left[\mathbf{S}_j \frac{a_3}{r^3} + \frac{\mathbf{L}_j^2}{r^2}\right]\mathbf{u}_{k,j}(r) = k^2 \mathbf{u}_{k,j}(r), \tag{85}$$

where we are considering N angular momentum channels. Notice that we have taken the chiral limit $m_\pi \to 0$, which means that only the tensor piece of the OPE potential survives; see Eq. (84). In the equation above, $\mathbf{S}_j$ is the tensor operator matrix, while $\mathbf{L}_j$ is a diagonal matrix representing the angular momentum operator $\vec{L}^2$:

$$\mathbf{L}_j^2 = \mathrm{diag}(l_1(l_1+1), \ldots, l_N(l_N+1)). \tag{86}$$

The reduced wave function $\mathbf{u}_{k,j}$ is an $N \times N$ matrix, where column j represents a solution that behaves as a free wave with angular momentum l_j when we take $a_3 \to 0$. The solution of the Schrödinger equation is a linear combination of the functions $\boldsymbol{\xi}$ and $\boldsymbol{\eta}$:

$$\mathbf{u}_{k,j}(r) = \sum_{\{l_j\}} [\alpha_{l_j} \boldsymbol{\xi}_{l_j}(r;k) + \beta_{l_j} \boldsymbol{\eta}_{l_j}(r;k)], \tag{87}$$

where we sum over the possible values of the angular momenta and with $\boldsymbol{\xi}$ and $\boldsymbol{\eta}$ N-component vectors that can be written as sums of Bessel functions:

$$\boldsymbol{\xi}_{l_j}(r;k) = \sum_{m=-\infty}^{\infty} \boldsymbol{b}_m(\nu_{l_j}) \sqrt{r} J_{m+\nu_{l_j}}(kr), \tag{88}$$

$$\boldsymbol{\eta}_{l_j}(r;k) = \sum_{m=-\infty}^{\infty} (-1)^m \boldsymbol{b}_{-m}(\nu_{l_j}) \sqrt{r} J_{-m-\nu_{l_j}}(kr), \tag{89}$$

where the ν_{l_j}'s are functions of $\kappa = ka_3$, i.e., $\nu_{l_j} = \nu_{l_j}(\kappa)$. The ν_{l_j}'s are the *renormalized* angular momenta that we previously introduced in Eq. (83). In turn the expansion of the reduced wave functions $\boldsymbol{\xi}$ and $\boldsymbol{\eta}$ in Eqs. (88) and (89) is simply the extension of Eq. (83) to arbitrary orders.[9] We have N different solutions for $\boldsymbol{\xi}$ and $\boldsymbol{\eta}$ that we have labeled with the subscript l_j to indicate that for $\kappa = 0$ they behave as a free wave of angular momentum l_j. The recursive relation from which one can compute $\boldsymbol{b}_m(\nu_{l_j})$ can be found in Ref. [45] but is of no concern if we are only interested in the ν_{l_j}'s. For $\kappa = 0$, only the $\boldsymbol{b}_m(\nu_{l_j})$ coefficient for $m = 0$ survives.

The renormalized angular momenta $\nu_{l_i} = \nu_{l_i}(\kappa)$ (with $\kappa = ka_3$) can be calculated as follows. First we define the following $N \times N$ matrix:

$$\mathbf{F}_j(\nu,\kappa) \equiv \mathbf{f}_j(\nu) - \frac{\kappa^2}{\nu}[\mathbf{R}_1(\nu) - \mathbf{R}_1(-\nu)], \tag{90}$$

which depends on two other matrices, $\mathbf{f}_j(\nu)$ and $\mathbf{R}_1(\nu)$; $\mathbf{f}_j(\nu)$ is a diagonal matrix defined as

$$\frac{\mathbf{f}_j(\nu)}{2\nu} = \mathrm{diag}\left(\nu^2 - \left(l_1 + \frac{1}{2}\right)^2, \ldots, \nu^2 - \left(l_N + \frac{1}{2}\right)^2\right), \tag{91}$$

while $\mathbf{R}_1(\nu)$ is given by the recursive relation

$$\mathbf{R}_n(\nu) = [\mathbf{f}_j(n+\nu) - \kappa^2 \mathbf{S}_j \mathbf{R}_{n+1}(\nu) \mathbf{S}_j]^{-1}, \tag{92}$$

[9]We note that Eq. (83) is written in terms of the standard wave function, while Eqs. (88) and (89) use the reduced wave function instead.

which can be accurately solved with between 20 and 30 iterations [45] (that is, one takes $\mathbf{R}_N = 0$ for large enough N, e.g., 20–30, and solves the recursion relation backwards). Once we have the matrix F_j, we obtain $\nu_{l_i} = \nu_{l_i}(\kappa)$ by finding the zeros of

$$\det\left(\mathbf{F}_j(\nu,\kappa)\right) = 0. \tag{93}$$

This equation admits N solutions, one for each value of the angular momentum. For $\kappa = 0$ these solutions behave as

$$\nu_{l_i}(\kappa = 0) = l_i + \frac{1}{2}, \tag{94}$$

with $i = 1, \ldots, N$. As κ increases $\nu_{l_i}(\kappa)$ moves slowly downwards. Once we reach $\nu_{l_i} = l_i$ at the critical value $\kappa = \kappa_c$, we have that ν_{l_i} splits into the complex conjugate solutions $\nu_{l_i}(\kappa) = l_i \pm i\rho_{l_i}(\kappa)$. This is a nonanalyticity which marks the point above which $\nu_{l_i}(\kappa)$ cannot be expressed as a perturbative series. This in turn defines κ_c, the critical value of κ for which there is a $\nu_{l_i}(\kappa)$ that becomes nonanalytic in κ. Usually the first ν_{l_j} to split is the one that corresponds to the smallest angular momentum and also the one that determines the breakdown of the perturbative series.

For computing the critical momenta we need first the matrix elements of the tensor operator in the channel under consideration. For the $B_{\bar{3}}\bar{B}_{\bar{3}}$, $B_6\bar{B}_6$, and $B_6^*\bar{B}_6^*$ molecules this is trivial: first we take the tensor force matrix $\mathbf{S}_j$, which can be found in Eq. (138) and Eqs. (A147)–(A150) of Appendix A, and then we plug this matrix into Eq. (92), from which finally we solve Eq. (93) to obtain κ_c. For the $B_3\bar{B}_6^*$ molecules the procedure is the same, with the tensor force matrices defined in Eqs. (A167) and (A168). The $B_6\bar{B}_6^*$ molecules are the most complicated because they contain both a direct and exchange tensor operators, which mediate the $B_6\bar{B}_6^* \to B_6\bar{B}_6^*$ and $B_6\bar{B}_6^* \to B_6^*\bar{B}_6$ potential, respectively. In addition the effective pion masses are different for the direct and exchange tensor operators. Here we ignore this effect: in the present calculation we are making the approximation that HQSS is exact and therefore there is no mass splitting between the B_6 and B_6^* heavy baryons. However, the length scale a_3 is different for the direct and exchange operators, i.e.,

$$2\mu\mathbf{V}_{B_6\bar{B}_6^*}(r) = \frac{a_3^D}{r^3}\mathbf{S}_j^D + \frac{a_3^E}{r^3}\mathbf{S}_j^E. \tag{95}$$

It happens that both scales are proportional to each other,

$$a_3^E = -\frac{3}{4}a_3^D, \tag{96}$$

as can be checked by inspecting the coupled-channel form of the potential in Eq. (A106) from Appendix A. Thus in the $B_6\bar{B}_6^*$ system we will be computing the critical values of the matrix

$$\mathbf{S}_j = \mathbf{S}_j^D - \frac{3}{4}\mathbf{S}_j^E. \tag{97}$$

TABLE VI. Reduced critical momenta κ_c for the different S-wave heavy baryon-antibaryon systems $B'\bar{B}$.

Channel	κ_c
$B_3\bar{B}_6(0^-)/B_6\bar{B}_6(0^-)$	…
$B_3\bar{B}_6(1^-)/B_6\bar{B}_6(1^-)$	0.6835
$B_3\bar{B}_6^*(1^-)$	1.412
$B_3\bar{B}_6^*(2^-)$	1.934
$B_6\bar{B}_6^*(1^{-+})$	0.8533
$B_6\bar{B}_6^*(1^{--})$	0.7264
$B_6\bar{B}_6^*(2^{-+})$	0.5784
$B_6\bar{B}_6^*(2^{--})$	0.6998
$B_6^*\bar{B}_6^*(0^{-+})$	0.6378
$B_6^*\bar{B}_6^*(1^{--})$	0.6674
$B_6^*\bar{B}_6^*(2^{-+})$	0.6833
$B_6^*\bar{B}_6^*(3^{--})$	0.5922

D. Critical momenta

The critical κ_c values for which the convergence criterion fails are listed in Table VI for the different possible heavy baryon-antibaryon states that contain an S-wave. The previous values have been obtained under the assumption that the effective pion mass can be taken to be zero. The effect of finite pion mass was considered in Ref. [32], where it was found that it increases the range of momenta where the tensor part of OPE is perturbative by the following factor,

$$\kappa_c(m_\pi) = \kappa_c e^{+m_\pi R_c}, \tag{98}$$

where R_c is the radius below which we do not expect the OPE potential to be valid. The value of this radius is rather ambiguous. In Ref. [32] the estimation $R_c = 0.5$–0.8 fm was proposed, yielding

$$\kappa_c(m_\pi) \simeq 1.5\kappa_c. \tag{99}$$

Higher values might be more appropriate indeed, but here we will stick to this value.

To obtain the critical momenta we multiply $\kappa_c(m_\pi)$ by the relation $k_c = \kappa_c(m_\pi)/|a_3|$, where a_3 is the tensor length scale. If we match the $m_\pi r \to 0$ limit of the OPE potential to the $1/r^3$ form we have used to derive κ_c, we find that

$$|a_3| = |R_1\bar{R}_2\tau|\frac{\mu g_i^2}{4\pi f_\pi^2}, \tag{100}$$

TABLE VII. The tensor scale Λ_T (in units of MeV) for a series of heavy baryon-antibaryon molecules. For momenta above this scale, $p > \Lambda_T$, the tensor force becomes nonperturbative. The tensor scale depends on the pion mass: $\Lambda_T(0)$ and $\Lambda_T(m_\pi)$ represent the value in the chiral limit and physical pion mass, respectively. The values of Λ_T are shown for the antitriplet-sextet and sextet-sextet molecules. In the latter case we concentrate on the isoscalar $\Sigma_Q^{(*)}\bar{\Sigma}_Q^{(*)}$ molecules, for which pion exchanges are stronger (for the isovector case, the value of Λ_T is twice that of the isoscalar case). For the $\Xi_Q^{(\prime/*)}\bar{\Xi}_Q^{(\prime/*)}$ molecules we only show the channel in which the tensor force is strongest. For comparison purposes, in the deuteron channel of the two-nucleon system the tensor scale is $\Lambda_T(0) = 66$ MeV and $\Lambda_T(m_\pi) = 99$ MeV, respectively.

Channel	I	$\Lambda_T(0)$	$\Lambda_T(m_\pi)$	Channel	I	$\Lambda_T(0)$	$\Lambda_T(m_\pi)$
$\Xi_c\bar{\Xi}_c'(1^{-\pm})$	0	246^{+23}_{-10}	368^{+34}_{-14}	$\Xi_b\bar{\Xi}_b'(1^{-\pm})$	0	200^{+100}_{-60}	300^{+150}_{-90}
$\Lambda_c\bar{\Sigma}_c(1^{-\pm})$	1	196^{+18}_{-7}	295^{+27}_{-11}	$\Lambda_b\bar{\Sigma}_b(1^{-\pm})$	1	150^{+80}_{-40}	230^{+110}_{-70}
$\Xi_c'\bar{\Xi}_c'(1^{--})$	0	180–490	270–740	$\Xi_b'\bar{\Xi}_b'(1^{--})$	0	210^{+160}_{-70}	320^{+230}_{-110}
$\Sigma_c\bar{\Sigma}_c(1^{--})$	0	70–190	110–290	$\Sigma_b\bar{\Sigma}_b(1^{--})$	0	80^{+60}_{-30}	120^{+90}_{-40}
$\Xi_c^*\bar{\Xi}_c'(2^{-+})$	0	150–410	230–610	$\Xi_b^*\bar{\Xi}_b'(2^{-+})$	0	180^{+130}_{-60}	270^{+200}_{-90}
$\Sigma_c^*\bar{\Sigma}_c(1^{-+})$	0	90–240	130–350	$\Sigma_b^*\bar{\Sigma}_b(1^{-+})$	0	100^{+80}_{-30}	150^{+110}_{-50}
$\Sigma_c^*\bar{\Sigma}_c(1^{--})$	0	70–200	110–300	$\Sigma_b^*\bar{\Sigma}_b(1^{--})$	0	90^{+60}_{-30}	130^{+90}_{-40}
$\Sigma_c^*\bar{\Sigma}_c(2^{-+})$	0	60–160	90–240	$\Sigma_b^*\bar{\Sigma}_b(2^{-+})$	0	70^{+50}_{-20}	100^{+80}_{-30}
$\Sigma_c^*\bar{\Sigma}_c(2^{--})$	0	70–190	110–290	$\Sigma_b^*\bar{\Sigma}_b(2^{--})$	0	80^{+60}_{-30}	130^{+90}_{-50}
$\Xi_c^*\bar{\Xi}_c'(3^{--})$	0	160–420	230–630	$\Xi_b^*\bar{\Xi}_b'(3^{--})$	0	190^{+130}_{-70}	280^{+200}_{-100}
$\Sigma_c^*\bar{\Sigma}_c^*(0^{-+})$	0	60–170	100–260	$\Sigma_b^*\bar{\Sigma}_b^*(0^{-+})$	0	80^{+50}_{-30}	110^{+80}_{-40}
$\Sigma_c^*\bar{\Sigma}_c^*(1^{--})$	0	70–180	100–270	$\Sigma_b^*\bar{\Sigma}_b^*(1^{--})$	0	80^{+60}_{-30}	120^{+90}_{-40}
$\Sigma_c^*\bar{\Sigma}_c^*(2^{-+})$	0	70–190	100–280	$\Sigma_b^*\bar{\Sigma}_b^*(2^{-+})$	0	80^{+60}_{-30}	120^{+90}_{-40}
$\Sigma_c^*\bar{\Sigma}_c^*(3^{--})$	0	60–160	90–240	$\Sigma_b^*\bar{\Sigma}_b^*(3^{--})$	0	70^{+50}_{-20}	100^{+80}_{-40}

where $\tau = \vec{T}_1 \cdot \vec{T}_2$ and $g_i = g_2$, g_3 depending on whether we are considering the $S\bar{S}$ or the $T\bar{S}$ potential. The factors R_1 and $\bar{R}_2$ and the proper isospin operator to use can be checked in Table IV. For the $B_6\bar{B}_6^*$ case we will use the factors corresponding to the direct channels, i.e., $B_6 \to B_6$ and $B_6^* \to B_6^*$, in agreement with the convention that we have used in Eq. (97) for writing their tensor matrices. From the previous, we can define the tensor scale as

$$\Lambda_T(m_\pi) = \frac{\kappa(m_\pi)}{|a_3|} = \frac{\kappa(m_\pi)}{|R_1\bar{R}_2\tau|}\frac{4\pi f_\pi^2}{\mu g_i^2}, \tag{101}$$

which is useful because it allows a direct comparison with the central scale Λ_C that we defined in Eq. (76). If we particularize for the $T\bar{S}$ and $S\bar{S}$ in the charm sector,

$$\Lambda_T^{T\bar{S}}(m_\pi, Q = c) \simeq \kappa_c(m_\pi)\frac{186^{+18}_{-8}\ \text{MeV}}{|R_1\bar{R}_2\tau|}, \tag{102}$$

$$\Lambda_3^{S\bar{S}}(m_\pi, Q = c) \simeq \kappa_c(m_\pi)\frac{90 - 250\ \text{MeV}}{|R_1\bar{R}_2\tau|}, \tag{103}$$

while for the bottom sector we obtain

$$\Lambda_T^{T\bar{S}}(m_\pi, Q = b) \simeq \kappa_c(m_\pi)\frac{140^{+80}_{-40}\ \text{MeV}}{|R_1\bar{R}_2\tau|}, \tag{104}$$

$$\Lambda_T^{S\bar{S}}(m_\pi, Q = b) \simeq \kappa_c(m_\pi)\frac{100^{+80}_{-40}\ \text{MeV}}{|R_1\bar{R}_2\tau|}, \tag{105}$$

where we have used the lattice QCD values of g_2 and g_3 [53]. These scales look rather soft at first sight but the factors R_1, $\bar{R}_2$, and τ will increase the values of Λ_T considerably in most cases. A few representative values of Λ_T are compiled in Table VII both for the chiral limit and the physical pion mass. In general we find that tensor OPE is considerably stronger than central OPE. For the $\Xi_Q\bar{\Xi}_Q'$ and $\Lambda_Q\bar{\Sigma}_Q$ molecules we find that Λ_T is markedly softer than Λ_C, and in the bottom sector the tensor force probably requires a nonperturbative treatment. For the isoscalar $\Sigma_Q\bar{\Sigma}_Q$, $\Sigma_Q^*\bar{\Sigma}_Q$, $\Sigma_Q^*\bar{\Sigma}_Q^*$ molecules the tensor scale Λ_T is moderately soft, particularly in the bottom sector. We notice that the same comments are also valid in the two-nucleon system, in which $\Lambda_T(0) = 66$ MeV in the chiral limit [45] and $\Lambda(m_\pi) = 99$ MeV for the physical pion mass.

V. POWER COUNTING FOR HEAVY BARYON MOLECULES

In this section we discuss the different possible power counting rules for the heavy baryon-antibaryon states. We are interested in the case where there are bound states. This excludes NDA, for which

TABLE VIII. Possible power countings for the heavy baryon-antibaryon system: NDA and the three scenarios (a), (b), (c) that we consider in Sec. V. Q refers to the soft scales in each power counting, which include the momenta p of the heavy baryons and pions, the mass m_π of the pions, the binding momentum $\sqrt{2\mu B_2}$ of a heavy baryon-antibaryon bound state (with μ the reduced mass and B_2 the binding energy) and the central and tensor scales Λ_C and Λ_T defined in Eqs. (76) and (101) and listed in Tables V and VII for a series of heavy baryon-antibaryon systems. The LO and NLO columns indicate the counting Q^ν of the leading order and first subleading correction. In the $V^{\rm LO}$ and $V^{\rm NLO}$ columns we write the contributions to the EFT potential in each case. C and $D(p^2+p'^2)$ refer to a contact-range potential without derivatives and with two derivatives of the heavy baryon field, respectively. $V_{\rm OPE}$ is the OPE potential, $V_{\rm OPE(C)}$ its central piece, and $V_{\rm OPE(T)}$ its tensor piece. Finally $V_{\rm TPE}$ refers to the two pion exchange potential (i.e., irreducible diagrams containing two pions), which we have not considered in this work.

Power counting	Q	LO	$V^{\rm LO}$	NLO	$V^{\rm NLO}$
NDA	p, m_π	Q^0	C, $V_{\rm OPE}$	Q^2	$D(p^2+p'^2)$, $V_{\rm TPE}$
(a)	p, m_π, $\sqrt{2\mu B_2}$	Q^{-1}	C	Q^0	$D(p^2+p'^2)$, $V_{\rm OPE}$
(b)	p, m_π, Λ_C	Q^{-1}	$V_{\rm OPE(C)}$	Q^0	C, $V_{\rm OPE(T)}$
(c)	p, m_π, Λ_T	Q^{-1}	C, $V_{\rm OPE}$	$Q^{3/2}$	$D(p^2+p'^2)$

$$V_C^{\rm LO}(\vec{q}) \sim Q^0, \qquad V_F^{\rm LO} \sim Q^0, \tag{106}$$

as this counting leads to purely perturbative heavy baryon-antibaryon interactions. The existence of bound states requires that at least one of the components of the potential is promoted to Q^{-1}; see the discussion in Sec. II B for details. There are different choices depending on which piece of the interaction is promoted. We will consider three scenarios:

(a) promotion of the contact terms,
(b) promotion of central OPE, and
(c) promotion of tensor OPE.

Each scenario represents a different binding mechanism:

(a) short range,
(b) long range, and
(c) a combination of both,

where we notice that (c) is not obvious but a consequence of the technicalities of power counting, as we will explain. We present an overview of these scenarios in Table VIII. But we stress that the discussion here will be theoretical: in the absence of experimental data it is not particularly useful to consider the subleading orders of the EFT expansion. The exploration in this section provides information about the theoretical uncertainties that are to be expected from a LO calculation in each scenario,

(a) (Q/M),
(b) (Q/M),
(c) $(Q/M)^{\frac{5}{2}}$,

where we will explain in detail how we obtain these uncertainties and also what is the general form of the first subleading corrections, which can actually be found in Table VIII. For a more in-depth discussion of the power counting of heavy meson-antimeson in particular and two-body systems in general we refer the reader to Refs. [32,44].

A. Counting with perturbative pions

The first possibility—scenario (a)—is that the binding mechanism for heavy baryon-antibaryon molecules is of a short-range nature. Within the EFT language this amounts to the promotion of the contact-range potential from Q^0 to Q^{-1}. Within this power counting, the leading order (LO $\equiv Q^{-1}$ in this case) potential will be composed of contact terms, while the next-to-leading order potential (NLO $\equiv Q^0$) will contain the OPE potential plus a few additional contact interactions:

$$V^{\rm LO} = V_C^{(-1)}, \tag{107}$$

$$V^{\rm NLO} = V_C^{(0)} + V_{\rm OPE}. \tag{108}$$

We do not have to promote all the possible contact interactions that we obtain from the heavy-light spin decomposition: in general a subset of it will be enough.

There is one important detail with this counting. If we consider the S-wave contact-range interactions in EFT, they admit the momentum expansion

$$\langle p'|V_C|p\rangle = C + D(p'^2+p^2) + \ldots, \tag{109}$$

where the dots denote couplings involving more derivatives of the baryon fields. Here we use C and D as a generic notation for the couplings of a contact-range potential with no derivatives (C) or with two derivatives (D). The naive expectation for the scaling of the C and D couplings is

$$C \sim \frac{1}{M^2}, \qquad D \sim \frac{1}{M^4}. \tag{110}$$

But if we promote the coupling C to LO, the coupling D must also be promoted [39–41]:

$$C \sim \frac{1}{MQ}, \qquad D \sim \frac{1}{M^2Q^2}. \tag{111}$$

As a consequence the ordering of the contact-range potential will be

$$\langle p'|V_C^{\rm LO}|p\rangle = C, \tag{112}$$

$$\langle p'|V_C^{\rm NLO}|p\rangle = D(p'^2+p^2). \tag{113}$$

That is, the NLO potential will contain a contact-range interaction with two derivatives on the baryon fields. As a consequence if we promote a particular C coupling to Q^{-1}, the corresponding derivative coupling with D will be promoted to Q^0. We notice that in this work we have not explicitly considered a contact-range potential with derivatives. The take-home message is that in this scenario the theoretical uncertainty of the calculations is Q/M because the first correction to a LO calculation is suppressed by one order in the EFT expansion.

B. Counting with nonperturbative central OPE

The second possibility is that the binding mechanism depends also on the attraction provided by the central OPE. We can distinguish two cases: (i) the binding depends on central OPE alone, i.e., scenario (b), and (ii) the binding depends on the interplay of the contact terms and central OPE, i.e., scenario (a + b).

In the first case—scenario (a)—we have a relatively simple power counting in which

$$V^{\rm LO} = V_{\rm OPE(C)}, \tag{114}$$

where OPE(C) means the central piece of OPE. The NLO potential contains the tensor OPE and the contact interactions

$$V^{\rm NLO} = V_{\rm OPE(T)} + V_{\rm C}^{(0)}, \tag{115}$$

where

$$\langle p'|V_C^{(0)}|p\rangle = C_0. \tag{116}$$

Contacts with $2n$ derivatives on the baryon fields will enter at order Q^{2n}. In this scenario the relative uncertainty of a LO calculation is Q/M because the first correction to the EFT potential enters at NLO.

The second case—scenario (a + b)—is identical to the power counting of scenario (a) except for the fact that we include OPE in the LO:

$$V^{\rm LO} = V_C^{\rm LO} + V_{\rm OPE(C)}, \tag{117}$$

$$V^{\rm NLO} = V_C^{\rm NLO} + V_{\rm OPE(T)}, \tag{118}$$

where $V_{\rm OPE(T)}$ is the tensor piece of OPE, while $V_C^{\rm LO}$ and $V_C^{\rm NLO}$ are the contact-range potentials of Eqs. (112) and (113). The uncertainty of the LO calculation is Q/M.

C. Counting with nonperturbative tensor OPE

The third possibility—scenario (c)—arises when tensor OPE is nonperturbative. This is the most involved of the three power countings considered. Tensor OPE is a singular potential, which means that it diverges as fast as (or faster than) $1/r^2$ for $r \to 0$. Singular potentials in general lead to nontrivial consequences in EFT [58–63]. The tensor force is not only singular, but also attractive for the case at hand: for an S-wave heavy baryon-antibaryon state that mixes with a D-wave, there is always a configuration for which the tensor force is attractive.[10] For attractive singular potentials short-range physics is enhanced: the nonperturbative treatment of attractive singular potentials requires the inclusion of a contact-range interaction at LO [60,61].

The application of these ideas for a heavy baryon-antibaryon S-wave molecule implies that a nonperturbative tensor force requires a nonperturbative contact potential. As a consequence, the LO potential will be

$$V^{\rm LO} = V_{\rm OPE} + V_C^{-1}, \tag{119}$$

with $V_C^{(-1)}$ the lowest order contact-range potential.[11] The counting of the contacts will be modified as follows [44,45]:

$$C \sim \frac{1}{MQ}, \qquad D \sim \frac{1}{M^{7/2}Q^{1/2}}, \tag{120}$$

or equivalently we can write

$$\langle p'|V_C^{(-1)}|p\rangle = C, \tag{121}$$

$$\langle p'|V_C^{(3/2)}|p\rangle = D(p'^2+p^2), \tag{122}$$

where the contacts with derivatives get promoted by half an order. Thus the theoretical uncertainty of a LO calculation is $(Q/M)^{5/2}$ (the first subleading correction, a derivative contact interaction, enters $Q^{5/2}$ orders after LO), which is considerably better than for the other scenarios.

The previous analysis is a simplification though: tensor forces mix channels with different orbital angular momentum, which might lead to complications in certain cases (in particular the power counting of contact interactions mixing partial waves). We have not addressed these problems here: they depend on the particular system under consideration and the aim of the present discussion is to provide

[10]This can be seen by inspecting the partial wave projection of the tensor operator S_{12}, which can be found in Appendix A. It happens that for these matrices there is always at least one positive and one negative eigenvalue.

[11]We have simply included the full OPE potential in LO because the addition of central OPE does not further modify the power counting induced by tensor OPE.

an overview of power counting rather than a detailed account.

VI. PREDICTING HEAVY BARYON MOLECULES

In this section we investigate the question of whether we can predict heavy baryon molecules. The answer to this question depends on which is the binding mechanism. If the binding mechanism is of a short-range nature, the prediction of bound states will rely on phenomenology. Within the EFT framework this is illustrated by the fact that the contact-range couplings are free parameters. If there is no preexisting experimental information about the heavy baryon-antibaryon system, we will have to determine the contact-range couplings by matching to a phenomenological model. Conversely if the binding mechanism is of a long-range nature, the prediction of bound states is possible within EFT. Examples are the $\Lambda_{c1}\bar{\Sigma}_c$ [29] and $DD^*_{s0}/D^*D^*_{s1}$ [64] systems, which interact via a long-range Yukawa potential that is strong enough to bind. This is not the standard situation though and more often than not we will need phenomenological input.

At this point it is interesting to notice the relation between power counting and the predictability of heavy baryon-antibaryon molecules. In Sec. V we proposed three power counting scenarios: (a), (b), and (c). Scenario (a) corresponds to a short-range binding mechanism, which requires phenomenological input. Scenario (b) corresponds to a long-range binding mechanism, which allows for EFT predictions. Finally scenario (c) is a mixture of short- and long-range binding, which in a few cases will lead to predictions. The heavy baryon-antibaryon system belongs to scenario (a) or (c) depending on the particular state and quantum numbers considered.

Theoretical studies of hadronic molecules have attributed the binding mechanism to either short- or long-range causes. In the pioneering work of Voloshin and Okun [1] it is the exchange of light mesons (π, σ, ρ, and ω) which generates heavy hadron molecules, i.e., a mixture of short- and long-range physics. Early speculations [2–5] often predicted binding from the OPE potential (long-range physics) alone. It is notable to mention that Ericson and Karl [4] indicated that hadronic molecules should be possible in the charm sector and that Törnqvist [5] predicted the existence of an isoscalar 1^{++} $D^*\bar{D}$ bound state. The experimental discovery of the $X(3872)$ a decade after [6] suggests that these theoretical speculations were on the right track. At this point we find it interesting to notice that a molecular $X(3872)$ also arises naturally from short-range physics [65]. Before the discovery of the $P_c(4450)$ by the LHCb [11], which is suspected (but not confirmed) to be a $\bar{D}^*\Sigma_c$ molecule [14,16–18], there were theoretical predictions of its existence too. The authors of Refs. [66,67] used contact-range interactions derived from vector meson exchange saturation to make quantitative predictions of an $I=\frac{1}{2}$, $J^P=\frac{3}{2}^-$ $\bar{D}^*\Sigma_c$ molecule (among others). Meanwhile the authors of Ref. [68] used the OPE potential instead to make qualitative predictions about probable hadronic molecules, including a possible $I=\frac{1}{2}$, $J^P=\frac{3}{2}^-$ $\bar{D}^*\Sigma_c$ molecule. Finally EFT and EFT-inspired works have explained the properties of shallow molecular states solely on the basis of short-range interactions [31,36,69], without making explicit assumptions about the binding mechanism.

In this section we will examine the short- and long-range binding mechanisms for heavy baryon-antibaryon molecules. The most obvious short-range mechanism is the saturation of the EFT contact-range couplings from scalar and vector meson exchange, while the most important long-range mechanism is the OPE potential. Now we will explain these binding mechanisms in detail.

A. Short-range binding dynamics

First we explore the short-range dynamics, in particular scalar and vector meson exchange. For taking this effect into account we saturate the contact-range couplings of the EFT with the exchange of a meson with mass m_S of the order of the hard scale of the EFT ($m_S \sim M$); see Ref. [70] for a detailed exposition of this idea. For this we expand the exchange potential V_S for momenta $\vec{q}^2 \ll m_S$ and match it with the expansion of the EFT contact-range potential

$$V_S(\vec{q}) = V_0 + V_2\vec{q}^2 + \ldots, \tag{123}$$

$$V_C(\vec{q}) = C + D\vec{q}^2 + \ldots, \tag{124}$$

from which we arrive to

$$C(\Lambda \sim m_S) \sim V_0 = V_S(|\vec{q}| = 0), \tag{125}$$

where Λ is the cutoff. Notice that we take $\Lambda \sim m_S$: this is because the saturation hypothesis is only expected to work if the cutoff is of the order of the mass of the exchange meson [70]. For a Yukawa-like meson exchange potential

$$V_S(\vec{q}) = \frac{g_S^2}{\vec{q}^2 + m_S^2}, \tag{126}$$

the saturated contact-range coupling is proportional to

$$C \propto \frac{g_S^2}{m_S^2}, \tag{127}$$

where the proportionality constant will depend on the details of the regularization process. This argument is independent of the nature of the exchanged meson; it only matters that the mass of this meson is of the order of the hard scale.

Next we calculate the scalar and vector meson exchange contribution to the saturation of the EFT coupling. We

TABLE IX. Contact-range coupling from saturation of vector and scalar meson exchange in units proportional to g_ρ^2/m_V^2 and $g_{\sigma qq}/m_\sigma^2$, with $g_\rho \simeq 2.9$ and $g_{\sigma qq} \simeq 3.4$. Scalar and vector meson exchange saturations of the spin-$\frac{3}{2}$ sextet heavy baryons (Σ_Q^*, Ξ_Q^*, Ω_Q^*) are identical to their spin-$\frac{1}{2}$ partners (Σ_Q, Ξ_Q, Ω_Q) and are not listed independently. The contributions to vector meson exchange are also listed separately as $C_V = C_\rho + C_\omega + C_\phi$. Though not listed, the saturation for the heavy baryon-baryon system can be obtained from the heavy baryon-antibaryon case by changing the sign of the ω and ϕ contributions. For comparison purposes we also include the NN (two-nucleon), $D^*\bar{D}$, and $\bar{D}^*\Sigma_c$ systems, which are related to the deuteron, the $X(3872)$, and the $P_c(4450)$, respectively.

System	Isospin	C_S	C_V	C_ρ	C_ω	C_ϕ
NN	0	−9	+6	−3	+9	0
NN	1	−9	+10	+1	+9	0
$D\bar{D}$	0	−1	−4	−3	−1	0
$D\bar{D}$	1	−1	0	+1	−1	0
$\Sigma_c\bar{D}$	$\frac{1}{2}$	−2	−2	−4	+2	0
$\Sigma_c\bar{D}$	$\frac{3}{2}$	−2	+4	+2	+2	0
$\Lambda_Q\bar{\Lambda}_Q$	0	−4	−4	0	−4	0
$\Xi_Q\bar{\Xi}_Q$	0	−1	−6	−3	−1	−2
$\Xi_Q\bar{\Xi}_Q$	1	−1	−2	+1	−1	−2
$\Xi'_Q\bar{\Xi}_Q$	0	−1	−6	−3	−1	−2
$\Xi'_Q\bar{\Xi}_Q$	1	−1	−2	+1	−1	−2
$\Sigma_c\bar{\Lambda}_Q$	1	−4	−4	0	−4	0
$\Omega_Q\bar{\Omega}_Q$	0	0	−8	0	0	−8
$\Xi_Q\bar{\Xi}_Q$	0	−1	−6	−3	−1	−2
$\Xi_Q\bar{\Xi}_Q$	1	−1	−2	+1	−1	−2
$\Sigma_Q\bar{\Sigma}_Q$	0	−4	−12	−8	−4	0
$\Sigma_Q\bar{\Sigma}_Q$	1	−4	−8	−4	−4	0
$\Sigma_Q\bar{\Sigma}_Q$	2	−4	0	+4	−4	0

begin by considering scalar meson exchange. The sigma meson exchange potential is

$$V_\sigma(\vec{q}) = -\frac{g_\sigma^2}{\vec{q}^2 + m_\sigma^2}, \tag{128}$$

with g_σ the sigma coupling. We can determine g_σ from the quark model, in which g_σ is simply proportional to the number of u and d quarks in the hadron. Here we take the sigma-nucleon-nucleon coupling as input, which in the nonlinear sigma model [71] is $g_{\sigma NN} = \sqrt{2}M_N/f_\pi \sim 10.2$, where M_N is the nucleon mass and f_π the pion decay constant. From this we have $g_\sigma = g_{\sigma NN}/3 \sim 3.4$ for Ξ_Q, Ξ'_Q, and Ξ_Q^* and $g_\sigma = 2g_{\sigma NN}/3 \sim 6.8$ for Λ_Q, Σ_Q, and Σ_Q^*. The contributions of the scalar meson to the saturation of the contact-range couplings are listed in Table IX.

We continue with the vector meson exchange potential, for which the starting point is the heavy baryon-vector-meson Lagrangian for the SSV and TTV vertices (where V represents the vector meson). If we consider interactions with no derivatives, which allow for saturation of the lowest order EFT couplings, we can write the following Lagrangians:

$$\mathcal{L}_{TTV} = \lambda_T \epsilon_{ikl}\epsilon_{jkm}\bar{T}_Q^l v_\mu (V^\mu)_j^i T_{Qm}, \tag{129}$$

$$\mathcal{L}_{SSV} = \lambda_S \bar{S}_{Q\nu ik} v_\mu (V^\mu)_j^i S_Q^{\nu jk}, \tag{130}$$

where the latin indices indicate the sum over the SU(3) components.[12] The vector meson nonet field is given by

$$V = \begin{pmatrix} \frac{\rho^0}{\sqrt{2}} + \frac{\omega^0}{\sqrt{2}} & \rho^+ & K^{*+} \\ \rho^- & -\frac{\rho^0}{\sqrt{2}} + \frac{\omega^0}{\sqrt{2}} & K^{*0} \\ K^{*-} & \bar{K}^{*0} & \phi \end{pmatrix}, \tag{131}$$

where the Lorentz index μ is implicitly understood. The vector meson exchange contribution to the potential can be worked out along the lines of Appendix A. A few representative examples are

$$\langle \Xi_Q\bar{\Xi}_Q|V|\Xi_Q\bar{\Xi}_Q\rangle = \frac{\lambda_T^2}{\vec{q}^2 + m_V^2}\frac{(\vec{\tau}_1\cdot\vec{\tau}_2 - 3)}{2}, \tag{132}$$

$$\langle \Xi'_Q\bar{\Xi}_Q|V|\Xi'_Q\bar{\Xi}_Q\rangle = \frac{\lambda_S\lambda_T}{\vec{q}^2 + m_V^2}\frac{(\vec{\tau}_1\cdot\vec{\tau}_2 - 3)}{4}, \tag{133}$$

$$\langle \Xi'_Q\bar{\Xi}'_Q|V|\Xi'_Q\bar{\Xi}'_Q\rangle = \frac{\lambda_S^2}{\vec{q}^2 + m_V^2}\frac{(\vec{\tau}_1\cdot\vec{\tau}_2 - 3)}{8}, \tag{134}$$

$$\langle \Sigma_Q\bar{\Sigma}_Q|V|\Sigma_Q\bar{\Sigma}_Q\rangle = \frac{\lambda_S^2}{\vec{q}^2 + m_V^2}\frac{(\vec{T}_1\cdot\vec{T}_2 - 1)}{2}, \tag{135}$$

which have been calculated in the SU(3) limit. We have taken $m_\rho = m_\omega = m_\phi = m_V$ with m_V the vector meson mass. Notice that we do not have to write explicitly the potential for the sextet spin-3/2 heavy baryons: the vector meson potentials for the Σ_Q^*, Ξ_Q^*, and Ω_Q^* are identical to the ones for Σ_Q, Ξ'_Q, and Ω_Q. The couplings λ_S and λ_T are not arbitrary: they can be determined from the universality of the ρ coupling constant [72]. If we consider the ρ-meson exchange potential between two isospin-1/2 baryons

$$V_\rho(\vec{q}) = \frac{g_\rho^2}{\vec{q}^2 + m_\rho^2}\vec{\tau}_1\cdot\vec{\tau}_2, \tag{136}$$

[12]Notice that we are not considering TSV vertices because they involve derivatives and do not saturate the LO contact-range couplings.

with $m_\rho = 770$ MeV, the universality of the ρ coupling implies that $g_\rho = m_\rho/2f_\pi \simeq 2.9$. If we match to the potentials in Eqs. (132) to (135), we find

$$\lambda_T = \sqrt{2}g_\rho \quad \text{and} \quad \lambda_S = 2\sqrt{2}g_\rho. \tag{137}$$

The saturation of the EFT contact couplings by the vector mesons is easy to obtain and can be found in Table IX. We mention that it is possible to consider the contributions of the different vector mesons separately:

$$C_V = C_\rho + C_\omega + C_\phi. \tag{138}$$

This form is interesting because it makes it easy to deduce the strength of the heavy baryon-baryon short-range interaction from the heavy baryon-antibaryon one. This merely involves changing the sign of the contributions from the negative G-parity mesons, the ω and the ϕ, yielding $C'_V = C_\rho - C_\omega - C_\phi$. Though the vector meson saturations of the heavy baryon-baryon system is not listed here, they can be obtained from Table IX where the C_ρ, C_ω, and C_ϕ contributions are listed.

Finally we add the contribution to the EFT contact couplings from scalar and vector meson exchange saturation, that is,

$$C(\Lambda \sim m_V, m_\sigma) \sim C_S + C_V, \tag{139}$$

where C_S and C_V are the scalar and vector meson contributions. At this point it is interesting to compare saturation in the heavy baryon-antibaryon system with the heavy meson-antimeson and heavy meson-antibaryon cases. The $X(3872)$ and $P_c(4450)$ are $D^*\bar{D}$ and $\bar{D}^*\Sigma_c$ molecular candidates for which we can apply the saturation argument as well, as can be seen in Table IX. If we compare the saturated contact-range couplings of the $X(3872)$ and $P_c(4450)$ with the ones for the heavy baryon-antibaryon system, we can identify the most promising molecular candidates. Heavy baryon-antibaryon systems for which the short-range interaction is expected to be more attractive than the $X(3872)$ include

$$\begin{aligned} &\Lambda_Q\bar{\Lambda}_Q, \quad \Xi_Q\bar{\Xi}_Q(I=0), \quad \Xi'_Q\bar{\Xi}_Q(I=0), \\ &\Sigma_Q\bar{\Lambda}_Q, \quad \Xi'_Q\bar{\Xi}'_Q(I=0), \quad \Sigma_Q\bar{\Sigma}_Q(I=0,1), \end{aligned} \tag{140}$$

to which we have to add the molecules containing the excited sextet baryons, i.e., the molecules we obtain from the substitutions $\Xi_Q \to \Xi^*_Q$ and $\Sigma_Q \to \Sigma^*_Q$. The systems for which there is more short-range attraction than for the $P_c(4450)$ include

$$\Lambda_Q\bar{\Lambda}_Q, \quad \Sigma_Q\bar{\Lambda}_Q, \quad \Sigma_Q\bar{\Sigma}_Q(I=0,1), \tag{141}$$

where we notice that they are a subset of Eq. (140). The obvious conclusion is that the heavy baryon-antibaryon pairs listed in Eq. (141) are the strongest candidates to bind. The particular case of $\Lambda_c\bar{\Lambda}_c$ has been recently studied in Ref. [73], leading to binding in agreement with our conclusions.

If we consider the heavy baryon-baryon system instead, the contribution of the ω and ϕ mesons is repulsive and in general there is less attraction than in the heavy baryon-antibaryon case. Yet for the following heavy baryon-baryon system,

$$\Sigma_Q\Sigma_Q(I=0), \tag{142}$$

there is more short-range attraction than in the $X(3872)$ and the $P_c(4450)$. Further candidates for binding can be inferred from a comparison with the deuteron, for which the short-range interaction is repulsive. In Table IX we see that for the nucleon-nucleon system there is a strong short-range repulsion from the exchange of the ω meson but also a strong attraction coming from the exchange of the σ meson. The existence of the deuteron indicates that attraction wins in this case. This is not surprising if we notice that $m_\sigma < m_\omega$ and $(g_{\sigma NN}/3) > g_\rho$, which suggests that σ meson saturation overcomes ω meson saturation ($|C_S| > |C_\omega|$). Here it is worth noticing that binding in nonrelativistic systems depends on the reduced potential, the product of the potential by twice the reduced mass of the system. This in turn implies that for the following systems,

$$\Lambda_Q\Lambda_Q, \qquad \Sigma_Q\Lambda_Q, \qquad \Sigma_Q\Sigma_Q(I=0,1), \tag{143}$$

the net effect of the short-range attraction from the σ meson will be larger than in the two-nucleon system, i.e.,

$$2\mu|C_S| > 2\mu_{\rm NN}|C_S^{\rm NN}|, \tag{144}$$

with μ and $\mu_{\rm NN}$ the reduced masses of the systems listed in Eq. (143) and the two-nucleon system, respectively, and C_S and $C_S^{\rm NN}$ their σ-saturated couplings. But we warn that this argument is incomplete: common wisdom in nuclear physics attributes binding in the deuteron to the interplay of short- and long-range physics, in particular the short-range repulsion from the ω meson, the attraction from the σ meson, and the tensor force from OPE. This suggests that, with the exception of the isoscalar $\Sigma_c\Sigma_c$ system, the other molecular candidates listed in Eq. (143) require a more thorough theoretical exploration to determine if there is binding.

The saturation argument probably provides incomplete information about the LO contact-range couplings. The saturated couplings are independent of the total light spin of the heavy hadron-antihadron system. This is compatible with HQSS—it represents a subset of the possible interactions that respect HQSS—but not necessarily with experiments. If we review the heavy meson-antimeson

TABLE X. Critical radius R_c for which OPE is able to bind certain heavy baryon-antibaryon molecules, where I refers to the isospin of the system. For the $\Sigma_Q\bar{\Sigma}_C(0^{-+})$, where there is no tensor force, the notation $0^{+0.23}$ indicates that there is only binding for $R_c \leq 0.23$ fm if the coupling g_2 lies on the high end of the lattice calculations. For comparison purposes, the critical radius for the deuteron and the $P_c^+(4450)$ pentaquark are 1.00 fm and 0.30–0.49 fm, respectively. If the system does not bind, we indicate it with the "…" notation.

Channel	$I=0$	$I=1$	$I=2$	Channel	$I=0$	$I=1$	$I=2$
$\Sigma_c\bar{\Sigma}_c(0^{-+})$	…	…	…	$\Sigma_b\bar{\Sigma}_b(0^{-+})$	$0^{+0.23}$	…	…
$\Sigma_c\bar{\Sigma}_c(1^{--})$	0.42–0.94	0.22–0.55	0.19–0.48	$\Sigma_b\bar{\Sigma}_b(1^{--})$	$0.86^{+0.30}_{-0.31}$	$0.49^{+0.21}_{-0.19}$	$0.43^{+0.21}_{-0.18}$
$\Sigma_c\bar{\Sigma}_c^*(1^{-+})$	0.39–1.00	0.19–0.53	0.15–0.36	$\Sigma_b\bar{\Sigma}_b^*(1^{-+})$	$0.88^{+0.38}_{-0.35}$	$0.46^{+0.23}_{-0.20}$	$0.32^{+0.13}_{-0.12}$
$\Sigma_c\bar{\Sigma}_c^*(1^{--})$	0.44–1.11	0.22–0.59	0.18–0.44	$\Sigma_b\bar{\Sigma}_b^*(1^{--})$	$0.99^{+0.40}_{-0.39}$	$0.52^{+0.26}_{-0.22}$	$0.39^{+0.16}_{-0.15}$
$\Sigma_c\bar{\Sigma}_c^*(2^{-+})$	0.46–1.01	0.24–0.59	0.25–0.64	$\Sigma_b\bar{\Sigma}_b^*(2^{-+})$	$0.91^{+0.31}_{-0.32}$	$0.51^{+0.21}_{-0.21}$	$0.56^{+0.24}_{-0.22}$
$\Sigma_c\bar{\Sigma}_c^*(2^{--})$	0.39–0.85	0.21–0.50	0.20–0.55	$\Sigma_b\bar{\Sigma}_b^*(2^{--})$	$0.77^{+0.27}_{-0.27}$	$0.45^{+0.18}_{-0.17}$	$0.48^{+0.23}_{-0.21}$
$\Sigma_c^*\bar{\Sigma}_c^*(0^{-+})$	0.56–1.36	0.27–0.75	0.18–0.41	$\Sigma_b^*\bar{\Sigma}_b^*(0^{-+})$	$1.20^{+0.46}_{-0.46}$	$0.64^{+0.32}_{-0.27}$	$0.36^{+0.14}_{-0.30}$
$\Sigma_c^*\bar{\Sigma}_c^*(1^{--})$	0.52–1.24	0.26–0.68	0.18–0.42	$\Sigma_b^*\bar{\Sigma}_b^*(1^{--})$	$1.09^{+0.42}_{-0.41}$	$0.59^{+0.29}_{-0.25}$	$0.37^{+0.15}_{-0.14}$
$\Sigma_c^*\bar{\Sigma}_c^*(2^{-+})$	0.44–1.02	0.22–0.57	0.20–0.50	$\Sigma_b^*\bar{\Sigma}_b^*(2^{-+})$	$0.91^{+0.34}_{-0.34}$	$0.50^{+0.23}_{-0.20}$	$0.43^{+0.18}_{-0.17}$
$\Sigma_c^*\bar{\Sigma}_c^*(3^{--})$	0.45–0.91	0.25–0.55	0.28–0.69	$\Sigma_b^*\bar{\Sigma}_b^*(3^{--})$	$0.82^{+0.27}_{-0.28}$	$0.48^{+0.20}_{-0.18}$	$0.60^{+0.28}_{-0.25}$

system, to which the $X(3872)$ is suspected to belong, scalar and vector meson exchange saturation predicts exactly the same potential for $D\bar{D}$, $D^*\bar{D}$, $D\bar{D}^*$, and $D^*\bar{D}^*$ irrespectively of the spin and C-parity quantum numbers. That is, the saturation argument leads to the prediction of six isoscalar heavy meson-antimeson molecules. This is to be compared with only one obvious molecular candidate, the $X(3872)$. Analogously, the application of this argument to the heavy meson-antibaryon molecules leads to the prediction of seven $\bar{D}\Sigma_c$, $\bar{D}\Sigma_c^*$, $\bar{D}^*\Sigma_c$, and $\bar{D}^*\Sigma_c^*$ molecules but only one experimental candidate, the $P_c(4450)$. This situation also happens in other theoretical approaches that derive heavy hadron interactions from vector meson saturation [65–67]. The probable conclusion is that we are probably missing something in the resonance saturation arguments we are using to derive the LO couplings. Be that as it may, for the set of molecules in Eq. (141) the short-range attraction is expected to be remarkably stronger than in the $X(3872)$ and $P_c(4450)$.

B. Long-range binding dynamics

The long-range dynamics of the heavy baryon-antibaryon system is driven by OPE. We assess the relative strength of the OPE potential for each channel in the following way: first we modify the OPE potential by including a cutoff

$$V_{\rm OPE}(r;r_c) = V_{\rm OPE}(r)\theta(r-r_c), \tag{145}$$

where r_c is the cutoff. Then we calculate the largest r_c for which OPE alone is able to bind a molecule. We call this radius $r_c = R_c$ the "critical radius." Notice that we are in fact assuming that (i) OPE is valid from infinity till the critical radius and (ii) there is no short-range physics. If this critical radius turns out to be *large enough*, we will consider that the system is likely to bind. By large enough we mean for instance that the critical radius is larger than the size of the hadrons or the range of other contributions to the hadron-hadron potential that have not been taken into account (e.g., two pion exchange).

It is important to notice that most heavy baryon-antibaryon molecules bind if r_c is sufficiently small because of the tensor force. Thus the crucial factor is not whether there is a critical radius for which the molecule binds, but whether the critical radius R_c is reasonable or not. The reason why the tensor force is able to bind in most cases is because for S-wave molecules it behaves as an attractive singular potential; see the discussion in Sec. V C. This is why it is important to consider whether the distance at which OPE binds is reasonable or not.

We list the critical radii for the $\Sigma_Q^{(*)}\bar{\Sigma}_Q^{(*)}$ molecules in Table X. We have chosen the $\Sigma_Q^{(*)}\bar{\Sigma}_Q^{(*)}$ system because this is the case in which the OPE potential is expected to be stronger owing to the higher isospin of the Σ_Q's. Besides, from scalar and vector meson exchange saturation we expect a very strong short-range attraction. The isoscalar molecules are the ones showing more attraction and higher critical radii, reaching in a few cases 1 fm. For the hidden charm molecules the uncertainty is really big as the value of g_2 is not experimentally known. To give a sense of scale we mention that for the deuteron the critical radius is 1.00 fm. For the $P_c(4450)$ pentaquarklike state as a $\Sigma_c\bar{D}^*$ molecule, the critical radius is 0.30–0.49 fm (where the uncertainty is again a consequence of g_2). In comparison, for the heavy meson-antimeson molecular candidates, the radii are 0.30, 0.10, and 0.26 fm for the $X(3872)$, $Z_c(3900)$, and $Z_b(10610)$, respectively. The rather small critical radii of the X, the Z_c, and the Z_b suggest that these hadron molecules depend on the short-range attraction (instead of OPE) to bind. For the deuteron the critical radius is

significantly larger, indicating that OPE is an important component of the binding mechanism. Lastly, the situation for the $P_c(4450)^+$ pentaquark seems to be in the middle. From Table X it is apparent that for the heavy baryon-antibaryon system OPE can provide as much attraction as in the deuteron. If we combine this observation with what we know about short-range physics according to Table IX, the conclusion is that there will be a rich $\Sigma_Q^{(*)}\bar{\Sigma}_Q^{(*)}$ molecular spectrum, particularly in the $I = 0$, 1 configurations.

VII. CONCLUSIONS

In this work we have presented a general EFT framework for the heavy baryon-antibaryon system. EFTs exploit the existence of a separation of scales to express the observable quantities of a low energy system as a power series. In the case at hand the size of a hadron molecule is expected to be larger than the hadrons forming it. As a consequence this type of system is amenable to an EFT description. Also, heavy hadron molecules are constrained by chiral, SU(2)-isospin, SU(3)-flavor, and HQSS symmetries. This degree of symmetry translates into a few interesting regularities in their spectrum.

EFT explains the heavy baryon-antibaryon interaction in terms of contact-range interactions and pion exchanges. The relative importance of these two contributions changes from system to system. In general the LO EFT description involves four-baryon contact-range interactions and pion exchanges (OPE), but this depends on the molecule. Pion exchanges are expected to be particularly important in the isoscalar $\Sigma_Q\bar{\Sigma}_Q$, $\Sigma_Q^*\bar{\Sigma}_Q$, and $\Sigma_Q^*\bar{\Sigma}_Q^*$ molecules (but less important for other configurations). In contrast, OPE vanishes in the $\Xi_Q\bar{\Xi}_Q$ and $\Lambda_Q\bar{\Lambda}_Q$ molecules, which can be described in terms of a contact theory at LO. For the $\Xi_Q'\bar{\Xi}_Q'$, $\Xi_Q^*\bar{\Xi}_Q'$, and $\Xi_Q^*\bar{\Xi}_Q^*$ molecules, particularly in the hidden charm sector, OPE is probably a NLO effect. We warn that the conclusions about the relevance of the OPE potential are only well established for the bottom sector. In the charm sector, the value of the g_2 axial coupling that appears in the $\Sigma_c \to \Sigma_c\pi$ amplitude is not known experimentally, and a determination either in a future experiment or in the lattice will be welcomed. Particle coupled channels, i.e., transitions in which a heavy baryon changes from the ground to the excited state ($B_6 \to B_6^*$), are subleading if the molecules are not too tightly bound, i.e., for binding momenta $\gamma = \sqrt{M_6|E_B|} \leq 350$–$400$ MeV. The previous findings regarding pion exchanges and coupled channels are analogous to the ones in the heavy meson-antimeson molecules [32]. It is also worth mentioning that right now the LO EFT is more than enough for the description of heavy hadron-antihadron molecules, where the scarcity of experimental data makes it superfluous to calculate subleading orders.

The EFT potential is constrained by HQSS. This is particularly evident for S-wave interactions, such as the LO contact-range potential and central OPE. Symmetries in the S-wave interaction are likely to translate into symmetries in the spectrum. For the $T\bar{T}$ case, the LO EFT potential does not depend on the total spin of the system:

$$\langle T\bar{T}|V_s(0^-)|T\bar{T}\rangle = \langle T\bar{T}|V_s(1^-)|T\bar{T}\rangle, \tag{146}$$

where the subscript s is used to indicate S-wave. That is, the $T\bar{T}$ heavy baryon molecules are expected to come in pairs. For the $T\bar{S}/S\bar{T}$ molecules we have the following two relations:

$$\langle T\bar{S}|V_s(0^{-\pm})|T\bar{S}\rangle = \langle T\bar{S}|V_s(2^{-\pm})|T\bar{S}\rangle, \tag{147}$$

$$\langle T\bar{B}_6|V_s(1^{-\pm})|T\bar{B}_6\rangle = \langle T\bar{B}_6^*|V_s(1^{-\mp})|T\bar{B}_6^*\rangle, \tag{148}$$

where in the second line we have explicitly indicated whether the sextet heavy baryon is in the ground or excited state. The conclusion is again that $T\bar{S}$ molecules appear in pairs. For $S\bar{S}$ molecules the contacts have a far richer structure, with only one obvious symmetry relation:

$$\langle S\bar{S}|V_s(2^{--})|S\bar{S}\rangle = \langle S\bar{S}|V_s(3^{--})|S\bar{S}\rangle. \tag{149}$$

Tensor OPE mixes partial waves and will induce deviations from the previous relations, which will be moderate if the bound states are shallow. At this point it is worth noticing the analogy with the heavy meson-antimeson case, where this type of twin structure also happens for (i) the 1^{+-} $D^*\bar{D}$ and 1^{+-} $D^*\bar{D}^*$ and (ii) the 1^{++} $D^*\bar{D}$ and 2^{++} $D^*\bar{D}^*$ molecules. The first of these relations explains why the Z_c's and Z_b's resonances appear in pairs [31,74], while the latter predicts that the $X(3872)$ should have a 2^{++} partner, the $X(4012)$ [32,33]. In the heavy meson-antimeson system there is a series of dynamical effects (besides the aforementioned tensor OPE) that might break these patterns, which include decays into nearby channels [75], coupled channel dynamics [76], the existence of nearby quarkonia [77], and annihilation [78]. Though they have not been studied in the heavy baryon-antibaryon case, these effects could be relevant.

Finally there is the important question of whether the existence of heavy baryon molecules can be predicted. EFTs are generic frameworks that usually require preexisting experimental input to make predictions. The EFT potential is composed of a long-range and short-range piece. The short-range piece involves unknown couplings, which have to be determined from external information. In the absence of experimental data, there is the possibility of using phenomenological arguments to estimate the contact-range couplings. If we assume the saturation of these couplings from ρ-, ω-, ϕ-, and σ-meson exchange, the most probable candidates for a heavy baryon-antibaryon bound state are the isoscalar $\Lambda_c\bar{\Lambda}_c$, $\Sigma_c\bar{\Sigma}_c$, $\Sigma_c^*\bar{\Sigma}_c$, and $\Sigma_c^*\bar{\Sigma}_c^*$ molecules, located at 4573, 4906, 4970, and 5035 MeV

and the isovector $\Lambda_c\bar{\Sigma}_c$ and $\Lambda_c\bar{\Sigma}_c^*$ molecules at 4740 and 4805 MeV. If we consider the heavy baryon-baryon system instead, saturation indicates that the isoscalar, doubly-charmed $\Sigma_c\Sigma_c$, $\Sigma_c^*\Sigma_c$, and $\Sigma_c^*\Sigma_c^*$ molecules are good candidates for binding, followed by their isovector counterparts, the isoscalar $\Lambda_c\Lambda_c$ and isovector $\Lambda_c\Sigma_c$ and $\Lambda_c\Sigma_c^*$ systems. For the heavy baryon-antibaryon system we supplement the saturation argument with an estimate of the relative strength of the OPE potential, which we assess by calculating the radius for which OPE would be able to bind the system by itself. This second argument also points to isoscalar molecules as the most likely to bind. It might be possible to observe these heavy baryon-antibaryon molecules in experiments such as LHCb and PANDA, which is expected to be particularly suited for the precision study of hidden charm exotic states [79], or alternatively in the lattice.

ACKNOWLEDGMENTS

M. P. V. thanks Johann Haidenbauer for discussions and the Institute de Physique Nucléaire d'Orsay, where part of this work was carried out, for its hospitality. We also thank Chu-Wen Xiao for his comments on the manuscript. This work is partly supported by the National Natural Science Foundation of China under Grants No. 11375024, No. 11522539, and No. 11735003; the Fundamental Research Funds for the Central Universities; and the Thousand Talents Plan for Young Professionals.

APPENDIX A: THE ONE PION EXCHANGE POTENTIAL IN HEAVY HADRON CHIRAL PERTURBATION THEORY

The OPE potential is the LO piece of the finite-range EFT potential. In this Appendix we explain how to compute it. The idea is to obtain nonrelativistic amplitudes for processes involving an incoming and outgoing heavy baryon and a pion, which we write as

$$\mathcal{A}(B \to B'\pi; \vec{q}), \tag{A1}$$

where $B(B')$ are the initial/final baryon and $\vec{q}$ the momentum of the pion if outgoing (if incoming we change the momentum to $-\vec{q}$). If written in a suitable normalization these amplitudes can be combined to compute the OPE potential (or for that matter any one boson exchange potential) as follows:

$$\langle B_1' B_2'|V|B_1 B_2\rangle = \frac{\mathcal{A}_1(\vec{q})\mathcal{A}_2(-\vec{q})}{\vec{q}^2+\mu_\pi^2}, \tag{A2}$$

where 1 and 2 refer to the pion vertices 1 and 2 and μ_π is the effective pion mass for this particular transition (which is not necessarily the physical pion mass because $m_{B_1'} - m_{B_1} \neq 0$ and gives the pion a nonvanishing zeroth component to its 4-momentum). The amplitudes $\mathcal{A}_1$ and $\mathcal{A}_2$ may refer to baryons or antibaryons indistinctively. In the following lines we will explain how to do the derivation in detail.

1. The heavy baryon field

Heavy baryons contain a heavy quark and two light quarks; i.e., they have the structure $|Qqq\rangle$. The total spin of the light quark pair is $S_L = 0, 1$. If the light quark spin is $S_L = 0$, we have an antitriplet spin-$1/2$ heavy baryon, which we denote by the Dirac field

$$\Psi_{\bar{3}Q}. \tag{A3}$$

If the light quark spin is $S_L = 1$, we have spin-$1/2$ and spin-$3/2$ heavy baryons which we denote by the Dirac and Rarita-Schwinger fields

$$\Psi_{6Q}, \qquad \Psi^*_{6Q\mu}. \tag{A4}$$

Notice that the Rarita-Schwinger field contains a Lorentz index: it is the external product of a Minkowsky vector and a Dirac spinor. The product contains a spurious spin-$\frac{1}{2}$ component that can be removed with the condition

$$\gamma^\mu \Psi^*_{6Q\mu} = 0. \tag{A5}$$

Within heavy hadron EFT it is customary to use the fields $T(v)$ and $S_\mu(v)$ instead, which have good transformation properties under rotations of the spin of the heavy quark (where v refers to the velocity of the heavy quark). For the $\Psi_{\bar{3}Q}$ heavy baryon, the definition is

$$T_Q(v) = \frac{1+\not{v}}{2}\Psi_{\bar{3}Q}, \tag{A6}$$

$$\bar{T}_Q(v) = \bar{\Psi}_{\bar{3}Q}\frac{1+\not{v}}{2}. \tag{A7}$$

The superfield $T_Q(v)$ transforms as

$$T_Q(v) \to e^{-i\vec{\epsilon}\cdot\vec{S}_v} T_Q(v), \tag{A8}$$

where $\vec{S}_v$ is related to $SU(2)_v$, the $SU(2)$ spin group of the heavy quark Q moving at velocity v. For the Ψ_{6Q} and $\Psi^*_{6Q\mu}$ sextet heavy baryons, the definition is

$$S_{Q\mu}(v) = \frac{1}{\sqrt{3}}(\gamma_\mu + v_\mu)\gamma_5 \frac{1+\not{v}}{2}\Psi_{6Q} + \frac{1+\not{v}}{2}\Psi^*_{6Q\mu}, \tag{A9}$$

$$\bar{S}_{Q\mu}(v) = -\frac{1}{\sqrt{3}}\bar{\Psi}_{6Q}\frac{1+\not{v}}{2}\gamma_5(\gamma_\mu + v_\mu) + \bar{\Psi}^*_{6Q\mu}\frac{1+\not{v}}{2}, \tag{A10}$$

where γ_μ, γ_5 are the Dirac matrices. The $S_{Q\mu}(v)$ superfield contains a Lorentz index that comes from the Rarita-Schwinger field $\Psi^*_{6Q\mu}$. It obeys a constraint analogous to Eq. (A5):

$$v^\mu S_{Q\mu}(v) = 0 \quad \text{and} \quad \not{v} S_{Q\mu}(v) = S_{Q\mu}(v). \tag{A11}$$

The $S_{Q\mu}(v)$ superfield transforms as

$$S_{Q\mu}(v) \to e^{-i\vec{\epsilon}\cdot\vec{S}_v} S_{Q\mu}(v). \tag{A12}$$

In general we take the velocity parameter to be $v = (1, \vec{0})$.

We are interested in heavy baryon-antibaryon molecules; i.e., we need the antibaryon fields. Here it is important to notice that

$$\bar{T}_Q(v) = T_Q^\dagger(v)\gamma_0, \tag{A13}$$

$$\bar{S}_{Q\mu}(v) = S_{Q\mu}^\dagger(v)\gamma_0, \tag{A14}$$

are the operators for creating heavy baryons, which are unrelated to the antibaryon fields. Heavy antibaryons require the definition of new $T_{\bar{Q}}(v)$, $\bar{T}_{\bar{Q}}(v)$, $S_{\bar{Q}}(v)$, and $\bar{S}_{\bar{Q}}(v)$ fields. We will not need to define them explicitly though. Instead we will use C- and G-parity transformations to deduce the interactions of the heavy antibaryons with the pions.

The heavy baryon fields have SU(2)-isospin and SU(3)-flavor structure. If we add SU(3)-flavor indices for the heavy baryons with $Q = b$ and $S_L = 0$, we have

$$\Psi_{\bar{3}b} = \begin{pmatrix} \Xi_b^- \\ -\Xi_b^0 \\ \Lambda_b^0 \end{pmatrix} \tag{A15}$$

while for $Q = b$, $S_L = 1$ we have

$$\Psi_{\bar{6}b} = \begin{pmatrix} \Sigma_b^+ & \frac{1}{\sqrt{2}}\Sigma_b^0 & \frac{1}{\sqrt{2}}\Xi_b^{0\prime} \\ \frac{1}{\sqrt{2}}\Sigma_b^0 & \Sigma_b^- & \frac{1}{\sqrt{2}}\Xi_b^{-\prime} \\ \frac{1}{\sqrt{2}}\Xi_b^{0\prime} & \frac{1}{\sqrt{2}}\Xi_b^{-\prime} & \Omega_b^- \end{pmatrix}, \tag{A16}$$

where the corresponding expressions for the spin-$\frac{3}{2}$ heavy baryons Ψ^*_{6c} are identical. For the $SU(3)$-flavor structure of the $Q = c$ charmed baryons we refer to Eqs. (20) and (21). In the following we will mostly consider the $SU(2)$-isospin structure: when we talk about the T_Q we could either be referring to Λ_Q (isoscalar) or Ξ_Q (isospinor), while when we talk about S_Q it could be Σ_Q (isovector), Ξ'_Q (isospinor), or Ω_Q (isoscalar).

Notice that we are interested in the OPE potential: the isoscalar Ω_Q cannot exchange a single pion and will not be further considered here. The isoscalar Λ_Q and the isospinor Ξ_Q can only exchange pions in vertices involving a Ξ'_Q and a $\Sigma_Q^{(*)}$ respectively; i.e., there is no $\Xi_Q\Xi_Q\pi$ or $\Lambda_Q\Lambda_Q\pi$ vertex but there are $\Xi_Q\Xi_Q^{(*)\prime}\pi$ and $\Lambda_Q\Sigma_Q^{(*)}\pi$ vertices.

2. The heavy baryon chiral Lagrangian at LO

The interaction of heavy baryons and pions can be written as [46,52]

$$\mathcal{L}_{TT\pi} = 0, \tag{A17}$$

$$\mathcal{L}_{ST\pi} = g_3[\epsilon_{ijk}\bar{T}^i_Q(A^\mu)^j_l S^{kl}_{Q\mu} + \epsilon^{ijk}\bar{S}^\mu_{Qkl}(A^\mu)^l_j T_{Qi}], \tag{A18}$$

$$\mathcal{L}_{SS\pi} = ig_2\epsilon_{\mu\nu\sigma\lambda}\bar{S}^\mu_{Qik}v^\nu(A^\sigma)^i_j(S^\lambda)^{jk}_Q, \tag{A19}$$

where the latin indices i, j, k, l indicate either the SU(2)-isospin or the SU(3)-flavor components; g_2, g_3 are coupling constants; and $\epsilon_{\mu\nu\sigma\lambda}$ is the four-dimensional Levi-Cività symbol. In the equation above, A^μ is the pseudo Goldstone boson field,

$$A^\mu = \frac{i}{2}(\xi^\dagger\partial^\mu\xi - \xi\partial^\mu\xi^\dagger), \tag{A20}$$

where ξ is defined as

$$\xi = e^{\frac{i}{f_\pi}M}, \tag{A21}$$

with the matrix M

$$M = \begin{pmatrix} \frac{\pi^0}{\sqrt{2}} + \frac{\eta}{\sqrt{6}} & \pi^+ & K^+ \\ \pi^- & -\frac{\pi^0}{\sqrt{2}} + \frac{\eta}{\sqrt{6}} & K^0 \\ K^- & \bar{K}^0 & -\sqrt{\frac{2}{3}}\eta \end{pmatrix}, \tag{A22}$$

which entails that we are taking the normalization choice $f_\pi \simeq 132$ MeV.

If we consider the $SU(2)$ subgroup of $SU(3)$, the A^μ field reduces to the following expansion in the pion field:

$$A^\mu = -\frac{1}{f_\pi}\partial^\mu\pi + \frac{1}{6f_\pi^3}[\pi,[\pi,\partial^\mu\pi]] + \ldots, \tag{A23}$$

where π refers to the $SU(2)$ submatrix in the equation above (after removing the contribution from the η), i.e.,

$$\pi = \begin{pmatrix} \frac{\pi^0}{\sqrt{2}} & \pi^+ \\ \pi^- & -\frac{\pi^0}{\sqrt{2}} \end{pmatrix}. \tag{A24}$$

3. The nonrelativistic limit

The potential is well defined in the nonrelativistic limit, where the heavy baryon fields reduce to

$$\Psi_{\bar{3}Q} \to \sqrt{2M_{\bar{3}}}\begin{pmatrix}\chi'_s\\0\end{pmatrix}, \tag{A25}$$

$$\Psi_{6Q} \to \sqrt{2M_6}\begin{pmatrix}\chi_s\\0\end{pmatrix}, \tag{A26}$$

$$\Psi^*_{6Q\mu} = \{\Psi^*_{6Q0}, \vec{\Psi}^*_{6Q}\} \to \sqrt{2M^*_6}\left\{\begin{pmatrix}0\\0\end{pmatrix}, \begin{pmatrix}\vec{\chi}_s\\0\end{pmatrix}\right\}, \tag{A27}$$

where χ'_s, χ_s are standard spinors, while $\vec{\chi}_s = (\chi_{s1}, \chi_{s2}, \chi_{s3})$ is a vector in which each component is a spinor. The vector $\vec{\chi}_s$ fulfills the condition

$$\vec{\sigma}\cdot\vec{\chi}_s = 0, \tag{A28}$$

i.e., the nonrelativistic version of Eq. (A5), which ensures that $\Psi^*_{6Q\mu}$ is a genuine spin-$\frac{3}{2}$ field. We have that $M_{\bar{3}}$ is the $S_L = 0$ heavy baryon mass, while M_6, M^*_6 are the $S_L = 1$ heavy baryon masses. In the heavy quark limit the $S_L = 1$ baryon masses are identical:

$$M_6 = M^*_6 \quad \text{for } m_Q \to \infty. \tag{A29}$$

However, this does not happen with the $M_{\bar{3}}$ mass, which remains different from M_6 and M^*_6 in the heavy quark limit. Putting all the pieces together, in the nonrelativistic limit the $S_L = 0$ heavy field reduces to

$$\frac{1}{\sqrt{2M_{\bar{3}}}}T_Q(v) \to \begin{pmatrix}B_{\bar{3}}\\0\end{pmatrix}, \tag{A30}$$

$$\frac{1}{\sqrt{2M_{\bar{3}}}}\bar{T}_Q(v) \to \begin{pmatrix}B^\dagger_{\bar{3}} & 0\end{pmatrix}, \tag{A31}$$

while the $S_L = 1$ heavy fields read

$$\frac{1}{\sqrt{2M_6}}\vec{S}_Q(v) \to \begin{pmatrix}\sqrt{\frac{1}{3}}\vec{\sigma}B_6 + \vec{B}^*_6\\0\end{pmatrix}, \tag{A32}$$

$$\frac{1}{\sqrt{2M_6}}\bar{\vec{S}}_Q(v) \to \begin{pmatrix}\sqrt{\frac{1}{3}}\vec{\sigma}B^\dagger_6 + \vec{B}^{*\dagger}_6 & 0\end{pmatrix}, \tag{A33}$$

with $B_{\bar{3}}$, B_6, and B^*_6 the nonrelativistic heavy baryon fields. The notation can be further simplified (i) by noticing that there is no difference between the $\bar{T}_Q/\bar{S}_Q$ and $T^\dagger_Q/S^\dagger_Q$ fields in the nonrelativistic limit, (ii) by ignoring the antibaryon components and (iii) by absorbing the normalization factors $\sqrt{2M_{\bar{3}}}$ and $\sqrt{2M_6}$ in a field redefinition. In this case we end up with

$$T_Q = B_{\bar{3}}, \tag{A34}$$

$$T^\dagger_Q = B^\dagger_{\bar{3}}, \tag{A35}$$

$$\vec{S}_Q = \sqrt{\frac{1}{3}}\vec{\sigma}B_6 + \vec{B}^*_6, \tag{A36}$$

$$\vec{S}^\dagger_Q = \sqrt{\frac{1}{3}}B^\dagger_6\vec{\sigma} + \vec{B}^{*\dagger}_6. \tag{A37}$$

The pion field A_μ reduces in the heavy baryon nonrelativistic limit to

$$\vec{A} = -\frac{1}{f_\pi}\vec{\nabla}\vec{\pi} + \mathcal{O}\left(\frac{\pi^3}{f^3_\pi}\right), \tag{A38}$$

where we ignore the zeroth component of A_μ because it couples to the zeroth component of $S_{Q\mu}(v)$, which vanishes in the nonrelativistic limit. From this we can rewrite the Lagrangian as

$$\mathcal{L}_{ST\pi} = -g_3[\epsilon_{ijk}T^{i\dagger}_Q(\vec{A})^j_l\cdot\vec{S}^{kl}_Q + \epsilon^{ijk}\vec{S}^\dagger_{Qkl}\cdot(\vec{A})^l_j T_{Qi}], \tag{A39}$$

$$\mathcal{L}_{SS\pi} = -ig_2\mathrm{Tr}[\vec{S}^\dagger_Q\cdot(\vec{A}\times\vec{S}_Q)], \tag{A40}$$

where the trace is over isospin space. Alternatively we can expand the Lagrangian in terms of the fields $B_{\bar{3}}$, B_6, and B^*_6:

$$\begin{aligned}\mathcal{L}_{ST\pi} = {}& \frac{g_3}{\sqrt{3}f_\pi}B^\dagger_{\bar{3}}\vec{\sigma}\cdot\vec{\nabla}\pi B_6 + \frac{g_3}{\sqrt{3}f_\pi}B^\dagger_6\vec{\sigma}\cdot\vec{\nabla}\pi B'_6\\ &+ \frac{g_3}{f_\pi}B^\dagger_{\bar{3}}\vec{\nabla}\pi\cdot\vec{B}^*_6 + \frac{g_3}{f_\pi}\vec{B}^{*\dagger}_6\cdot\vec{\nabla}\pi B_{\bar{3}}\end{aligned} \tag{A41}$$

$$\begin{aligned}\mathcal{L}_{SS\pi} = {}& i\frac{g_2}{3f_\pi}B^\dagger_6\vec{\sigma}\cdot(\vec{\nabla}\vec{\pi}\times\sigma)B_6 + i\frac{g_2}{f_\pi}\vec{B}^{*\dagger}_6\cdot(\vec{\nabla}\vec{\pi}\times\vec{B}^*_6)\\ &+ i\frac{g_2}{\sqrt{3}f_\pi}B^\dagger_6\vec{\sigma}\cdot(\vec{\nabla}\vec{\pi}\times\vec{B}^*_6)\\ &+ i\frac{g_2}{\sqrt{3}f_\pi}\vec{B}^{*\dagger}_6\cdot(\vec{\nabla}\vec{\pi}\times\vec{\sigma})B_6,\end{aligned} \tag{A42}$$

where we have removed the isospin/flavor indices to make the expressions shorter.

4. The spin and isospin factors

Now we calculate the matrix elements of the different vertices, which depend on a series of spin and isospin factors. In the charm sector ($Q = c$), the relations between the isospin and particle basis are

$$B_{\bar{3}}(\Lambda_c) = \Lambda^+_c, \tag{A43}$$

$$B_{\bar{3}}(\Xi_c) = \begin{pmatrix}\Xi^{+\prime}_c\\ \Xi^{0\prime}_c\end{pmatrix}, \tag{A44}$$

$$B_6(\Xi_c') = \begin{pmatrix} \Xi_c^{+\prime} \\ \Xi_c^{0\prime} \end{pmatrix}, \tag{A45}$$

$$B_6(\Sigma_c) = \begin{pmatrix} \Sigma_c^{++} & \frac{1}{\sqrt{2}}\Sigma_c^{+} \\ \frac{1}{\sqrt{2}}\Sigma_c^{+} & \Sigma_c^{0} \end{pmatrix}, \tag{A46}$$

for the Λ_c, Ξ_c, Ξ_c', and Σ_c baryons, respectively. The relations for the excited $\Xi_c'^*$ and Σ_c^* sextet baryons are identical to those of the Ξ_c' and Σ_c baryons. Alternatively if we consider isospin vectors we can write

$$\Lambda_c^+ = |00\rangle_I, \tag{A47}$$

$$\{\Xi_c^+, \Xi_c^0\} = \left\{ \left|\frac{1}{2}, \frac{1}{2}\right\rangle_I, \left|\frac{1}{2}, -\frac{1}{2}\right\rangle_I \right\}, \tag{A48}$$

$$\{\Xi_c^{+\prime}, \Xi_c^{0\prime}\} = \left\{ \left|\frac{1}{2}, \frac{1}{2}\right\rangle_I, \left|\frac{1}{2}, -\frac{1}{2}\right\rangle_I \right\}, \tag{A49}$$

$$\{\Sigma_c^{++}, \Sigma_c^{+}, \Sigma_c^{0}\} = \{|1,1\rangle_I, |1,0\rangle_I, |1,-1\rangle_I\}. \tag{A50}$$

The isospin factors can be extracted by first expanding the isospin/flavor indices in the particle basis and later reinterpreting the result in terms of matrices in the isospin space. We begin with the $ST\pi$ Lagrangian, for which

$$\Lambda_c^\dagger \pi^a \Sigma_c = t^a, \tag{A51}$$

$$\Xi_c^\dagger \pi^a \Xi_c' = \frac{\tau^a}{2}, \tag{A52}$$

where π^a is the pion field in the Cartesian basis, τ^a are the Pauli matrices, and t^a are given by

$$t^1 = \begin{pmatrix} \frac{1}{\sqrt{2}} \\ 0 \\ -\frac{1}{\sqrt{2}} \end{pmatrix}, \tag{A53}$$

$$t^2 = \begin{pmatrix} \frac{i}{\sqrt{2}} \\ 0 \\ \frac{i}{\sqrt{2}} \end{pmatrix}, \tag{A54}$$

$$t^3 = \begin{pmatrix} 0 \\ 1 \\ 0 \end{pmatrix}. \tag{A55}$$

In the $SS\pi$ case we have

$$\Xi_c'^\dagger \pi^a \Xi_c' = \frac{\tau^a}{2\sqrt{2}}, \tag{A56}$$

$$\Sigma_c^\dagger \pi^a \Sigma_c = \frac{T^a}{\sqrt{2}}, \tag{A57}$$

where T_a are the $J = 1$ angular momentum matrices in isospin space. The isospin factors for the Ξ_c^* and Σ_c^* baryons are identical to those of the Ξ_c and Σ_c baryons.

Next we factor out the spin in terms of angular momentum matrices or equivalent expressions. For the $ST\pi$ vertices the factors are

$$B_{\bar{3}}^\dagger \vec{\sigma}\cdot\vec{q} B_6 = \vec{\sigma}\cdot\vec{q}, \tag{A58}$$

$$B_{\bar{3}}^\dagger \vec{q}\cdot\vec{B}_6^* = \vec{S}\cdot\vec{q}, \tag{A59}$$

while for the $SS\pi$ vertices we have

$$B_6^\dagger \vec{\sigma}\cdot(\vec{q}\times\vec{\sigma}) B_6 = -i2\vec{\sigma}\cdot\vec{q}, \tag{A60}$$

$$\vec{B}_6^{*\dagger}\cdot(\vec{q}\times\vec{B}_6^*) = -i\frac{2}{3}\vec{\Sigma}\cdot\vec{q}, \tag{A61}$$

$$B_6^\dagger \vec{\sigma}\cdot(\vec{q}\times\vec{B}_6^*) = -i\vec{S}\cdot\vec{q}, \tag{A62}$$

$$\vec{B}_6^{*\dagger}\cdot(\vec{q}\times\vec{\sigma}) B_6 = -i\vec{S}^\dagger\cdot\vec{q}, \tag{A63}$$

where $\vec{\sigma}$ are the Pauli matrices, $\vec{\Sigma}$ are the $J = \frac{3}{2}$ angular momentum matrices, and $\vec{S}$ are 2×4 matrices that connect the spin-$\frac{1}{2}$ and spin-$\frac{3}{2}$ baryons. These $\vec{S}$ matrices read

$$S_1 = \begin{pmatrix} \frac{1}{\sqrt{2}} & 0 & -\frac{1}{\sqrt{6}} & 0 \\ 0 & \frac{1}{\sqrt{6}} & 0 & -\frac{1}{\sqrt{2}} \end{pmatrix}, \tag{A64}$$

$$S_2 = \begin{pmatrix} \frac{i}{\sqrt{2}} & 0 & \frac{i}{\sqrt{6}} & 0 \\ 0 & \frac{i}{\sqrt{6}} & 0 & \frac{i}{\sqrt{2}} \end{pmatrix}, \tag{A65}$$

$$S_3 = \begin{pmatrix} 0 & -\sqrt{\frac{2}{3}} & 0 & 0 \\ 0 & 0 & -\sqrt{\frac{2}{3}} & 0 \end{pmatrix}, \tag{A66}$$

which are normalized as follows:

$$S_i S_j^\dagger = \frac{2\delta_{ij} - i\epsilon_{ijk}\sigma_k}{3}. \tag{A67}$$

Now we define the nonrelativistic amplitudes as

$$\mathcal{A}(B \to B\pi^a) = -i\langle B\pi^a|\mathcal{L}|B\rangle, \tag{A68}$$

with $B = B_{\bar{3}}$, B_6, B_6^*. For the transitions involving Λ_c we have

$$\mathcal{A}(\Lambda_c \to \Sigma_c \pi^a) = \frac{g_3}{\sqrt{3} f_\pi} t^a \vec{\sigma} \cdot \vec{q}, \tag{A69}$$

$$\mathcal{A}(\Lambda_c \to \Sigma_c^* \pi^a) = \frac{g_3}{f_\pi} t^a \vec{S}^\dagger \cdot \vec{q}, \tag{A70}$$

$$\mathcal{A}(\Sigma_c^* \to \Lambda_c \pi^a) = \frac{g_3}{f_\pi} t^a \vec{S} \cdot \vec{q}. \tag{A71}$$

For the transitions involving Ξ_c we have

$$\mathcal{A}(\Xi_c' \to \Xi_c \pi^a) = \frac{g_3}{\sqrt{3} f_\pi} \frac{\tau^a}{2} \vec{\sigma} \cdot \vec{q}, \tag{A72}$$

$$\mathcal{A}(\Xi_c' \to \Xi_c^* \pi^a) = \frac{g_3}{f_\pi} \frac{\tau^a}{2} \vec{S}^\dagger \cdot \vec{q}, \tag{A73}$$

$$\mathcal{A}(\Xi_c^* \to \Xi_c' \pi^a) = \frac{g_3}{f_\pi} \frac{\tau^a}{2} \vec{S} \cdot \vec{q}. \tag{A74}$$

For the ones with the Ξ_c' and Ξ_c^*, the amplitudes read

$$\mathcal{A}(\Xi_c' \to \Xi_c' \pi^a) = \frac{2 g_2}{3 f_\pi} \frac{\tau^a}{2\sqrt{2}} \vec{\sigma} \cdot \vec{q}, \tag{A75}$$

$$\mathcal{A}(\Xi_c'^* \to \Xi_c'^* \pi^a) = \frac{2 g_2}{3 f_\pi} \frac{\tau^a}{2\sqrt{2}} \vec{\Sigma} \cdot \vec{q}, \tag{A76}$$

$$\mathcal{A}(\Xi_c'^* \to \Xi_c' \pi^a) = \frac{g_2}{\sqrt{3} f_\pi} \frac{\tau^a}{2\sqrt{2}} \vec{S} \cdot \vec{q}, \tag{A77}$$

$$\mathcal{A}(\Xi_c \to \Xi_c'^* \pi^a) = \frac{g_2}{\sqrt{3} f_\pi} \frac{\tau^a}{2\sqrt{2}} \vec{S}^\dagger \cdot \vec{q}. \tag{A78}$$

Finally for the transitions with the Σ_c and Σ_c^*, we have the following amplitudes:

$$\mathcal{A}(\Sigma_c \to \Sigma_c \pi^a) = \frac{2 g_2}{3 f_\pi} \frac{T^a}{\sqrt{2}} \vec{\sigma} \cdot \vec{q}, \tag{A79}$$

$$\mathcal{A}(\Sigma_c^* \to \Sigma_c^* \pi^a) = \frac{2 g_2}{3 f_\pi} \frac{T^a}{\sqrt{2}} \vec{\Sigma} \cdot \vec{q}, \tag{A80}$$

$$\mathcal{A}(\Sigma_c^* \to \Sigma_c \pi^a) = \frac{g_2}{\sqrt{3} f_\pi} \frac{T^a}{\sqrt{2}} \vec{S} \cdot \vec{q}, \tag{A81}$$

$$\mathcal{A}(\Sigma_c \to \Sigma_c^* \pi^a) = \frac{g_2}{\sqrt{3} f_\pi} \frac{T^a}{\sqrt{2}} \vec{S}^\dagger \cdot \vec{q}. \tag{A82}$$

5. G-parity and heavy antibaryons

The amplitudes in Eqs. (A69)–(A82) are for the heavy baryons. Here we deduce the amplitudes for the heavy antibaryons by working in the isospin basis and applying a G-parity transformation, which is a combination of a C-parity transformation and a rotation in isospin space [47]:

$$G = C e^{i\pi I_2}, \tag{A83}$$

with I_2 the second Cartesian component of the isospin matrix. Now we will determine how G operates on the different fields we consider here. For instance, pions have well-defined G-parity:

$$G|\pi\rangle = -|\pi\rangle. \tag{A84}$$

We can write it in terms of the components of the pion field for completeness:

$$G \begin{pmatrix} |\pi^+\rangle \\ |\pi^0\rangle \\ |\pi^-\rangle \end{pmatrix} = - \begin{pmatrix} |\pi^+\rangle \\ |\pi^0\rangle \\ |\pi^-\rangle \end{pmatrix}. \tag{A85}$$

If we consider baryons instead, G will transform a baryon into an antibaryon in the same isospin state. If we consider nucleons or other isospin-$\frac{1}{2}$ baryons, the G-parity transformation works as follows:

$$G \begin{pmatrix} |p\rangle \\ |n\rangle \end{pmatrix} = \begin{pmatrix} |\bar{n}\rangle \\ -|\bar{p}\rangle \end{pmatrix}. \tag{A86}$$

Now we can identify antiparticle states with isospinors as follows:

$$|\bar{n}\rangle = \left|\frac{1}{2} + \frac{1}{2}\right\rangle_I, \tag{A87}$$

$$|\bar{p}\rangle = -\left|\frac{1}{2} - \frac{1}{2}\right\rangle_I, \tag{A88}$$

where we use the subscript I to indicate that we are indeed referring to isospinors. From the nucleon/antinucleon example we can appreciate that the idea of a G-parity transformation is to have a good mapping between the isospin and the particle/antiparticle basis. The crucial point in the G-parity transformation for the baryons is the relative minus sign between the isospin vectors of the antineutron and antiproton, which in turn allows for the use of the same SU(2) Clebsch-Gordan coefficients in the baryon and antibaryon cases.

For the heavy baryons the idea is the same as for the nucleons. But there is a subtlety: we are considering different C-parity conventions for the spin-$\frac{1}{2}$ and spin-$\frac{3}{2}$ fields,

$$C|B\rangle = |\bar{B}\rangle, \tag{A89}$$

$$C|B_6^*\rangle = -|\bar{B}_6^*\rangle, \tag{A90}$$

where $B = B_{\bar{3}}, B_6$. For the antitriplet and sextet spin-$\frac{1}{2}$ heavy cascades, the transformation works exactly as in nucleons,

$$G\begin{pmatrix} |\Xi_c^{+(\prime)}\rangle \\ |\Xi_c^{0(\prime)}\rangle \end{pmatrix} = \begin{pmatrix} |\bar{\Xi}_c^{0(\prime)}\rangle \\ -|\Xi_c^{-(\prime)}\rangle \end{pmatrix}, \tag{A91}$$

while for the sextet spin-3/2 heavy cascades we have

$$G\begin{pmatrix} |\Xi_c^{+*}\rangle \\ |\Xi_c^{0*}\rangle \end{pmatrix} = -\begin{pmatrix} |\bar{\Xi}_c^{0*}\rangle \\ -|\Xi_c^{-*}\rangle \end{pmatrix}. \tag{A92}$$

For the isotriplet heavy baryons $\{\Sigma_c^{++}, \Sigma_c^{+}, \Sigma_c^{0}\}$, we have instead

$$G\begin{pmatrix} |\Sigma_c^{++}\rangle \\ |\Sigma_c^{+}\rangle \\ |\Sigma_c^{0}\rangle \end{pmatrix} = \begin{pmatrix} |\bar{\Sigma}_c^{0}\rangle \\ -|\Sigma_c^{-}\rangle \\ |\Sigma_c^{--}\rangle \end{pmatrix}, \tag{A93}$$

plus the transformation for the excited isotriplet heavy baryons, which will carry an extra minus sign.

With the G-parity transformation we can deduce the amplitudes for the antibaryons from the ones we already know for the baryons:

$$\mathcal{A}(\bar{B} \to \bar{B}\pi^a) = -\mathcal{A}(B \to B\pi^a), \tag{A94}$$

$$\mathcal{A}(\bar{B} \to \bar{B}_6^*\pi^a) = +\mathcal{A}(B \to B_6^*\pi^a), \tag{A95}$$

$$\mathcal{A}(\bar{B}_6^* \to \bar{B}\pi^a) = +\mathcal{A}(B_6^* \to B\pi^a), \tag{A96}$$

$$\mathcal{A}(\bar{B}_6^* \to \bar{B}_6^*\pi^a) = -\mathcal{A}(B_6^* \to B_6^*\pi^a), \tag{A97}$$

where $B = B_{\bar{3}}, B_6$. The signs simply reflect the sign for the G-parity transformation of the pion, plus the extra sign involved in the $B_{\bar{3}}/B_6 \to B_6^*$ and $B_6^* \to B_{\bar{3}}/B_6$ transitions. For a detailed example we consider

$$\begin{aligned} \mathcal{A}(\bar{B}_6 \to \bar{B}_6\pi^a) &= i\langle \bar{B}_6\pi^a|\mathcal{L}|\bar{B}_6\rangle \\ &= -i\langle G(B_6\pi^a)|\mathcal{L}|GB_6\rangle \\ &= -i\langle B_6\pi^a|G^\dagger\mathcal{L}G|B_6\rangle \\ &= -i\langle B_6\pi^a|\mathcal{L}|B_6\rangle \\ &= -\mathcal{A}(B_6 \to B_6\pi^a), \end{aligned} \tag{A98}$$

where we have used that $G^2|B_6\rangle = \pm 1$ (-1 for Ξ_Q', $+1$ for Σ_Q), $G^2|\pi\rangle = +1$, and $G^\dagger\mathcal{L}G = \mathcal{L}$.

6. The OPE potential

With the amplitudes of Eqs. (A69)–(A82) we can derive the potential by using Eq. (A2). For simplicity we will consider the heavy quark limit, in which the B_6 and B_6^* heavy baryons are degenerate. For the $T\bar{S} = \Lambda_c\bar{\Sigma}_c, \Lambda_c\bar{\Sigma}_c^*$ and $T\bar{S} = \Xi_c\bar{\Xi}_c', \Xi_c\bar{\Xi}_c^*$ potentials, we write the potential in the bases,

$$\mathcal{B}_{\Lambda_c\bar{\Sigma}_c} = \{\Lambda_c\bar{\Sigma}_c, \Sigma_c\bar{\Lambda}_c, \Lambda_c\bar{\Sigma}_c^*, \Sigma_c^*\bar{\Lambda}_c\}, \tag{A99}$$

$$\mathcal{B}_{\Xi_c'\bar{\Xi}_c} = \{\Xi_c\bar{\Xi}_c', \Xi_c'\bar{\Xi}_c, \Xi_c\bar{\Xi}_c^*, \Xi_c^*\bar{\Xi}_c\}, \tag{A100}$$

in which the potential reads as

$$V_{\rm OPE}^{S\bar{T}}(\vec{q}) = \frac{g_3^2}{f_\pi^2}\tau\frac{1}{\vec{q}^2+\mu_\pi^2}\begin{pmatrix} 0 & \frac{1}{3}\vec{\sigma}_1\cdot\vec{q}\vec{\sigma}_2\cdot\vec{q} & 0 & \frac{1}{\sqrt{3}}\vec{S}_1\cdot\vec{q}\vec{\sigma}_2\cdot\vec{q} \\ \frac{1}{3}\vec{\sigma}_1\cdot\vec{q}\vec{\sigma}_2\cdot\vec{q} & 0 & \frac{1}{\sqrt{3}}\vec{\sigma}_1\cdot\vec{q}\vec{S}_2\cdot\vec{q} & 0 \\ 0 & \frac{1}{\sqrt{3}}\vec{\sigma}_1\cdot\vec{q}\vec{S}_2^\dagger\cdot\vec{q} & 0 & \vec{S}_1^\dagger\cdot\vec{q}\vec{S}_2^\dagger\cdot\vec{q} \\ \frac{1}{\sqrt{3}}\vec{S}_1^\dagger\cdot\vec{q}\vec{\sigma}_2\cdot\vec{q} & 0 & \vec{S}_1^\dagger\cdot\vec{q}\vec{S}_2\cdot\vec{q} & 0 \end{pmatrix} + \mathcal{O}\left(\frac{1}{m_Q}\right), \tag{A101}$$

where the isospin factor τ is

$$\tau(\Lambda_c\bar{\Sigma}_c) = 1, \tag{A102}$$

$$\tau(\Xi_c\bar{\Xi}_c') = \frac{\vec{\tau}_1\cdot\vec{\tau}_2}{4}. \tag{A103}$$

The effective pion mass in the heavy quark limit is given by $\mu_\pi^2 = m_\pi^2 - (m_{\Sigma_c} - m_{\Lambda_c})^2$ or $\mu_\pi^2 = m_\pi^2 - (m_{\Xi_c'} - m_{\Xi_c})^2$, respectively. For the $S\bar{S}$ potential we use the bases

$$\mathcal{B}_{\Xi_c'\bar{\Xi}_c'} = \{\Xi_c'\bar{\Xi}_c', \Xi_c'\bar{\Xi}_c^*, \Xi_c^*\bar{\Xi}_c', \Xi_c^*\bar{\Xi}_c^*\}, \tag{A104}$$

$$\mathcal{B}_{\Sigma_c\bar{\Sigma}_c} = \{\Sigma_c\bar{\Sigma}_c, \Sigma_c\bar{\Sigma}_c^*, \Sigma_c^*\bar{\Sigma}_c, \Sigma_c^*\bar{\Sigma}_c^*\}, \tag{A105}$$

in which the potential reads

$$V_{\rm OPE}^{S\bar{S}}(\vec{q}) = \frac{2g_2^2}{9f_\pi^2}\tau\frac{1}{\vec{q}^2+m_\pi^2}\begin{pmatrix} +\vec{\sigma}_1\cdot\vec{q}\vec{\sigma}_2\cdot\vec{q} & -\lambda\vec{\sigma}_1\cdot\vec{q}\vec{S}_2\cdot\vec{q} & +\lambda\vec{S}_1\cdot\vec{q}\vec{\sigma}_2\cdot\vec{q} & -\lambda^2\vec{S}_1\cdot\vec{q}\vec{S}_2\cdot\vec{q} \\ -\lambda\vec{\sigma}_1\cdot\vec{q}\vec{S}_2\cdot\vec{q} & +\vec{\sigma}_1\cdot\vec{q}\vec{\Sigma}_2\cdot\vec{q} & -\lambda^2\vec{S}_1\cdot\vec{q}\vec{S}_2^\dagger\cdot\vec{q} & +\lambda\vec{S}_1\cdot\vec{q}\vec{\Sigma}_2\cdot\vec{q} \\ +\lambda\vec{S}_1^\dagger\cdot\vec{q}\vec{\sigma}_2\cdot\vec{q} & -\lambda^2\vec{S}_1^\dagger\cdot\vec{q}\vec{S}_2\cdot\vec{q} & +\vec{\Sigma}_1\cdot\vec{q}\vec{\sigma}_2\cdot\vec{q} & -\lambda\vec{\Sigma}_1\cdot\vec{q}\vec{S}_2\cdot\vec{q} \\ -\lambda^2\vec{S}_1^\dagger\cdot\vec{q}\vec{S}_2^\dagger\cdot\vec{q} & +\lambda\vec{S}_1^\dagger\cdot\vec{q}\vec{\Sigma}_2\cdot\vec{q} & -\lambda\vec{\Sigma}_1\cdot\vec{q}\vec{S}_2^\dagger\cdot\vec{q} & +\vec{\Sigma}_1\cdot\vec{q}\vec{\Sigma}_2\cdot\vec{q} \end{pmatrix} + \mathcal{O}\left(\frac{1}{m_Q}\right), \quad \text{(A106)}$$

where $\lambda = \frac{\sqrt{3}}{2}$ and where the isospin factor is

$$\tau(\Xi_c'\bar{\Xi}_c') = \frac{\vec{\tau}_1\cdot\vec{\tau}_2}{4}, \quad \text{(A107)}$$

$$\tau(\Sigma_c\bar{\Sigma}_c) = \vec{T}_1\cdot\vec{T}_2. \quad \text{(A108)}$$

7. Coordinate space

The general form of the $S\bar{T}$ and $S\bar{S}$ potential in momentum space can be written as

$$V_{\rm OBE}^{T\bar{S}} = -R_1\bar{R}_2\frac{g_3^2}{2f_\pi^2}\vec{I}_1\cdot\vec{I}_2\frac{\vec{a}_1\cdot\vec{q}\vec{a}_2\cdot\vec{q}}{q^2+\mu_\pi^2}, \quad \text{(A109)}$$

$$V_{\rm OPE}^{S\bar{S}} = -R_1\bar{R}_2\frac{g_2^2}{2f_\pi^2}\vec{I}_1\cdot\vec{I}_2\frac{\vec{a}_1\cdot\vec{q}\vec{a}_2\cdot\vec{q}}{q^2+\mu_\pi^2}, \quad \text{(A110)}$$

where R_1 and $\bar{R}_2$ are numerical factors; μ_π is the effective pion mass at the vertices (as explained in the previous section); I_1, I_2 the appropriate isospin matrices; and $\vec{a}_1$, $\vec{a}_1$ are the spin matrices acting on vertex 1 and 2. The specific factors can be worked out easily from Eqs. (A101) and (A106) to obtain the results of Table IV. The coordinate space potential is obtained by Fourier transforming the momentum space potential:

$$V^{(0)}(\vec{r}) = \int\frac{d^3q}{(2\pi)^3}V^{(0)}(\vec{q})e^{-i\vec{q}\cdot\vec{r}} = R_1\bar{R}_2\frac{g_i^2}{2f_\pi^2}\vec{I}_1\cdot\vec{I}_2(\vec{a}_1\cdot\nabla)(\vec{a}_2\cdot\nabla)\frac{e^{-\mu_\pi r}}{4\pi r}, \quad \text{(A111)}$$

where $g_i = g_2$ or g_3 depending on the case. From this we obtain the expressions we already wrote in Eqs. (61)–(65).

Here we will write the coordinate space potential in coupled channels, in which case we obtain

$$V_{S\bar{T}}^{(0)}(\vec{r}) = \tau\frac{g_3^2}{3f_\pi^2}\mathbf{C}_{12}^{S\bar{T}}\delta^3(\vec{r}) - \tau[\mathbf{C}_{12}^{S\bar{T}}W_C(r) + \mathbf{S}_{12}^{S\bar{T}}(\hat{r})W_T(r)], \quad \text{(A112)}$$

$$V_{S\bar{S}}^{(0)}(\vec{r}) = \tau\frac{2g_3^2}{27f_\pi^2}\mathbf{C}_{12}^{S\bar{S}}\delta^3(\vec{r}) - \tau\frac{2}{9}[\mathbf{C}_{12}^{S\bar{S}}W_C(r) + \mathbf{S}_{12}^{S\bar{S}}(\hat{r})W_T(r)], \quad \text{(A113)}$$

where W_C and W_T are defined in Eqs. (64) and (65), and with the central and tensor matrices given by

$$\mathbf{C}_{12}^{S\bar{T}} = \begin{pmatrix} 0 & \frac{1}{3}\vec{\sigma}_1\cdot\vec{\sigma}_2 & 0 & \frac{1}{\sqrt{3}}\vec{S}_1\cdot\vec{\sigma}_2 \\ \frac{1}{3}\vec{\sigma}_1\cdot\vec{\sigma}_2 & 0 & \frac{1}{\sqrt{3}}\vec{\sigma}_1\cdot\vec{S}_2 & 0 \\ 0 & \frac{1}{\sqrt{3}}\vec{\sigma}_1\cdot\vec{S}_2^\dagger & 0 & \vec{S}_1^\dagger\cdot\vec{S}_2^\dagger \\ \frac{1}{\sqrt{3}}\vec{S}_1^\dagger\cdot\vec{\sigma}_2 & 0 & \vec{S}_1^\dagger\cdot\vec{S}_2 & 0 \end{pmatrix}, \quad \text{(A114)}$$

$$\mathbf{C}_{12}^{S\bar{S}} = \begin{pmatrix} +\vec{\sigma}_1\cdot\vec{\sigma}_2 & -\lambda\vec{\sigma}_1\cdot\vec{S}_2 & +\lambda\vec{S}_1\cdot\vec{\sigma}_2 & -\lambda^2\vec{S}_1\cdot\vec{S}_2 \\ -\lambda\vec{\sigma}_1\cdot\vec{S}_2 & +\vec{\sigma}_1\cdot\vec{\Sigma}_2 & -\lambda^2\vec{S}_1\cdot\vec{S}_2^\dagger & +\lambda\vec{S}_1\cdot\vec{\Sigma}_2 \\ +\lambda\vec{S}_1^\dagger\cdot\vec{\sigma}_2 & -\lambda^2\vec{S}_1^\dagger\cdot\vec{S}_2 & +\vec{\Sigma}_1\cdot\vec{\sigma}_2 & -\lambda\vec{\Sigma}_1\cdot\vec{S}_2 \\ -\lambda^2\vec{S}_1^\dagger\cdot\vec{S}_2^\dagger & +\lambda\vec{S}_1^\dagger\cdot\vec{\Sigma}_2 & -\lambda\vec{\Sigma}_1\cdot\vec{S}_2^\dagger & +\vec{\Sigma}_1\cdot\vec{\Sigma}_2 \end{pmatrix}, \quad \text{(A115)}$$

$$\mathbf{S}_{12}^{S\bar{T}}(\hat{r}) = \begin{pmatrix} 0 & \frac{1}{3}S_{12}(\vec{\sigma}_1,\vec{\sigma}_2,\hat{r}) & 0 & \frac{1}{\sqrt{3}}S_{12}(\vec{S}_1,\vec{\sigma}_2,\hat{r}) \\ \frac{1}{3}S_{12}(\vec{\sigma}_1,\vec{\sigma}_2,\hat{r}) & 0 & \frac{1}{\sqrt{3}}S_{12}(\vec{\sigma}_1,\vec{S}_2,\hat{r}) & 0 \\ 0 & \frac{1}{\sqrt{3}}S_{12}(\vec{\sigma}_1,\vec{S}_2^\dagger,\hat{r}) & 0 & S_{12}(\vec{S}_1^\dagger,\vec{S}_2^\dagger,\hat{r}) \\ \frac{1}{\sqrt{3}}S_{12}(\vec{S}_1^\dagger,\vec{\sigma}_2,\hat{r}) & 0 & S_{12}(\vec{S}_1^\dagger,\vec{S}_2,\hat{r}) & 0 \end{pmatrix}, \quad \text{(A116)}$$

$$\mathbf{S}_{12}^{S\bar{S}}(\hat{r}) = \begin{pmatrix} +S_{12}(\vec{\sigma}_1,\vec{\sigma}_2,\hat{r}) & -\lambda S_{12}(\vec{\sigma}_1,\vec{S}_2,\hat{r}) & +\lambda S_{12}(\vec{S}_1,\vec{\sigma}_2,\hat{r}) & -\lambda^2 S_{12}(\vec{S}_1,\vec{S}_2,\hat{r}) \\ -\lambda S_{12}(\vec{\sigma}_1,\vec{S}_2,\hat{r}) & +S_{12}(\vec{\sigma}_1,\vec{\Sigma}_2,\hat{r}) & -\lambda^2 S_{12}(\vec{S}_1,\vec{S}_2^\dagger,\hat{r}) & +\lambda S_{12}(\vec{S}_1,\vec{\Sigma}_2,\hat{r}) \\ +\lambda S_{12}(\vec{S}_1^\dagger,\vec{\sigma}_2,\hat{r}) & -\lambda^2 S_{12}(\vec{S}_1^\dagger,\vec{S}_2,\hat{r}) & +S_{12}(\vec{\Sigma}_1,\vec{\sigma}_2,\hat{r}) & -\lambda S_{12}(\vec{\Sigma}_1,\vec{S}_2,\hat{r}) \\ -\lambda^2 S_{12}(\vec{S}_1^\dagger,\vec{S}_2^\dagger,\hat{r}) & +\lambda S_{12}(\vec{S}_1^\dagger,\vec{\Sigma}_2,\hat{r}) & -\lambda S_{12}(\vec{\Sigma}_1,\vec{S}_2^\dagger,\hat{r}) & +S_{12}(\vec{\Sigma}_1,\vec{\Sigma}_2,\hat{r}) \end{pmatrix}. \tag{A117}$$

8. The partial wave projection

Heavy baryon-antibaryon bound states have well-defined J^P quantum numbers. Hence we can simplify the OPE potential by projecting it into partial waves with well-defined parity and angular momentum. For this we define the states

$$|S\bar{T}(jm)\rangle = \sum_{lm_l sm_s} Y_{lm_l}(\hat{r})|sm_s\rangle\langle lm_l sm_s|jm\rangle, \tag{A118}$$

$$|S\bar{S}(jm)\rangle = \sum_{lm_l sm_s} Y_{lm_l}(\hat{r})|sm_s\rangle\langle lm_l sm_s|jm\rangle, \tag{A119}$$

where j, m is the total angular momentum and its third component for the heavy baryon-antibaryon pair, while l, m_l and s, m_s refer to the angular momentum and spin of the pair. The product $\langle lm_l sm_s|jm\rangle$ is the Clebsch-Gordan coefficient for that particular combination of total, orbital, and spin angular momentum (notice that, when applied to the coupling of angular momentum, the Clebsch-Gordan coefficients are independent of whether we have particles or antiparticles). The spin wave function can be further decomposed as

$$|sm_s\rangle = \sum_{m_1 m_2} |s_1 m_1\rangle|s_2 m_2\rangle\langle s_1 m_1 s_2 m_2|sm_s\rangle, \tag{A120}$$

with s_1 and s_2 the spin of the heavy baryon 1 and 2 (either $\frac{1}{2}$ or $\frac{3}{2}$).

In this basis we can compute the partial wave projection of $\mathbf{C}_{12}$ and $\mathbf{S}_{12}$ as

$$\begin{aligned} &\langle (s'l')j'm'|\mathbf{O}_{12}|(sl)jm\rangle \\ &= \int d^2\hat{r}\langle (s'l')j'm'|\mathbf{O}_{12}(\hat{r})|(sl)jm\rangle \\ &= \delta_{jj'}\delta_{mm'}\mathbf{O}^j_{ss'll'}, \end{aligned} \tag{A121}$$

where the total angular momentum and its third component are conserved. The central force C_{12} conserves in addition the orbital angular momentum and the spin:

$$\mathbf{C}^j_{ss'll'} = \delta_{ss'}\delta_{ll'}\mathbf{C}^j_{ls}. \tag{A122}$$

The tensor force is more involved. Owing to conservation of parity, $|l - l'|$ must be an even number. The spin transitions are more complicated because in the general case $|s - s'|$ can be even or odd. The exceptions are the $B_{\bar{3}}\bar{B}_{\bar{3}}$, $B_6\bar{B}_6$, and $B_6^*\bar{B}_6^*$ systems: these systems usually have well-defined C- or G-parity, which implies that $|s - s'|$ is even. Even when C-/G-parity is not well defined, like in the $\Xi_c^*\bar{\Sigma}_c^*$ system, the tensor operator involves identical spin-matrices and is symmetrical under the exchange of particles 1 and 2:

$$S_{12}^{B_{\bar{3}}\bar{B}_{\bar{3}}} = S_{12}^{B_6\bar{B}_6} = 3\vec{\sigma}_1\cdot\hat{r}\vec{\sigma}_2\cdot\hat{r} - \vec{\sigma}_1\cdot\vec{\sigma}_2, \tag{A123}$$

$$S_{12}^{B_6^*\bar{B}_6^*} = 3\vec{\Sigma}_1\cdot\hat{r}\vec{\Sigma}_2\cdot\hat{r} - \vec{\Sigma}_1\cdot\vec{\Sigma}_2. \tag{A124}$$

As a consequence, the matrix elements for the tensor operator vanish for odd $|s - s'|$. But if we consider the $B_{\bar{3}}\bar{B}_6^*$ and $B_6\bar{B}_6^*$ systems (for example, the $\Xi_c\bar{\Xi}_c^*$ and $\Sigma_c'\bar{\Sigma}_c^*$ systems), it is perfectly possible to have a mix of even and odd spin. The odd $|s - s'|$ transitions have a particularity that it is worth mentioning. The matrix element for the tensor operator for odd $|s - s'|$ changes sign as follows:

$$\langle B\bar{B}_6^*|\mathbf{S}^j_{s(s\pm1)ll'}|B\bar{B}_6^*\rangle = -\langle B_6^*\bar{B}|\mathbf{S}^j_{s(s\pm1)ll'}|B_6^*\bar{B}\rangle, \tag{A125}$$

$$\langle B\bar{B}_6^*|\mathbf{S}^j_{s(s\pm1)ll'}|B_6^*\bar{B}\rangle = -\langle B_6^*\bar{B}|\mathbf{S}^j_{s(s\pm1)ll'}|B\bar{B}_6^*\rangle, \tag{A126}$$

with $B = B_{\bar{3}}$ or B_6. In fact, the previous two equations indicate that it is actually a good idea to take explicitly into account the particle coupled channel structure. Now if we consider the bases

$$\mathcal{B}' = \{B_{\bar{3}}\bar{B}_6^*, B_6^*\bar{B}_{\bar{3}}\}, \tag{A127}$$

$$\mathcal{B} = \{B_6\bar{B}_6^*, B_6^*\bar{B}_6\}, \tag{A128}$$

then for $\mathcal{B}'$ we can write the central and tensor operators as

$$C'_{12} = \begin{pmatrix} 0 & \vec{S}_1^\dagger\cdot\vec{S}_2 \\ \vec{S}_1\cdot\vec{S}_2^\dagger & 0 \end{pmatrix}, \tag{A129}$$

$$S'_{12}(\hat{r}) = \begin{pmatrix} & S_{12}(\vec{S}_1^\dagger,\vec{S}_2,\hat{r}) \\ S_{12}(\vec{S}_1,\vec{S}_2^\dagger,\hat{r}) & 0 \end{pmatrix}, \tag{A130}$$

while for $\mathcal{B}$ they read

$$C_{12} = \begin{pmatrix} \vec{\sigma}_1 \cdot \vec{\Sigma}_2 & \vec{S}_1^\dagger \cdot \vec{S}_2 \\ \vec{S}_1 \cdot \vec{S}_2^\dagger & \vec{\Sigma}_1 \cdot \vec{\sigma}_2 \end{pmatrix}, \tag{A131}$$

$$S_{12}(\hat{r}) = \begin{pmatrix} S_{12}(\vec{\sigma}_1, \vec{\Sigma}_2, \hat{r}) & S_{12}(\vec{S}_1^\dagger, \vec{S}_2, \hat{r}) \\ S_{12}(\vec{S}_1, \vec{S}_2^\dagger, \hat{r}) & S_{12}(\vec{\Sigma}_1, \cdot\vec{\sigma}_2, \hat{r}) \end{pmatrix}. \tag{A132}$$

This increases the complexity of the partial wave projection. However, in most cases we can define states with good C- or G-parity, which effectively amounts to reducing the previous coupled channel systems to a single channel problem.

The calculation of the matrix elements is straightforward in most cases. We begin with the $B\bar{B}$ system (with $B = B_{\bar{3}}$ or B_6), for which we have the partial waves

$$|B\bar{B}(0^-)\rangle = \{^1S_0\}, \tag{A133}$$

$$|B\bar{B}(1^-)\rangle = \{^3S_1, ^3D_1\}, \tag{A134}$$

which lead to the matrix elements

$$\mathbf{C}_{12}^{B\bar{B}}(0^-) = -3, \tag{A135}$$

$$\mathbf{C}_{12}^{B\bar{B}}(1^-) = \begin{pmatrix} 1 & 0 \\ 0 & 1 \end{pmatrix}, \tag{A136}$$

$$\mathbf{S}_{12}^{B\bar{B}}(0^-) = 0, \tag{A137}$$

$$\mathbf{S}_{12}^{B\bar{B}}(1^-) = \begin{pmatrix} 0 & 2\sqrt{2} \\ 2\sqrt{2} & -2 \end{pmatrix}. \tag{A138}$$

In terms of complexity, the next case is the $B_6^*\bar{B}_6^*$ system, for which the partial waves are

$$|B_6^*\bar{B}_6^*(0^-)\rangle = \{^1S_0, ^5D_0\}, \tag{A139}$$

$$|B_6^*\bar{B}_6^*(1^-)\rangle = \{^3S_1, ^3D_1, ^7D_1, ^7G_1\}, \tag{A140}$$

$$|B_6^*\bar{B}_6^*(2^-)\rangle = \{^1D_2, ^5S_2, ^5D_2, ^5G_2\}, \tag{A141}$$

$$|B_6^*\bar{B}_6^*(3^-)\rangle = \{^3D_3, ^3G_3, ^7S_3, ^7D_3, ^7G_3, ^7I_3\}, \tag{A142}$$

which translate into the following matrices:

$$\mathbf{C}_{12}^{B_6^*\bar{B}_6^*}(0^-) = \begin{pmatrix} -\frac{15}{4} & 0 \\ 0 & -\frac{3}{4} \end{pmatrix}, \tag{A143}$$

$$\mathbf{C}_{12}^{B_6^*\bar{B}_6^*}(1^-) = \begin{pmatrix} -\frac{11}{4} & 0 & 0 & 0 \\ 0 & -\frac{11}{4} & 0 & 0 \\ 0 & 0 & +\frac{9}{4} & 0 \\ 0 & 0 & 0 & +\frac{9}{4} \end{pmatrix}, \tag{A144}$$

$$\mathbf{C}_{12}^{B_6^*\bar{B}_6^*}(2^-) = \begin{pmatrix} -\frac{15}{4} & 0 & 0 & 0 \\ 0 & -\frac{3}{4} & 0 & 0 \\ 0 & 0 & -\frac{3}{4} & 0 \\ 0 & 0 & 0 & -\frac{3}{4} \end{pmatrix}, \tag{A145}$$

$$\mathbf{C}_{12}^{B_6^*\bar{B}_6^*}(3^-) = \begin{pmatrix} -\frac{11}{4} & 0 & 0 & 0 & 0 & 0 \\ 0 & -\frac{11}{4} & 0 & 0 & 0 & 0 \\ 0 & 0 & +\frac{9}{4} & 0 & 0 & 0 \\ 0 & 0 & 0 & +\frac{9}{4} & 0 & 0 \\ 0 & 0 & 0 & 0 & +\frac{9}{4} & 0 \\ 0 & 0 & 0 & 0 & 0 & +\frac{9}{4} \end{pmatrix}, \tag{A146}$$

$$\mathbf{S}_{12}^{B_6^*\bar{B}_6^*}(0^-) = \begin{pmatrix} 0 & -3 \\ -3 & -3 \end{pmatrix}, \tag{A147}$$

$$\mathbf{S}_{12}^{B_6^*\bar{B}_6^*}(1^-) = \begin{pmatrix} 0 & \frac{17}{5\sqrt{2}} & -\frac{3\sqrt{7}}{5} & 0 \\ \frac{17}{5\sqrt{2}} & -\frac{17}{10} & \frac{3}{5}\sqrt{\frac{2}{7}} & -\frac{9}{5}\sqrt{\frac{6}{7}} \\ -\frac{3\sqrt{7}}{5} & \frac{3}{5}\sqrt{\frac{2}{7}} & -\frac{108}{35} & \frac{9\sqrt{3}}{35} \\ 0 & -\frac{9}{5}\sqrt{\frac{6}{7}} & \frac{9\sqrt{3}}{35} & -\frac{45}{14} \end{pmatrix}, \tag{A148}$$

$$\mathbf{S}_{12}^{B_6^*\bar{B}_6^*}(2^-) = \begin{pmatrix} 0 & -\frac{3}{\sqrt{5}} & 3\sqrt{\frac{2}{7}} & -9\sqrt{\frac{2}{35}} \\ -\frac{3}{\sqrt{5}} & 0 & 3\sqrt{\frac{7}{10}} & 0 \\ 3\sqrt{\frac{2}{7}} & 3\sqrt{\frac{7}{10}} & \frac{9}{14} & \frac{18}{7\sqrt{5}} \\ -9\sqrt{\frac{2}{35}} & 0 & \frac{18}{7\sqrt{5}} & -\frac{15}{7} \end{pmatrix}, \tag{A149}$$

$$\mathbf{S}_{12}^{B_6^*\bar{B}_6^*}(3^-) = \begin{pmatrix} -\frac{17}{35} & \frac{51\sqrt{3}}{35} & -\frac{3\sqrt{3}}{5} & \frac{36}{35} & -\frac{3\sqrt{66}}{35} & 0 \\ \frac{51\sqrt{3}}{35} & -\frac{17}{14} & 0 & -\frac{3\sqrt{3}}{35} & \frac{9}{7}\sqrt{\frac{2}{11}} & -3\sqrt{\frac{3}{11}} \\ -\frac{3\sqrt{3}}{5} & 0 & 0 & \frac{9\sqrt{3}}{5} & 0 & 0 \\ \frac{36}{35} & -\frac{3\sqrt{3}}{35} & \frac{9\sqrt{3}}{5} & \frac{99}{70} & \frac{9\sqrt{66}}{35} & 0 \\ -\frac{3\sqrt{66}}{35} & \frac{9}{7}\sqrt{\frac{2}{11}} & 0 & \frac{9\sqrt{66}}{35} & -\frac{27}{77} & \frac{9}{11}\sqrt{\frac{3}{2}} \\ 0 & -3\sqrt{\frac{3}{11}} & 0 & 0 & \frac{9}{11}\sqrt{\frac{3}{2}} & -\frac{63}{22} \end{pmatrix}. \tag{A150}$$

We will continue with the $B_{\bar{3}}\bar{B}_6$ system, where we have the partial waves

$$|B_{\bar{3}}\bar{B}_6(0^-)\rangle = \{^1S_0\}, \tag{A151}$$

$$|B_{\bar{3}}\bar{B}_6(1^-)\rangle = \{^3S_1, ^3D_1\}. \tag{A152}$$

For these systems OPE is nondiagonal: the $B_{\bar{3}}B_{\bar{3}}\pi$ vertex is zero and OPE involves the $B_{\bar{3}}\bar{B}_6 \to B_6\bar{B}_{\bar{3}}$ transition. In fact there is only one case, the $\Xi_c\Xi_c'$ system, in which OPE does not cancel. For this system either C- or G-parity is well defined, for which we define the standard states

$$|B_{\bar{3}}\bar{B}_6(\eta)\rangle = \frac{1}{\sqrt{2}}[|B_{\bar{3}}\bar{B}_6\rangle + \eta|B_6\bar{B}_{\bar{3}}\rangle], \tag{A153}$$

with $C = \eta(-1)^{L+S}$. With this definition in mind, the projection of the central and tensor operators read

$$\mathbf{C}_{12}^{B_{\bar{3}}\bar{B}_6}(0^-) = -3\eta, \tag{A154}$$

$$\mathbf{C}_{12}^{B_{\bar{3}}\bar{B}_6}(1^-) = \eta\begin{pmatrix} 1 & 0 \\ 0 & 1 \end{pmatrix}, \tag{A155}$$

$$\mathbf{S}_{12}^{B_{\bar{3}}\bar{B}_6}(0^-) = 0, \tag{A156}$$

$$\mathbf{S}_{12}^{B_{\bar{3}}\bar{B}_6}(1^-) = \eta\begin{pmatrix} 0 & 2\sqrt{2} \\ 2\sqrt{2} & -2 \end{pmatrix}. \tag{A157}$$

The next case is the $B_{\bar{3}}\bar{B}_6^*$ system. As happened with the $B_{\bar{3}}\bar{B}_6$ case, the $B_{\bar{3}}\bar{B}_6^*$ system involves only nondiagonal OPE transitions, i.e., $B_{\bar{3}}\bar{B}_6^* \to \bar{B}_{\bar{3}}B_6$. We have the partial waves

$$|B_{\bar{3}}\bar{B}_6^*(1^-)\rangle = \{^3S_1, ^3D_1, ^5D_1\}, \tag{A158}$$

$$|B_{\bar{3}}\bar{B}_6^*(2^-)\rangle = \{^3D_1, ^5S_2, ^5D_2, ^5G_2\}. \tag{A159}$$

If we are considering states with well-defined C-parity

$$|B_{\bar{3}}\bar{B}_6^*(\eta)\rangle = \frac{1}{\sqrt{2}}[|B_{\bar{3}}\bar{B}_6^*\rangle + \eta|B_6^*\bar{B}_{\bar{3}}\rangle], \tag{A160}$$

where $C = \eta(-1)^{L+S}$, we find the combinations

$$|B_{\bar{3}}\bar{B}_6^*(1^{-+})\rangle = \{^3S_1(-), ^3D_1(-), ^5D_1(+)\}, \tag{A161}$$

$$|B_{\bar{3}}\bar{B}_6^*(2^{-+})\rangle = \{^3D_2(-), ^5S_2(+), ^5D_2(+), ^5G_2(+)\}, \tag{A162}$$

$$|B_{\bar{3}}\bar{B}_6^*(1^{--})\rangle = \{^3S_1(+), ^3D_1(+), ^5D_1(-)\}, \tag{A163}$$

$$|B_{\bar{3}}\bar{B}_6^*(2^{--})\rangle = \{^3D_2(+), ^5S_2(-), ^5D_2(-), ^5G_2(-)\}, \tag{A164}$$

where the number in parentheses is the value of $\eta = \pm 1$. That is, there is the complication that each partial wave in a particular channel can have a different η. Concrete calculations yield the following matrices:

$$\mathbf{C}_{12}^{E}(1^{-\pm}) = \pm\begin{pmatrix} -\frac{1}{3} & 0 & 0 \\ 0 & -\frac{1}{3} & 0 \\ 0 & 0 & 1 \end{pmatrix}, \tag{A165}$$

$$\mathbf{C}_{12}^{E}(2^{-\pm}) = \pm\begin{pmatrix} -\frac{1}{3} & 0 & 0 & 0 \\ 0 & 1 & 0 & 0 \\ 0 & 0 & 1 & 0 \\ 0 & 0 & 0 & 1 \end{pmatrix}, \tag{A166}$$

$$\mathbf{S}_{12}^{E}(1^{-\pm}) = \pm\begin{pmatrix} 0 & \frac{5}{3\sqrt{2}} & \frac{1}{\sqrt{2}} \\ \frac{5}{3\sqrt{2}} & -\frac{5}{6} & \frac{1}{2} \\ \frac{1}{\sqrt{2}} & \frac{1}{2} & \frac{1}{2} \end{pmatrix}, \tag{A167}$$

$$\mathbf{S}_{12}^{E}(2^{-\pm}) = \pm\begin{pmatrix} \frac{5}{6} & -\sqrt{\frac{3}{10}} & \frac{1}{2}\sqrt{\frac{3}{7}} & 2\sqrt{\frac{3}{35}} \\ -\sqrt{\frac{3}{10}} & 0 & -\sqrt{\frac{7}{10}} & 0 \\ \frac{1}{2}\sqrt{\frac{3}{7}} & -\sqrt{\frac{7}{10}} & -\frac{3}{14} & -\frac{6}{7\sqrt{5}} \\ 2\sqrt{\frac{3}{35}} & 0 & -\frac{6}{7\sqrt{5}} & \frac{5}{7} \end{pmatrix}. \tag{A168}$$

Here we have departed from the previous notation of indicating the channel with a superindex. Instead, we use the superindex ^{E} to indicate that it is exchange or nondiagonal OPE.

Lastly, the most complex cases are the $B_6\bar{B}_6^*$ system. The partial wave and C-parity structure is identical to the $B_{\bar{3}}\bar{B}_6^*$ case, but now there is also a diagonal or direct piece of OPE (besides the nondiagonal piece). The vertex factors R_1 and $\bar{R}_2$ are different for the direct and exchange pieces, which has to be taken into account when writing down the potential:

$$\begin{aligned} V_{\rm OPE} &= V^D_{\rm OPE} + V^E_{\rm OPE} \\ &= R_1^D \bar{R}_2^D \vec{I}_1 \cdot \vec{I}_2 [\mathbf{C}^D_{12} W_C + \mathbf{S}^D_{12} W_T] \\ &\quad + R_1^E \bar{R}_2^E \vec{I}_1 \cdot \vec{I}_2 [\mathbf{C}^E_{12} W_C + \mathbf{S}^E_{12} W_T]. \end{aligned} \tag{A169}$$

If we ignore the fact that the direct and exchange pieces can have a different effective pion mass μ_π, we can merge together the direct and exchange central and tensor matrices. For this we notice the relation

$$R_1^E \bar{R}_2^E = -\frac{3}{4} R_1^D \bar{R}_2^D. \tag{A170}$$

This implies that we can reexpress the OPE potential as

$$\begin{aligned} V_{\rm OPE} &= V^D_{\rm OPE} + V^E_{\rm OPE} \\ &= R_1^D \bar{R}_2^D \vec{I}_1 \cdot \vec{I}_2 [\mathbf{C}_{12} W_C + \mathbf{S}_{12} W_T], \end{aligned} \tag{A171}$$

where the central and tensor matrices $\mathbf{C}_{12}$ and $\mathbf{S}_{12}$ are a sum of the direct and exchange pieces

$$\mathbf{C}_{12}(J^{PC}) = \mathbf{C}^D_{12}(J^{PC}) - \frac{3}{4}\mathbf{C}^E_{12}(J^{PC}), \tag{A172}$$

$$\mathbf{S}_{12}(J^{PC}) = \mathbf{S}^D_{12}(J^{PC}) - \frac{3}{4}\mathbf{S}^E_{12}(J^{PC}). \tag{A173}$$

The $\mathbf{C}^D_{12}$ and $\mathbf{S}^E_{12}$ are identical to the ones we discussed in the $B_{\bar{3}}\bar{B}_6^*$ case; see Eqs. (A165)–(A168). The direct matrices are given by

$$\mathbf{C}^D_{12}(1^{-\pm}) = \begin{pmatrix} -\frac{5}{2} & 0 & 0 \\ 0 & -\frac{5}{2} & 0 \\ 0 & 0 & \frac{3}{2} \end{pmatrix}, \tag{A174}$$

$$\mathbf{C}^D_{12}(2^{-\pm}) = \begin{pmatrix} -\frac{5}{2} & 0 & 0 & 0 \\ 0 & +\frac{3}{2} & 0 & 0 \\ 0 & 0 & +\frac{3}{2} & 0 \\ 0 & 0 & 0 & +\frac{3}{2} \end{pmatrix}, \tag{A175}$$

$$\mathbf{S}^D_{12}(1^{-\pm}) = \begin{pmatrix} 0 & -\frac{1}{\sqrt{2}} & \frac{3}{\sqrt{2}} \\ -\frac{1}{\sqrt{2}} & \frac{1}{2} & \frac{3}{2} \\ \frac{3}{\sqrt{2}} & \frac{3}{2} & -\frac{3}{2} \end{pmatrix}, \tag{A176}$$

$$\mathbf{S}^D_{12}(2^{-\pm}) = \begin{pmatrix} -\frac{1}{2} & -3\sqrt{\frac{3}{10}} & \frac{3}{2}\sqrt{\frac{3}{7}} & 6\sqrt{\frac{3}{35}} \\ -3\sqrt{\frac{3}{10}} & 0 & 3\sqrt{\frac{7}{10}} & 0 \\ \frac{3}{2}\sqrt{\frac{3}{7}} & 3\sqrt{\frac{7}{10}} & \frac{9}{14} & \frac{18}{7\sqrt{5}} \\ 6\sqrt{\frac{3}{35}} & 0 & \frac{18}{7\sqrt{5}} & -\frac{15}{7} \end{pmatrix}. \tag{A177}$$

Now there is a $B_6\bar{B}_6^*$ system for which good G-parity states cannot be defined, which is

$$\mathcal{B}'' = \{\Xi_c'\bar{\Sigma}^*, \Xi_c^*\bar{\Sigma}_c\}. \tag{A178}$$

This system is more involved than usual because we have to consider the two particle channels $\alpha = \Xi_c\bar{\Sigma}_c^*$ and $\beta = \Xi_c^*\bar{\Sigma}_c$ separately. We can define the central and tensor matrices in the particle basis as

$$\mathbf{C}_{12} = \begin{pmatrix} \mathbf{C}^{\alpha\alpha}_{12} & \mathbf{C}^{\alpha\beta}_{12} \\ \mathbf{C}^{\beta\alpha}_{12} & \mathbf{C}^{\beta\beta}_{12} \end{pmatrix} \text{ and } \mathbf{S}_{12} = \begin{pmatrix} \mathbf{S}^{\alpha\alpha}_{12} & \mathbf{S}^{\alpha\beta}_{12} \\ \mathbf{S}^{\beta\alpha}_{12} & \mathbf{S}^{\beta\beta}_{12} \end{pmatrix}. \tag{A179}$$

In this particle basis, the diagonal central matrices are

$$\mathbf{C}^{\alpha\alpha}_{12}(1^-) = \mathbf{C}^{\beta\beta}_{12}(1^-) = \mathbf{C}^D_{12}(1^{-\pm}), \tag{A180}$$

$$\mathbf{C}^{\alpha\alpha}_{12}(2^-) = \mathbf{C}^{\beta\beta}_{12}(2^-) = \mathbf{C}^D_{12}(2^{-\pm}), \tag{A181}$$

while the nondiagonal are given by

$$\mathbf{C}^{\alpha\beta}_{12}(1^-) = \mathbf{C}^{\beta\alpha}_{12}(1^-) = \begin{pmatrix} \frac{1}{3} & 0 & 0 \\ 0 & \frac{1}{3} & 0 \\ 0 & 0 & 1 \end{pmatrix}, \tag{A182}$$

$$\mathbf{C}^{\alpha\beta}_{12}(2^-) = \mathbf{C}^{\beta\alpha}_{12}(2^-) = \begin{pmatrix} \frac{1}{3} & 0 & 0 & 0 \\ 0 & 1 & 0 & 0 \\ 0 & 0 & 1 & 0 \\ 0 & 0 & 0 & 1 \end{pmatrix}. \tag{A183}$$

For the tensor matrices we have

$$\mathbf{S}_{12}^{\alpha\alpha}(1^-) = \begin{pmatrix} 0 & -\frac{1}{\sqrt{2}} & \frac{3}{\sqrt{2}} \\ -\frac{1}{\sqrt{2}} & \frac{1}{2} & \frac{3}{2} \\ \frac{3}{\sqrt{2}} & \frac{3}{2} & -\frac{3}{2} \end{pmatrix}, \quad \text{(A184)}$$

$$\mathbf{S}_{12}^{\alpha\beta}(1^-) = \begin{pmatrix} 0 & -\frac{5}{3\sqrt{2}} & \frac{1}{\sqrt{2}} \\ -\frac{5}{3\sqrt{2}} & \frac{5}{6} & \frac{1}{2} \\ -\frac{1}{\sqrt{2}} & -\frac{1}{2} & \frac{1}{2} \end{pmatrix}, \quad \text{(A185)}$$

$$\mathbf{S}_{12}^{\beta\alpha}(1^-) = \begin{pmatrix} 0 & -\frac{5}{3\sqrt{2}} & -\frac{1}{\sqrt{2}} \\ -\frac{5}{3\sqrt{2}} & \frac{5}{6} & -\frac{1}{2} \\ \frac{1}{\sqrt{2}} & \frac{1}{2} & \frac{1}{2} \end{pmatrix}, \quad \text{(A186)}$$

$$\mathbf{S}_{12}^{\beta\beta}(1^-) = \begin{pmatrix} 0 & -\frac{1}{\sqrt{2}} & -\frac{3}{\sqrt{2}} \\ -\frac{1}{\sqrt{2}} & \frac{1}{2} & -\frac{3}{2} \\ -\frac{3}{\sqrt{2}} & -\frac{3}{2} & -\frac{3}{2} \end{pmatrix}, \quad \text{(A187)}$$

$$\mathbf{S}_{12}^{\alpha\alpha}(2^-) = \begin{pmatrix} -\frac{1}{2} & -3\sqrt{\frac{3}{10}} & \frac{3}{2}\sqrt{\frac{3}{7}} & 6\sqrt{\frac{3}{35}} \\ -3\sqrt{\frac{3}{10}} & 0 & 3\sqrt{\frac{7}{10}} & 0 \\ \frac{3}{2}\sqrt{\frac{3}{7}} & 3\sqrt{\frac{7}{10}} & \frac{9}{14} & \frac{18}{7\sqrt{5}} \\ 6\sqrt{\frac{3}{35}} & 0 & \frac{18}{7\sqrt{5}} & -\frac{15}{7} \end{pmatrix}, \quad \text{(A188)}$$

$$\mathbf{S}_{12}^{\alpha\beta}(2^-) = \begin{pmatrix} -\frac{5}{6} & -\sqrt{\frac{3}{10}} & \frac{1}{2}\sqrt{\frac{3}{7}} & 2\sqrt{\frac{3}{35}} \\ \sqrt{\frac{3}{10}} & 0 & -\sqrt{\frac{7}{10}} & 0 \\ -\frac{1}{2}\sqrt{\frac{3}{7}} & -\sqrt{\frac{7}{10}} & -\frac{3}{14} & -\frac{6}{7\sqrt{5}} \\ -2\sqrt{\frac{3}{35}} & 0 & -\frac{6}{7\sqrt{5}} & \frac{5}{7} \end{pmatrix}, \quad \text{(A189)}$$

$$\mathbf{S}_{12}^{\beta\alpha}(2^-) = \begin{pmatrix} -\frac{5}{6} & \sqrt{\frac{3}{10}} & -\frac{1}{2}\sqrt{\frac{3}{7}} & -2\sqrt{\frac{3}{35}} \\ -\sqrt{\frac{3}{10}} & 0 & -\sqrt{\frac{7}{10}} & 0 \\ \frac{1}{2}\sqrt{\frac{3}{7}} & -\sqrt{\frac{7}{10}} & -\frac{3}{14} & -\frac{6}{7\sqrt{5}} \\ 2\sqrt{\frac{3}{35}} & 0 & -\frac{6}{7\sqrt{5}} & \frac{5}{7} \end{pmatrix}, \quad \text{(A190)}$$

$$\mathbf{S}_{12}^{\beta\beta}(2^-) = \begin{pmatrix} -\frac{1}{2} & 3\sqrt{\frac{3}{10}} & -\frac{3}{2}\sqrt{\frac{3}{7}} & -6\sqrt{\frac{3}{35}} \\ 3\sqrt{\frac{3}{10}} & 0 & 3\sqrt{\frac{7}{10}} & 0 \\ -\frac{3}{2}\sqrt{\frac{3}{7}} & 3\sqrt{\frac{7}{10}} & \frac{9}{14} & \frac{18}{7\sqrt{5}} \\ -6\sqrt{\frac{3}{35}} & 0 & \frac{18}{7\sqrt{5}} & -\frac{15}{7} \end{pmatrix}. \quad \text{(A191)}$$

APPENDIX B: THE ONE PSEUDOSCALAR MESON EXCHANGE POTENTIAL IN HEAVY HADRON CHIRAL PERTURBATION THEORY

1. General form of the potential

The potential generated from the exchange of the kaon and the eta can be derived from the same rules we have used to calculate the OPE potential. We will not present a complete derivation here, but simply a quick overview. The one pseudoscalar meson exchange (OME) potentials are formally identical to the OPE potential. For a general pseudo Nambu-Goldstone boson P we can write

$$V_{\rm OME}^{T\bar{S}} = -R_1^P \bar{R}_2^P \frac{g_3^2}{2f_P^2} F_1^P F_2^P \frac{\vec{a}_1 \cdot \vec{q}\, \vec{a}_2 \cdot \vec{q}}{q^2 + \mu_P^2}, \quad \text{(B1)}$$

$$V_{\rm OME}^{S\bar{S}} = -R_1^P \bar{R}_2^P \frac{g_2^2}{2f_P^2} F_1^P F_2^P \frac{\vec{a}_1 \cdot \vec{q}\, \vec{a}_2 \cdot \vec{q}}{q^2 + \mu_P^2}, \quad \text{(B2)}$$

with f_P the weak decay constant for the meson P; R_1^P, $\bar{R}_2^P$ numerical factors that depend on the meson P; F_1^P and F_2^P flavor factors (which for $P = \pi$ are the isospin factors we have previously used for OPE); $\vec{a}_1$ and $\vec{a}_1$ spin operators; and μ_P the effective mass of the meson P, which is $\mu_P^2 = m_P^2 - \Delta^2$, where m_P is the mass of the meson. Notice the analogy between Eqs. (B1) and (B2) and Eqs. (A109) and (A110) of Appendix A.

The numerical, flavor, and isospin factors of the one eta exchange potential are listed in Table XI for all vertices in which eta exchange is allowed. The format is similar to Table IV, which was dedicated to OPE. There is a difference worth mentioning: the G-parity of the η meson is positive (in contrast to the negative G-parity of the pion), which implies that the signs of the numerical factors R_i^η and $\bar{R}_i^\eta$ are not the same as for the pion factors R_i and $\bar{R}_i$ of Table IV. In particular we have that

$$R_i^\eta \bar{R}_i^\eta > 0 \Rightarrow R_i \bar{R}_i < 0, \quad \text{(B3)}$$

and vice versa. Besides this, it is easy to see that the strength of the flavor factors $F_1^\eta F_2^\eta$ is in general much weaker than the corresponding isospin factors for OPE. For example, in the $\Sigma_c \bar{\Sigma}_c$ system we have that $F_1^\eta F_2^\eta = 1/3$ for

TABLE XI. Numerical, isospin, and spin factor associated with each vertex of the one eta exchange potential for the $S\bar{T}$ and $S\bar{S}$ systems. The arrows are used to indicate the final baryon state in the vertex and P indicates the pseudo Goldstone meson in that vertex. The numerical factors R_i^P and $\bar{R}_i^P$ are for baryons and antibaryons respectively, while F_i^P are the flavor factors. $\vec{\sigma}_i$ are the Pauli matrices, $\vec{\Sigma}_i$ are the spin $S=3/2$ matrices, and $\vec{S}_i$ are the 2×4 matrices that are used for the transitions from a spin-1/2 to a spin-3/2 baryon.

Vertex	P	R_i^P	$\bar{R}_i^P$	$\vec{I}_i$	$\vec{a}_i$
$\Xi_c\to\Xi_c'$	η	$\sqrt{\frac{2}{3}}$	$\sqrt{\frac{2}{3}}$	$\frac{1}{2}\sqrt{3}$	$\vec{\sigma}_i$
$\Xi_c\to\Xi_c^*$	η	$\sqrt{2}$	$-\sqrt{2}$	$\frac{1}{2}\sqrt{3}$	$\vec{S}_i^\dagger$
$\Sigma_c\to\Sigma_c$	η	$\frac{2}{3}$	$\frac{2}{3}$	$\frac{1}{\sqrt{3}}$	$\vec{\sigma}_i$
$\Sigma_c^*\to\Sigma_c$	η	$\frac{1}{\sqrt{3}}$	$-\frac{1}{\sqrt{3}}$	$\frac{1}{\sqrt{3}}$	$\vec{S}_i$
$\Sigma_c\to\Sigma_c^*$	η	$\frac{1}{\sqrt{3}}$	$-\frac{1}{\sqrt{3}}$	$\frac{1}{\sqrt{3}}$	$\vec{S}_i^\dagger$
$\Sigma_c^*\to\Sigma_c^*$	η	$\frac{2}{3}$	$\frac{2}{3}$	$\frac{1}{\sqrt{3}}$	$\vec{\Sigma}_i$
$\Xi_c'\to\Xi_c'$	η	$\frac{2}{3}$	$\frac{2}{3}$	$\frac{1}{2\sqrt{3}}$	$\vec{\sigma}_i$
$\Xi_c^*\to\Xi_c'$	η	$\frac{1}{\sqrt{3}}$	$-\frac{1}{\sqrt{3}}$	$\frac{1}{2\sqrt{3}}$	$\vec{S}_i$
$\Xi_c'\to\Xi_c^*$	η	$\frac{1}{\sqrt{3}}$	$-\frac{1}{\sqrt{3}}$	$\frac{1}{2\sqrt{3}}$	$\vec{S}_i^\dagger$
$\Xi_c^*\to\Xi_c^*$	η	$\frac{2}{3}$	$\frac{2}{3}$	$\frac{1}{2\sqrt{3}}$	$\vec{\Sigma}_i$
$\Omega_c\to\Omega_c$	η	$\frac{2}{3}$	$\frac{2}{3}$	$\frac{2}{\sqrt{3}}$	$\vec{\sigma}_i$
$\Omega_c^*\to\Omega_c$	η	$\frac{1}{\sqrt{3}}$	$-\frac{1}{\sqrt{3}}$	$\frac{2}{\sqrt{3}}$	$\vec{S}_i$
$\Omega_c\to\Omega_c^*$	η	$\frac{1}{\sqrt{3}}$	$-\frac{1}{\sqrt{3}}$	$\frac{2}{\sqrt{3}}$	$\vec{S}_i^\dagger$
$\Omega_c^*\to\Omega_c^*$	η	$\frac{2}{3}$	$\frac{2}{3}$	$\frac{2}{\sqrt{3}}$	$\vec{\Sigma}_i$

eta exchange in contrast to $\vec{T}_1\cdot\vec{T}_2=-2$, -1 and 1 for $I=0$, 1, 2 with the OPE potential.

For the one kaon exchange potential we list the different factors in Table XII for half the nonvanishing vertices. We write the vertices in order of decreasing strangeness for the heavy baryons, with a final kaon. The vertices with an initial antikaon are indeed identical:

$$\mathcal{A}(B\to B'K)=\mathcal{A}(\bar{K}B\to B'), \tag{B4}$$

where B and B' denote the initial and final heavy baryons. The flavor factors in Table XII are listed as numbers, or as the symbol θ_i^a, which is a matrix in isospin space. When the flavor factor is a number, it is implicitly understood that they are multiplied by the identity in isospin space (all vertices conserve isospin). The matrices θ_i^a, where $a=\pm\frac{1}{2}$ refers to the isospin state of the kaon, mediate the transitions from isospin-1 to isospin-$\frac{1}{2}$ baryons (e.g., $\Sigma_c\to\Xi_c'K$). Their explicit expressions are

TABLE XII. Numerical, isospin, and spin factor associated with each vertex of the one kaon exchange potential for the $S\bar{T}$ and $S\bar{S}$ systems. The arrows are used to indicate the final baryon state in the vertex and P indicates the pseudo Goldstone meson in that vertex. The numerical and spin factors (R_i^P, $\bar{R}_i^P$ and $\vec{\sigma}_i$, $\vec{\Sigma}_i$, $\vec{S}_i$) are as in Table XI. The flavor factors F_i^P are in most cases a number (implicitly multiplied by the identity in isospin space to guarantee isospin conservation). The exceptions are the $\Sigma_c\to\Xi_c$ family of transitions in which the flavor factors are 2×3 matrices θ_i^a, with a denoting which of the two isospin states of the kaon have been exchanged.

Vertex	P	R_i^P	$\bar{R}_i^P$	F_i^P	$\vec{a}_i$
$\Lambda_c\to\Xi_c'$	K	$\sqrt{\frac{2}{3}}$	$\sqrt{\frac{2}{3}}$	1	$\vec{\sigma}_i$
$\Lambda_c\to\Xi_c^*$	K	$\sqrt{2}$	$-\sqrt{2}$	1	$\vec{S}_i^\dagger$
$\Sigma_c\to\Xi_c$	K	$\sqrt{\frac{2}{3}}$	$\sqrt{\frac{2}{3}}$	$-\theta_i$	$\vec{\sigma}_i$
$\Sigma_c^*\to\Xi_c$	K	$\sqrt{2}$	$-\sqrt{2}$	$-\theta_i$	$\vec{S}_i$
$\Xi_c\to\Omega_c$	K	$\sqrt{\frac{2}{3}}$	$\sqrt{\frac{2}{3}}$	1	$\vec{\sigma}_i$
$\Xi_c\to\Omega_c$	K	$\sqrt{2}$	$-\sqrt{2}$	1	$\vec{S}_i^\dagger$
$\Sigma_c\to\Xi_c'$	K	$\frac{2}{3}$	$\frac{2}{3}$	θ_i	$\vec{\sigma}_i$
$\Sigma_c^*\to\Xi_c'$	K	$\frac{1}{\sqrt{3}}$	$-\frac{1}{\sqrt{3}}$	θ_i	$\vec{S}_i$
$\Sigma_c\to\Xi_c^*$	K	$\frac{1}{\sqrt{3}}$	$-\frac{1}{\sqrt{3}}$	θ_i	$\vec{S}_i^\dagger$
$\Sigma_c^*\to\Xi_c^*$	K	$\frac{2}{3}$	$\frac{2}{3}$	θ_i	$\vec{\Sigma}_i$
$\Xi_c'\to\Omega_c$	K	$\frac{2}{3}$	$\frac{2}{3}$	1	$\vec{\sigma}_i$
$\Xi_c^*\to\Omega_c$	K	$\frac{1}{\sqrt{3}}$	$-\frac{1}{\sqrt{3}}$	1	$\vec{S}_i$
$\Xi_c'\to\Omega_c^*$	K	$\frac{1}{\sqrt{3}}$	$-\frac{1}{\sqrt{3}}$	1	$\vec{S}_i^\dagger$
$\Xi_c^*\to\Omega_c^*$	K	$\frac{2}{3}$	$\frac{2}{3}$	1	$\vec{\Sigma}_i$

$$\theta_i^{+1/2}=\begin{pmatrix}1&0&0\\0&\frac{1}{\sqrt{2}}&0\end{pmatrix},\quad \theta_i^{-1/2}=\begin{pmatrix}0&\frac{1}{\sqrt{2}}&0\\0&0&1\end{pmatrix}. \tag{B5}$$

The evaluation of the product of two θ_i^a matrices can be done in terms of isospin matrices

$$\sum_a \theta_1^{a\dagger}\theta_2^a=\frac{1}{2}[\vec{\tau}_1\cdot\vec{T}_2+1], \tag{B6}$$

where $\vec{\tau}_1$ and $\vec{T}_2$ refer to the isospin matrices as evaluated for the initial or final state.

2. Strength of the eta and kaon exchange potentials

The strength of eta and kaon exchange can be compared to that of OPE using the techniques of Sec. IV. The central scale Λ_C^P for the OME potential can be defined as follows:

$$\Lambda_C^P=\frac{1}{|\sigma F_1^P F_2^P|}\frac{24\pi f_P^2}{\mu|R_1^P\bar{R}_2^P|g_i^2}, \tag{B7}$$

which is analogous to Eq. (76), except for the changes

$$f_\pi \to f_P \quad \text{and} \quad \tau \to F_1^P F_2^P, \tag{B8}$$

while $|R_1\bar{R}_2| = |R_1^P \bar{R}_2^P|$. The comparison is in fact direct if we write it as

$$\Lambda_C^P = \left(\frac{|\tau|}{|F_1^P F_2^P|}\right) \times \left(\frac{f_P^2}{f_\pi^2}\right) \times \Lambda_C, \tag{B9}$$

which merely involves the evaluation of a few numerical factors. For the eta meson we have

$$\frac{|\tau|}{|F_1^\eta F_2^\eta|} = 3, 6, 9 \quad \text{and} \quad \frac{f_\eta^2}{f_\pi^2} \sim 1.5, \tag{B10}$$

where we have taken $f_\eta \simeq f_K \sim 160$ MeV. By multiplying these factors it is apparent that Λ_C^η is considerably harder than Λ_C. The conclusion is that one eta exchange is very suppressed with respect to OPE. For one kaon exchange the factors are

$$\frac{|\tau|}{|F_1^K F_2^K|} = 1, 2 \quad \text{and} \quad \frac{f_K^2}{f_\pi^2} \sim 1.5, \tag{B11}$$

which are not particularly large. The flavor factor suppression is larger for the lower isospin states, for which the OPE is stronger. The outcome is that the one kaon exchange potential is perturbative.

The comparison of the tensor scales Λ_T^P and Λ_T is similar except for the existence of factors of the type $e^{m_P R_c}$ and $e^{m_\pi R_c}$ that are included to take into account that the OME and OPE potentials cease to be valid below a certain distance; see Eq. (98). If we add these factors, we end up with

$$\Lambda_T^P(m_P) = \left(\frac{|\tau|}{|F_1^P F_2^P|}\right) \times \left(\frac{f_P^2}{f_\pi^2}\right) \times \left(\frac{e^{m_P R_c}}{e^{m_\pi R_c}}\right) \times \Lambda_T(m_p), \tag{B12}$$

where $e^{(m_P - m_\pi)R_c} \sim 3$–$5$ and 2.5–4 for the eta and kaon, respectively. The addition of this factor means that the tensor scale Λ_T^P is in general considerably larger than the one for OPE. In particular it can be regarded as a hard scale.

APPENDIX C: THE CONTACT-RANGE POTENTIAL

The calculation of the contact-range potential will use a different set of techniques than the one of the OPE potential. While we derived the OPE potential from the lowest-dimensional Lagrangian compatible with HQSS and chiral symmetry, for the contact-range potential we will use HQSS without any explicit reference to a Lagrangian. We will first take into account that the lowest order contact-range potential is simply a constant in momentum space,

$$\langle \vec{p}' | V_C^{(0)} | \vec{p} \rangle = C, \tag{C1}$$

where $\vec{p}$ and $\vec{p}'$ are the initial and final center-of-mass momentum of the heavy baryon-antibaryon pair and C a coupling. In principle the coupling C depends on a specific baryon-antibaryon system and its quantum numbers. But HQSS precludes C to depend on the heavy quark spin, which will translate into a reduction of the number of couplings. We will explain in the following lines how to do that.

Heavy baryons are $|Qqq\rangle$ states with the structure

$$B_{\bar{3}} = |Q(qq)_{s_L=0}\rangle_{j=\frac{1}{2}}, \tag{C2}$$

$$B_6 = |Q(qq)_{s_L=1}\rangle_{j=\frac{1}{2}}, \tag{C3}$$

$$B_6^* = |Q(qq)_{s_L=1}\rangle_{j=\frac{3}{2}}, \tag{C4}$$

with $s_L = 0, 1$ the light quark pair spin and j the total spin. The application of HQSS to the contact-range couplings C implies that they depend on the total light spin $\vec{S}_L = \vec{s}_{L1} + \vec{s}_{L2}$, but not on the total spin $\vec{J} = \vec{j}_1 + \vec{j}_2$ or the total heavy spin $\vec{S}_H = \vec{s}_{H1} + \vec{s}_{H2}$. To determine the exact structure we have to study the coupling of the light quark spin for different types of heavy baryon-antibaryon molecules. In the following lines we will explain how to do this for the $B_6^{(*)}\bar{B}_6^{(*)}$, $B_{\bar{3}}\bar{B}_6^{(*)}$ systems, ordered by decreasing degree of complexity. We did not list the system

$$B_{\bar{3}}\bar{B}_{\bar{3}} \Rightarrow S_L = 0, \tag{C5}$$

for which the light spin structure is trivial because $s_{L1} = s_{L2} = 0$.

1. The $S\bar{S}$ contact potential

For a heavy $S\bar{S}$ baryon-antibaryon system (i.e., $S_L = 1$ for both baryons) we can decompose the spin wave function into heavy and light components as follows:

$$|B_6^{(*)}\bar{B}_6^{(*)}(J^-)\rangle = \sum_{S_H, S_L} D_{S_H, S_L}(J) S_H \otimes S_L|_J, \tag{C6}$$

where D are the coefficients for this change of basis. They fulfill the condition

$$\sum_{S_H, S_L} |D_{S_H, S_L}(J)|^2 = 1. \tag{C7}$$

From this decomposition we can calculate the light spin components of the contact-range potential:

$$\langle S_H' \otimes S_L' | V | S_H \otimes S_L \rangle = \delta_{S_H S_H'} \delta_{S_L S_L'} V_{S_L}, \tag{C8}$$

where the light and heavy spin decouple.

The general way to carry on the heavy-light spin decomposition is to consider the spin wave function of the heavy hadrons

$$|H_1\rangle = |s_{H_1} s_{L_1} j_1\rangle, \qquad |H_2\rangle = |s_{H_2} s_{L_2} j_2\rangle, \quad \text{(C9)}$$

where s_{H_1}, s_{H_2} is the heavy spin; s_{L_1}, s_{L_2} the light spin; and j_1, j_2 the angular momenta of the two hadrons. When we couple the two hadrons, we have:

$$\begin{aligned}|H_1 H_2\rangle &= |s_{H_1} s_{L_1} j_1\rangle |s_{H_2} s_{L_2} j_2\rangle \\ &= \sum_{S_H, S_L} D_{S_H, S_L}(J) |(s_{H_1} s_{H_2}) S_H (s_{L_1} s_{L_2}) S_L (j_1 j_2) J\rangle,\end{aligned} \quad \text{(C10)}$$

which is merely a detailed version of Eq. (C6), where the notation indicates that the heavy spins coupled to S_H, the light spins to S_L, and the angular momenta to J. The coefficients $D_{S_H,S_L}(J)$ can in fact be expressed in terms of 9-J symbols:

$$\begin{aligned}&D_{S_H,S_L}(J) \\ &= \langle s_{H_1} s_{L_1} j_1 s_{H_2} s_{L_2} j_2 || (s_{H_1} s_{H_2}) S_H (s_{L_1} s_{L_2}) S_L (j_1 j_2) J\rangle \\ &= \sqrt{(2j_1+1)(2j_2+1)(2S_H+1)(2S_L+1)} \begin{Bmatrix} s_{H1} & s_{L_1} & j_1 \\ s_{H2} & s_{L_2} & j_2 \\ S_H & S_L & J \end{Bmatrix}.\end{aligned} \quad \text{(C11)}$$

Finally if we are considering antihadrons, we should consider their behaviors under C-parity to define their spin wave functions consistently: they might differ by a sign from the ansatz $|s_H s_L j\rangle$.

If we go back to the $S\bar{S}$ heavy baryon-antibaryon system, for the $B_6\bar{B}_6$ case we find the following:

$$|B_6\bar{B}_6(0^-)\rangle = \frac{1}{\sqrt{3}} 0_H \otimes 0_L + \sqrt{\frac{2}{3}} 1_H \otimes 1_L \Big|_{J=0}, \quad \text{(C12)}$$

$$\begin{aligned}|B_6\bar{B}_6(1^-)\rangle = &\frac{\sqrt{2}}{3} 0_H \otimes 1_L - \frac{1}{3\sqrt{3}} 1_H \otimes 0_L \\ &+ \frac{2}{3}\sqrt{\frac{5}{3}} 1_H \otimes 2_L \Big|_{J=1}.\end{aligned} \quad \text{(C13)}$$

For the $B_6\bar{B}_6^*$ and $B_6^*\bar{B}_6$ cases, we include a minus sign in front of the states containing a $\bar{B}_6^*$ to highlight the C-parity convention that we employ here:

$$\begin{aligned}-|B_6\bar{B}_6^*(1^-)\rangle = &+\frac{1}{3} 0_H \otimes 1_L - \frac{2}{3}\sqrt{\frac{2}{3}} 1_H \otimes 0_L \\ &+ \frac{1}{\sqrt{2}} 1_H \otimes 1_L \Big|_{J=1} - \frac{1}{3}\sqrt{\frac{5}{6}} 1_H \otimes 2_L \Big|_{J=1},\end{aligned} \quad \text{(C14)}$$

$$\begin{aligned}+|B_6^*\bar{B}_6(1^-)\rangle = &-\frac{1}{3} 0_H \otimes 1_L + \frac{2}{3}\sqrt{\frac{2}{3}} 1_H \otimes 0_L \\ &+ \frac{1}{\sqrt{2}} 1_H \otimes 1_L \Big|_{J=1} + \frac{1}{3}\sqrt{\frac{5}{6}} 1_H \otimes 2_L \Big|_{J=1},\end{aligned} \quad \text{(C15)}$$

$$\begin{aligned}-|B_6\bar{B}_6^*(2^-)\rangle = &+\frac{1}{\sqrt{3}} 0_H \otimes 2_L - \frac{1}{\sqrt{6}} 1_H \otimes 1_L \Big|_{J=2} \\ &+ \frac{1}{\sqrt{2}} 1_H \otimes 2_L \Big|_{J=2},\end{aligned} \quad \text{(C16)}$$

$$\begin{aligned}+|B_6^*\bar{B}_6(2^-)\rangle = &-\frac{1}{\sqrt{3}} 0_H \otimes 2_L + \frac{1}{\sqrt{6}} 1_H \otimes 1_L \Big|_{J=2} \\ &+ \frac{1}{\sqrt{2}} 1_H \otimes 2_L \Big|_{J=2}.\end{aligned} \quad \text{(C17)}$$

Finally, for the $B_6^*\bar{B}_6^*$ case we have

$$-|B_6^*\bar{B}_6^*(0^-)\rangle = \sqrt{\frac{2}{3}} 0_H \otimes 0_L - \frac{1}{\sqrt{3}} 1_H \otimes 1_L \Big|_{J=0}, \quad \text{(C18)}$$

$$\begin{aligned}-|B_6^*\bar{B}_6^*(1^-)\rangle = &\frac{\sqrt{5}}{3} 0_H \otimes 1_L + \frac{1}{3}\sqrt{\frac{10}{3}} 1_H \otimes 0_L \\ &- \frac{1}{3}\sqrt{\frac{2}{3}} 1_H \otimes 2_L \Big|_{J=1},\end{aligned} \quad \text{(C19)}$$

$$-|B_6^*\bar{B}_6^*(2^-)\rangle = \frac{1}{\sqrt{3}} 0_H \otimes 2_L + \sqrt{\frac{2}{3}} 1_H \otimes 1_L \Big|_{J=2}, \quad \text{(C20)}$$

$$-|B_6^*\bar{B}_6^*(3^-)\rangle = 1_H \otimes 2_L|_{J=3}, \quad \text{(C21)}$$

where we have included the minus sign to stress the convention.

Finally for the $B_6\bar{B}_6^*$ we can also write the decomposition in the basis with well-defined C-parity for those cases where it applies:

$$|B_6^*\bar{B}_6(1^{-+})\rangle = 1_H \otimes 1_L|_{J=1}, \quad \text{(C22)}$$

$$\begin{aligned}|B_6^*\bar{B}_6(1^{--})\rangle = &\frac{\sqrt{2}}{3} 0_H \otimes 1_L - \frac{4}{3\sqrt{3}} 1_H \otimes 0_L \\ &- \frac{1}{3}\sqrt{\frac{5}{3}} 1_H \otimes 2_L \Big|_{J=1}\end{aligned} \quad \text{(C23)}$$

$$|B_6^*\bar{B}_6(2^{-+})\rangle = \sqrt{\frac{2}{3}}0_H \otimes 2_L - \frac{1}{\sqrt{3}}1_H \otimes 1_L\Big|_{J=2}.$$
$$|B_6^*\bar{B}_6(2^{--})\rangle = 1_H \otimes 2_L|_{J=2}. \quad \text{(C24)}$$

From the previous decomposition and applying Eq. (C8) we obtain the contact-range potentials of Sec. III.

2. The $T\bar{S}/S\bar{T}$ contact potential

For a heavy $T\bar{S}/S\bar{T}$ baryon-antibaryon system we have to pay attention to the fact that one baryon has $S_L = 0$ and the other $S_L = 1$. The expectation is that there will be a direct (exchange) contact term for the transition $T\bar{S} \to T\bar{S}$ ($T\bar{S} \to S\bar{T}$). The heavy-light decomposition of the potential is in this case

$$\langle S'_H \otimes (S'_{L_1} \otimes S'_{L_2})_{S'_L}|V|S_H \otimes (S_{L_1} \otimes S_{L_2})_{S_L}\rangle = \delta_{S_H S'_H}\delta_{S_L S'_L}\langle S'_{L_1} S'_{L_2}|V_{S_L}|S_{L_1} S_{L_2}\rangle, \quad \text{(C25)}$$

where now we have take into account that the light quark spin of particles 1 and 2 is different. If we have a particle-antiparticle system, C-parity implies

$$\langle S'_{L_1} S'_{L_2}|V_{S_L}|S_{L_1} S_{L_2}\rangle = \langle S'_{L_2} S'_{L_1}|V_{S_L}|S_{L_2} S_{L_1}\rangle. \quad \text{(C26)}$$

As a consequence, for the $T\bar{S}/S\bar{T}$ case there are two contact couplings corresponding to

$$\langle 01|V_1|01\rangle = \langle 10|V_1|10\rangle, \quad \text{(C27)}$$

$$\langle 01|V_1|10\rangle = \langle 10|V_1|01\rangle. \quad \text{(C28)}$$

That is, a contact term that conserves the spin of particles 1 and 2 and a contact that exchanges it. For the $B_{\bar{3}}\bar{B}_6$ and $B_6\bar{B}_{\bar{3}}$ the heavy-light spin decomposition reads

$$|B_{\bar{3}}\bar{B}_6(0^-)\rangle = +1_H \otimes 1_{\bar{q}\bar{q}}|_{J=0}, \quad \text{(C29)}$$

$$|B_6\bar{B}_{\bar{3}}(0^-)\rangle = -1_H \otimes 1_{qq}|_{J=0}, \quad \text{(C30)}$$

$$|B_{\bar{3}}\bar{B}_6(1^-)\rangle = -\frac{1}{\sqrt{3}}0_H \otimes 1_{\bar{q}\bar{q}} + \sqrt{\frac{2}{3}}1_H \otimes 1_{\bar{q}\bar{q}}\Big|_{J=1}, \quad \text{(C31)}$$

$$|B_6\bar{B}_{\bar{3}}(1^-)\rangle = +\frac{1}{\sqrt{3}}0_H \otimes 1_{qq} + \sqrt{\frac{2}{3}}1_H \otimes 1_{qq}\Big|_{J=1}, \quad \text{(C32)}$$

while for the $B_{\bar{3}}\bar{B}_6^*$ and $B_6^*\bar{B}_{\bar{3}}$ we include the minus sign in front of the states to make the C-parity convention manifest:

$$-|B_{\bar{3}}\bar{B}_6^*(1^-)\rangle = \sqrt{\frac{2}{3}}0_H \otimes 1_{\bar{q}\bar{q}} + \frac{1}{\sqrt{3}}1_H \otimes 1_{\bar{q}\bar{q}}\Big|_{J=1}, \quad \text{(C33)}$$

$$+|B_6^*\bar{B}_{\bar{3}}(1^-)\rangle = \sqrt{\frac{2}{3}}0_H \otimes 1_{qq} - \frac{1}{\sqrt{3}}1_H \otimes 1_{qq}\Big|_{J=1}, \quad \text{(C34)}$$

$$-|B_{\bar{3}}\bar{B}_6^*(2^-)\rangle = 1_H \otimes 1_{\bar{q}\bar{q}}|_{J=2}, \quad \text{(C35)}$$

$$+|B_6^*\bar{B}_{\bar{3}}(2^-)\rangle = 1_H \otimes 1_{qq}|_{J=2}. \quad \text{(C36)}$$

In the decomposition above only the quark pair with $S_L = 1$ is written. The other quark pair is implicitly understood, i.e.,

$$1_{qq} = 1_{qq} \otimes 0_{\bar{q}\bar{q}}, \quad \text{(C37)}$$

$$1_{\bar{q}\bar{q}} = 0_{qq} \otimes 1_{\bar{q}\bar{q}}. \quad \text{(C38)}$$

From the decomposition and the definitions

$$B_{D1} = \langle 1_{qq}|V|1_{qq}\rangle = \langle 1_{\bar{q}\bar{q}}|V|1_{\bar{q}\bar{q}}\rangle, \quad \text{(C39)}$$

$$B_{E1} = \langle 1_{qq}|V|1_{\bar{q}\bar{q}}\rangle = \langle 1_{\bar{q}\bar{q}}|V|1_{qq}\rangle, \quad \text{(C40)}$$

we obtain the contact-range potentials of Sec. III.

[1] M. Voloshin and L. Okun, JETP Lett. **23**, 333 (1976).
[2] N. A. Törnqvist, Phys. Rev. Lett. **67**, 556 (1991), revised version.
[3] A. V. Manohar and M. B. Wise, Nucl. Phys. **B399**, 17 (1993).
[4] T. E. O. Ericson and G. Karl, Phys. Lett. B **309**, 426 (1993).
[5] N. A. Törnqvist, Z. Phys. C **61**, 525 (1994).
[6] S. K. Choi *et al.* (Belle Collaboration), Phys. Rev. Lett. **91**, 262001 (2003).
[7] M. Ablikim *et al.* (BESIII Collaboration), Phys. Rev. Lett. **110**, 252001 (2013).
[8] Z. Q. Liu *et al.* (Belle Collaboration), Phys. Rev. Lett. **110**, 252002 (2013).
[9] Q. Wang, C. Hanhart, and Q. Zhao, Phys. Rev. Lett. **111**, 132003 (2013).
[10] F.-K. Guo, C. Hidalgo-Duque, J. Nieves, and M. Pavón Valderrama, Phys. Rev. D **88**, 054007 (2013).
[11] R. Aaij *et al.* (LHCb Collaboration), Phys. Rev. Lett. **115**, 072001 (2015).
[12] R. Chen, X. Liu, X.-Q. Li, and S.-L. Zhu, Phys. Rev. Lett. **115**, 132002 (2015).

[13] H.-X. Chen, W. Chen, X. Liu, T. G. Steele, and S.-L. Zhu, Phys. Rev. Lett. **115**, 172001 (2015).
[14] L. Roca, J. Nieves, and E. Oset, Phys. Rev. D **92**, 094003 (2015).
[15] J. He, Phys. Lett. B **753**, 547 (2016).
[16] C. W. Xiao and U. G. Meißner, Phys. Rev. D **92**, 114002 (2015).
[17] T. J. Burns, Eur. Phys. J. A **51**, 152 (2015).
[18] L. Geng, J. Lu, and M. P. Valderrama, Phys. Rev. D **97**, 094036 (2018).
[19] A. Bondar *et al.* (Belle Collaboration), Phys. Rev. Lett. **108**, 122001 (2012).
[20] I. Adachi *et al.* (Belle Collaboration), arXiv:1207.4345.
[21] M. Voloshin, Phys. Rev. D **84**, 031502 (2011).
[22] M. Cleven, F.-K. Guo, C. Hanhart, and U.-G. Meissner, Eur. Phys. J. A **47**, 120 (2011).
[23] B. Aubert *et al.* (*BABAR* Collaboration), Phys. Rev. Lett. **90**, 242001 (2003).
[24] D. Besson *et al.* (CLEO Collaboration), Phys. Rev. D **68**, 032002 (2003); **75**, 119908(E) (2007).
[25] F.-K. Guo, P.-N. Shen, H.-C. Chiang, R.-G. Ping, and B.-S. Zou, Phys. Lett. B **641**, 278 (2006).
[26] F.-K. Guo, P.-N. Shen, and H.-C. Chiang, Phys. Lett. B **647**, 133 (2007).
[27] F.-K. Guo and U.-G. Meissner, Phys. Rev. D **84**, 014013 (2011).
[28] M. Altenbuchinger, L. S. Geng, and W. Weise, Phys. Rev. D **89**, 014026 (2014).
[29] L.-S. Geng, J.-X. Lu, M. P. Valderrama, and X.-L. Ren, Phys. Rev. D **97**, 091501 (2018).
[30] M. T. AlFiky, F. Gabbiani, and A. A. Petrov, Phys. Lett. B **640**, 238 (2006).
[31] T. Mehen and J. W. Powell, Phys. Rev. D **84**, 114013 (2011).
[32] M. Pavón Valderrama, Phys. Rev. D **85**, 114037 (2012).
[33] J. Nieves and M. Pavón Valderrama, Phys. Rev. D **86**, 056004 (2012).
[34] C. Hidalgo-Duque, J. Nieves, and M. Pavón Valderrama, Phys. Rev. D **87**, 076006 (2013).
[35] F.-K. Guo, C. Hidalgo-Duque, J. Nieves, and M. Pavón Valderrama, Phys. Rev. D **88**, 054014 (2013).
[36] E. Braaten and M. Kusunoki, Phys. Rev. D **69**, 074005 (2004).
[37] S. Fleming, M. Kusunoki, T. Mehen, and U. van Kolck, Phys. Rev. D **76**, 034006 (2007).
[38] D. L. Canham, H. W. Hammer, and R. P. Springer, Phys. Rev. D **80**, 014009 (2009).
[39] D. B. Kaplan, M. J. Savage, and M. B. Wise, Phys. Lett. B **424**, 390 (1998).
[40] D. B. Kaplan, M. J. Savage, and M. B. Wise, Nucl. Phys. **B534**, 329 (1998).
[41] U. van Kolck, Nucl. Phys. **A645**, 273 (1999).
[42] M. C. Birse, J. A. McGovern, and K. G. Richardson, Phys. Lett. B **464**, 169 (1999).
[43] M. Pavón Valderrama and D. R. Phillips, Phys. Rev. Lett. **114**, 082502 (2015).
[44] M. Pavón Valderrama, Int. J. Mod. Phys. E **25**, 1641007 (2016).
[45] M. C. Birse, Phys. Rev. C **74**, 014003 (2006).
[46] P. L. Cho, Nucl. Phys. **B396**, 183 (1993); **B421**, 683 (1994).
[47] T. D. Lee and C.-N. Yang, Nuovo Cimento **3**, 749 (1956).
[48] T. A. Kaeding, At. Data Nucl. Data Tables **61**, 233 (1995).
[49] S. H. Lee *et al.* (Belle Collaboration), Phys. Rev. D **89**, 091102 (2014).
[50] H.-Y. Cheng and C.-K. Chua, Phys. Rev. D **92**, 074014 (2015).
[51] T.-M. Yan, H.-Y. Cheng, C.-Y. Cheung, G.-L. Lin, Y. C. Lin, and H.-L. Yu, Phys. Rev. D **46**, 1148 (1992); **55**, 5851(E) (1997).
[52] P. L. Cho, Phys. Lett. B **285**, 145 (1992).
[53] W. Detmold, C. J. D. Lin, and S. Meinel, Phys. Rev. D **85**, 114508 (2012).
[54] S. Fleming, T. Mehen, and I. W. Stewart, Nucl. Phys. **A677**, 313 (2000).
[55] M. Pavón Valderrama, M. S. Sánchez, C. J. Yang, B. Long, J. Carbonell, and U. van Kolck, Phys. Rev. C **95**, 054001 (2017).
[56] M. Cavagnero, Phys. Rev. A **50**, 2841 (1994).
[57] B. Gao, Phys. Rev. A **59**, 2778 (1999).
[58] S. R. Beane, P. F. Bedaque, L. Childress, A. Kryjevski, J. McGuire, and U. van Kolck, Phys. Rev. A **64**, 042103 (2001).
[59] M. Pavón Valderrama and E. R. Arriola, Phys. Rev. C **72**, 054002 (2005).
[60] M. Pavón Valderrama and E. R. Arriola, Phys. Rev. C **74**, 054001 (2006).
[61] M. Pavón Valderrama and E. R. Arriola, Phys. Rev. C **74**, 064004 (2006).
[62] M. Pavón Valderrama and E. R. Arriola, Phys. Rev. C **79**, 044001 (2009).
[63] M. Pavón Valderrama and E. R. Arriola, Phys. Rev. C **83**, 044002 (2011).
[64] M. Sánchez Sánchez, L.-S. Geng, J.-X. Lu, T. Hyodo, and M. P. Valderrama, Phys. Rev. D **98**, 054001 (2018).
[65] D. Gamermann and E. Oset, Eur. Phys. J. A **33**, 119 (2007).
[66] J.-J. Wu, R. Molina, E. Oset, and B. S. Zou, Phys. Rev. Lett. **105**, 232001 (2010).
[67] C. W. Xiao, J. Nieves, and E. Oset, Phys. Rev. D **88**, 056012 (2013).
[68] M. Karliner and J. L. Rosner, Phys. Rev. Lett. **115**, 122001 (2015).
[69] M. Voloshin, Int. J. Mod. Phys. A **21**, 1239 (2006).
[70] E. Epelbaum, U. G. Meissner, W. Gloeckle, and C. Elster, Phys. Rev. C **65**, 044001 (2002).
[71] M. Gell-Mann and M. Lévy, Nuovo Cimento **16**, 705 (1960).
[72] J. J. Sakurai, Ann. Phys. (N.Y.) **11**, 1 (1960).
[73] R. Chen, A. Hosaka, and X. Liu, Phys. Rev. D **96**, 116012 (2017).
[74] A. E. Bondar, A. Garmash, A. I. Milstein, R. Mizuk, and M. B. Voloshin, Phys. Rev. D **84**, 054010 (2011).
[75] M. Albaladejo, F. K. Guo, C. Hidalgo-Duque, J. Nieves, and M. Pavón Valderrama, Eur. Phys. J. C **75**, 547 (2015).
[76] V. Baru, E. Epelbaum, A. A. Filin, C. Hanhart, U.-G. Meißner, and A. V. Nefediev, Phys. Lett. B **763**, 20 (2016).
[77] E. Cincioglu, J. Nieves, A. Ozpineci, and A. U. Yilmazer, Eur. Phys. J. C **76**, 576 (2016).
[78] L.-Y. Dai, J. Haidenbauer, and U.-G. Meißner, J. High Energy Phys. 07 (2017) 078.
[79] G. Barucca *et al.* (PANDA Collaboration), Eur. Phys. J. C **A55**, 42 (2019).